Vestigial-Like Co-Factors in *Drosophila* Development

by

Virginia L Pimmett

A thesis submitted in partial fulfillment of the requirements for the degree of

Doctor of Philosophy

Department of Cell Biology

University of Alberta

Abstract

Cells require the ability to modulate function in response to their surroundings so that they are able to contribute to the survival of the organism. A key mechanism that allows tunable responses to changes in environment is by differential control of gene expression by transcriptional regulators. In *Drosophila*, the Vestigial-like (VGLL) family of transcriptional co-factors is comprised of two genes*, vestigial* (*vg*) and *Tondu domain-containing Growth Inhibitor* (*Tgi*). Regulation of these co-factors is key during development of metazoans, and their dysregulation in humans is associated with several types of cancers.

Vg, the *Drosophila* orthologue of the mammalian VGLL1-3 proteins, is regulated by phosphorylation at the Serine-215 residue. This phosphorylation is mediated by association with the transcription factor Scalloped (Sd), and the residue is a target of the p38 mitogen-associated protein kinase (MAPK) pathway. Interfering with phosphorylation at Serine-215 causes developmental defects in the adult *Drosophila* wing, as well as altering terminal specification of the embryonic somatic musculature.

Tgi, the *Drosophila* orthologue of the mammalian VGLL4 protein, is a recently identified second member of the VGLL gene family in *Drosophila*. Tgi is able to interact with Sd similarly to Vg, but Tgi and Vg are unable to form a co-complex. A potential explanation for this is that Tgi and Vg are competing and excluding the other from interaction with Sd. Ectopic expression of Tgi causes wing size reduction and fate defects in the adult wing, and this wing size reduction is dose-sensitive to the level of *vg* expression. Additionally, overexpression of *Tgi* in *Drosophila* Kc167 cells causes an exclusion of Vg to the

cytoplasmic domain, and Tgi and Vg direct Sd to differentially regulate target genes. Finally, Tgi induces the expression of *vg*, setting up a negative feedback loop to repress its own activity.

Preface

Portions of Chapters 2 and 4 of this thesis were published as:

Pimmett, V. L., Deng, H., Haskins, J. A., Mercier, R. J., LaPointe, P. and Simmonds, A. J. (2017). The activity of the Drosophila Vestigial protein is modified by Scalloped-dependent phosphorylation. *Dev. Biol.* **425**, 58–69.

The paper cited represents a collaborative work between all authors. I was responsible for data collection and replication, analysis, manuscript writing and editing. H. Deng and J. Haskins also performed data collection and analysis, R. Mercier provided data collection, and A. Simmonds provided data analysis and manuscript writing and editing. P. LaPointe and A. Simmonds were supervisory authors. Chapter 2 contains data from this publication, and Chapter 5 contains methods and materials used to generate this data.

No portions of Chapter 3 have been published.

I gratefully acknowledge the family and friends who have supported me in my journey.

Thank you for your patience, wisdom, advice and strength.

This thesis is dedicated to the memory of James Van Eindhoven (1989-2008)

Acknowledgements

I would like to express my sincere gratitude to my supervisor, Dr. Andrew Simmonds. His patience, guidance, and expertise has been invaluable over the course of my PhD. I have been incredibly fortunate to have a supervisor and mentor who has constantly supported my growth, and who has been a source of advice and encouragement since the beginning.

I must gratefully acknowledge my committee members, Dr. Fred Berry (Department of Surgery) and Dr. Gary Eitzen (Department of Cell Biology) for their insight and input into my project. Thank you as well to my PhD examiners Dr. Roseline Godbout (Department of Oncology) and Dr. Douglas Allan (Department of Cellular & Physiological Sciences, University of British Columbia), and my candidacy examiner Dr. Alan Underhill (Department of Oncology).

Funding for this research was provided by the Motyl Graduate Studentship in Cardiac Sciences from the University of Alberta Faculty of Medicine and Dentistry, the Women's and Children's Health Research Institute at the University of Alberta, and the Natural Sciences and Engineering Research Council.

Table of Contents

List of Figures and Illustrations

List of Tables

Chapter 1: General Introduction

One of the most important functions of both individual cells and cells that comprise entire organisms is the ability to recognize and respond to change. There is a wide range of signals that cells need to be able to integrate and react appropriately to, such as intracellular communication, nutrient availability, or physical cues (reviewed in Baker, 2017; Danielsen et al., 2013; West and Harris, 2016; Zhang et al., 2018). Failure to recognize these cues or to implement an appropriate reaction can lead to cell stress and possibly cell death. A key mechanism that allows for a graded response to shifts in cellular demands is differential control of gene expression. This process is especially important during development of complex multicellular organisms (reviewed in Murakawa et al., 2016; Reiter et al., 2017; Voss and Hager, 2014). The process of development requires maintaining a balance between cell proliferation to expand tissue volume, fate determination/differentiation to develop specific physiological structures, and cell death to eliminate damaged or unnecessary cells. Implementation of specific cell fates requires cells to differentially express specific subsets of genes, a process regulated in part by the combinatorial expression of specific transcriptional regulators (reviewed in Heinz et al., 2015; Todeschini et al., 2014).

1.1 Modeling Disease in Drosophila

Drosophila melanogaster has historically been an excellent model system to probe transcriptional regulation by virtue of a deep body of knowledge of developmental processes across multiple tissue types and stages of development (reviewed in Arbeitman et al., 2002;

Schwarzer and Spitz, 2014). It also presents a useful mid-level model system, wherein the complexity of the system is reduced with fewer redundant or partially redundant genes while still presenting all three germ layers and multiple tissue types comparable to humans (reviewed in Adams et al., 2000). A rich and well-developed system of genetic manipulation exists to investigate the functional consequences of gene mutation, inactivation, and overexpression (reviewed in Hales et al., 2015; St Johnston, 2002). Practical considerations such as the short generation time, comparative ease of culture, and amenability of tissue for macroscopic and microscopic visualization have assisted the use of *Drosophila* as an effective model for human development and disease.

An estimated 75% of disease-associated genes in humans have a homologue in *Drosophila* (reviewed in Pandey and Nichols, 2011; Reiter et al., 2001). The founding members of many human disease-associated gene families were originally discovered in *Drosophila*, such as *wingless* (*wg*), orthologous to the mammalian *Wnt* family (reviewed in Klaus and Birchmeier, 2008); *hedgehog (hh)* with the human orthologues *sonic hedgehog, desert hedgehog* and *indian hedgehog* (reviewed in Ingham et al., 2011). This also includes *vestigial (vg)*, orthologous to the mammalian *Vestigial-like* (*VGLL*) family of transcriptional co-factors (reviewed in Simon et al., 2016). *Drosophila* has a considerably less complex genome compared to mammals and other metazoan model systems, with fewer functionally redundant homologous genes compared to humans and mice. For example, the *Hh* family mentioned above has only a single *Drosophila* orthologue in comparison to multiple mammalian homologues. Interestingly, the *VGLL* gene family has two paralogous genes in *Drosophila* compared to four in mice and humans (reviewed in Simon et al., 2016).

1.2 The Vestigial-like Family of Transcriptional co-factors

The founding member of the VGLL family of transcriptional co-factors, *vg*, was initially described via a mutant allele resulting in a 'vestigial' wing structure in a screen of adult flies by Thomas Hunt Morgan (Morgan and Bridges, 1919). Subsequently, Vg was identified as a nuclear protein involved in development of adult wings and halteres (Williams et al., 1991). It is best described as a "selector" gene, as its ectopic expression in different tissues results in conversion to a wing fate (Simmonds et al., 1998). This family of genes is broadly conserved across evolution, appearing in Eumetazoans from the tunicate *Ciona intestinalis* through invertebrates such as *Caenorhabditis elegans* and the *Drosophilid* family and higher vertebrates such as *Danio rerio* and *Xenopus laevis* as well as mice and humans (Waterhouse et al., 2011). Interestingly, no member of the Vestigial-like family is present outside of the Opisthokonts or fungi such as *Saccharomyces cerevisiae* or *Schizosaccharomyces pombe* (Simon et al., 2016).

The defining characteristic of the VGLL family is the presence of one or more TONDU functional domains in the gene product (**Figure 1.1A**) (Simmonds et al., 1998; Vaudin et al., 1999). This domain is a 24 amino acid region that is significantly conserved across multiple species (Simmonds et al., 1998; Vaudin et al., 1999). It is required for interaction with the transcription factor Scalloped (Sd), as deletion of the region results in a loss of interaction *in vitro* between Vg and Sd; *in vivo*, deletion of the TONDU domain in Vg causes impaired adult *Drosophila* wing development (MacKay et al., 2003; Simmonds et al., 1998). All known members of the Vestigial-like family are obligate partners of the TEF-1/TEC-1/ABAA DNA-

binding (TEA domain, or TEAD) (Bürglin, 1991) domain containing family of transcription factors (Pobbati and Hong, 2013). In *Drosophila*, the sole TEAD family member is encoded by the *sd* gene (Campbell et al., 1991; Campbell et al., 1992). This interaction is mediated by a direct binding of the carboxyl-terminal half of Sd to the TONDU domain of Vg (Simmonds et al., 1998). This effectively forms a complete unit wherein Sd provides the DNA binding capabilities and Vg is able to recruit the basal transcriptional machinery, as TEAD proteins alone do not display the ability to activate their target enhancers (MacKay et al., 2003; Xiao et al., 1991).

1.3 Subfamilies of the Vestigial-like Transcription co-factors

Two subfamilies of Vestigial-like genes have been identified. This division is based on the number of TONDU domains encoded. The first subfamily, of which *vg* is a member, contains only one TONDU domain; the second family is comprised of genes with >1 TONDU domain (**Figure 1.2**). These subfamilies may have arisen at separate points over evolution (Simon et al., 2016), as genes of the second subfamily are present in a wider range of species compared to a more restricted subset of species with genes identified as members of the single TONDU domain subfamily (Koontz et al., 2013). Historically, the VGLL family has undergone a series of gene renaming events as previously named genes were discovered to be homologues or orthologues to each other. Initially, VGLL1 was named in mice as *vrf-1* and *TONDU* in humans; VGLL2 was named *VITO-1* or *Vgl-2* in both mice and humans; VGLL3 was named *VITO-1b* or *VITO-2* in both mice and humans, followed with a shift to *Vgl-3*; and VGLL4 was named *Vgl-4* in both mice and humans (Chen et al., 2004a; Chen et al., 2004b; Günther et al., 2004; Mann et al., 2007;

Mielcarek et al., 2002). As functional and sequential homology was clarified both experimentally and bioinformatically, gene names were modified to the sequential *VGLL* standard to reduce confusion in the mammalian system and comply with the HUGO Gene Nomenclature Committee. *Drosophila* gene nomenclature has not adopted this system for the *VGLL* family, likely owing in part to historical continuity and in part to the incongruent number of mammalian orthologues to *vg*.

Identification of other Vestigial-like family proteins outside *Drosophila* resulted from a series of experiments showing that the human TEAD1 protein, a Sd homologue, was able to bind Vg and functionally substitute for it during development (Deshpande et al., 1997). This lead to a search for Vestigial-like family binding partners in humans and other species. In humans, four *Vestigial-like* genes were identified (Chen et al., 2004a; Maeda et al., 2002a; Vaudin et al., 1999) and named *VGLL1-4*. VGLL1-3 are paralogues with only a single TONDU domain, and show a high degree of conservation, while VGLL4 is relatively more divergent in comparison and has two TONDU domains. Mice also have 4 *VGLL* genes (Chen et al., 2004a; Halperin et al., 2013; Maeda et al., 2002a; Mielcarek et al., 2002), and follow a similar pattern to humans with VGLL1-3 having a single TONDU domain and VGLL4 having two. *Caenorhabditis elegans* is unique among the most common model organisms in that it has a single putative VGLL4 subfamily orthologue but no orthologue to Vg/VGLL1-3 (Simon et al., 2016). *Xenopus laevis* and *Danio rerio* both have five *VGLL* genes (Faucheux et al., 2010; Mann et al., 2007; Melvin et al., 2013). Unlike mice and humans, they retain the *VGLL1-3* genes with a single TONDU domain but have two highly similar VGLL4 paralogues (VGLL4 and VGLL4L), each with two TONDU domains, that likely resulted from a genome duplication event.

1.4 Expression Patterns of VGLLs in Drosophila and Other Model Systems

Drosophila vg has a highly restricted pattern of expression that stretches from mid-embryogenesis through to the adult fly. Vg expression is first apparent in stage 10 embryos as lateral stripes from the first thoracic to seventh abdominal segments. By stage 11, additional clusters in the second and third thoracic segments fated to become the wing and haltere imaginal discs form, as well as some expression in the presumptive ventral nerve cord (VNC; Williams et al., 1991). The Vg-positive cells of the VNC by stage 12 number approximately 10-12 cells per segment (Guss et al., 2008). At stage 13, expression of the mRNA transcript in the head region is apparent, as well as expression in a select group of embryonic muscles, namely the dorsal acute 1-3, lateral longitudinal 1 and ventral lateral 1-4 muscles (Baylies et al., 1998; Tixier et al., 2010; Williams et al., 1991). By stage 16, VNC cells in the thoracic segments expressing Vg have multiplied into 41-43 cells divided into dorsal and ventral subgroups, while cells in the abdominal segments are fewer in number. These cells go on to form a subset of interneurons, as well as three midline ventral unpaired motor neurons (Guss et al., 2008). The ventral clusters of proto-wing and -haltere disc cells continue to express Vg transcript in stages 16-17, and are maintained through hatching into the first instar larvae (Williams et al., 1991).

The larval expression pattern of Vg is complex and varies substantially through the larval stage. In the first and early second instar stages, Vg^{+} cells are present throughout the entire wing and haltere disc. By mid-second instar, the wing disc shows a slowly restricting pattern with loss in the distal portion of the disc (Williams et al., 1993). The third instar expression pattern has been

very well established, along with the cis-regulatory elements controlling it. Vg is expressed at a very low level throughout the disc, but is significantly concentrated along the dorsal/ventral (D/V) boundary as well as in the notum/presumptive wing hinge region (James and Bryant, 1981; Williams et al., 1993). This overlaps with the expression pattern of Sd in the wing disc, which also shows a gradient across the presumptive blade region with a peak at the D/V boundary (Campbell et al., 1992; Williams et al., 1993).

Very little is understood about the expression and regulation of Tgi within the developing embryo. It is ubiquitously expressed at a low level in larval wing and eye discs, as well as the entire adult carcass and the ovaries, as determined by RNA-FISH (Koontz et al., 2013); the embryonic expression pattern has yet to be fully determined. This contrasts to the very specific pattern of Vg, indicating that Tgi may not be an identity factor like Vg but instead have broader functions. It also overlaps with the previously described Sd expression pattern in the larval wing disc, although it is also expressed outside of the Sd domain as well. Whether this indicates other binding partners for Tgi is unknown, as no other interacting partners have been conclusively established.

The expression pattern of the mammalian VGLL genes has diversified from the *Drosophila* orthologues, partially due to the gain and loss of specific structures such as wings across the evolutionary tree. In humans, VGLL1 and VGLL3 are both expressed in the placenta, while VGLL2 seems to be restricted to skeletal muscle (Chen et al., 2004b; Maeda et al., 2002a; Mielcarek et al., 2002). VGLL4 expression is more diverse in terms of expression than the first

three VGLL genes, and is detectable in the brain, heart, skeletal muscle, colon, thymus, spleen, kidney, liver, small intestine, placenta and lung (Chen et al., 2004a).

Expression of VGLL genes in model systems other than *Drosophila* is not as well characterized as that of flies and humans. Mice express VGLL2 and VGLL3 in skeletal muscle and somites, while *Xenopus laevis* and *Danio rerio* share the VGLL2 somite expression although as yet have not been shown to have skeletal muscle expression (Faucheux et al., 2010; Maeda et al., 2002a; Mann et al., 2007; Mielcarek et al., 2002; Mielcarek et al., 2009). *VGLL2*$^{-/-}$ mice show a conversion from slow-twitch muscle fibres to fast twitch muscle fibres, but had no major developmental defects (Honda et al., 2017). VGLL4 has a common expression pattern in the mouse, frog and fish brain and lungs/pharyngeal pouches (Barrionuevo et al., 2014; Faucheux et al., 2010; Thisse et al., 2001; Zhang et al., 2014).

1.5 Scalloped and the TEAD Family Transcription Factors

Sd is a member of the TEAD transcription factor family and is the essential binding partner of Vg. The founding member of the family is the human TEAD1 protein, originally named TEF-1 and identified on the basis of its ability to bind and activate the SV40 enhancer (Xiao et al., 1991). Since then, a large number of related proteins have been identified in multiple species, including 4 in humans and mice (TEAD1-4) and one in *Drosophila* (Sd; Campbell et al., 1991; Campbell et al., 1992).

All known TEAD proteins have the same general domain architecture and conformation. The N-terminal of the protein contains the TEA/ATTS domain necessary for DNA binding, and conforms into a triple helical homeodomain-like fold (Anbanandam et al., 2006; Bürglin, 1991; Hwang et al., 1993). This domain is also able to interact with the Myocyte enhancer factor 2 (MEF2) via its MADS domain, which is a key regulatory step in muscle gene expression (Gupta et al., 2001; Maeda et al., 2002b). The C-terminal region, which binds to Sd co-factors like Vg and Yki, takes on a modified β-sandwich fold conformation with two extra helix-turn-helix inserts (Tian et al., 2010). As Sd lacks the ability to recruit the basal transcriptional machinery alone, this C-terminal region provides a platform for recruitment of co-factors that can then nucleate the transcriptional machinery (Xiao et al., 1991).

The target motif for TEAD proteins is known as the muscle-specific cytosine-adenine-thymidine (MCAT) motif. It was first identified in the promoter of the chicken cardiac troponin-T gene (Farrance et al., 1992; Mar and Ordahl, 1988). The MCAT motif is a heptameric sequence of 5'-CATTCCT-3', although there is substantial flexibility in the motif as the sequence of three MCAT elements in the SV40 enhancer do not conform exactly to the optimal sequence (Davidson et al., 1988; Larkin and Ordahl, 1999; Larkin et al., 1996; Stewart et al., 1994; Xiao et al., 1987). Interestingly, the targeting of Sd can be significantly impacted by its cognate co-factor, as binding of Sd and Vg causes a shift in motif grammar preference from a single MCAT element to a pair of side-by-side sequences requiring the coordination of two Sd and two Vg proteins in a four part complex (**Figure 1.1B**) (Halder and Carroll, 2001). It is unknown whether Tgi, with the potential to coordinate Sd proteins in a 1:2 ratio instead of the Vg:Sd 2:2 stoichiometry due to its paired TONDU domain structure, would have any impact on coordinate

gene regulation in the same fashion, or if this is an obligate heterotetramer for regulation of all target genes.

Throughout development, the expression of *sd* is spread across multiple different tissue types. During embryogenesis, *sd* is expressed in the central and peripheral nervous systems beginning at stage 10, approximately 4h40 after the egg is laid (AEL), and continues through at least the beginning of stage 14 (10h20 AEL) (Guss et al., 2013). Expression of Sd is detectable at the protein level in all somatic muscle cells at early stage 16 (13h AEL), although mRNA is detectable even earlier via *in situ* hybridization at stages 12-13 (7h20-10h20 AEL), where its expression progresses from the ventral to lateral regions (Deng et al., 2009; Guss et al., 2013). Sd is also a key transcription factor for cardiac development in the embryo, where interestingly its expression does not overlap with Vg but does overlap with Tgi (Deng et al., 2009; Yu et al., 2015). The structure of the embryonic heart differs in *Drosophila* when compared to mammals, as *Drosophila* does not have a closed circulatory system (Vanderploeg and Jacobs, 2017). Instead, cardiac muscle cells are surrounded by pericardial cells in a structure known as the dorsal vessel that acts as a single chamber heart with an aorta (reviewed in Ahmad, 2017). Sd expression is detectable in the heart muscle at stage 13 (9h20 AEL) but is entirely absent by stage 16 (13h AEL). Finally, Sd protein is also detectable in the embryonic wing and haltere primordia as well as myoblasts fated to become IFMs, both of which overlap with Vg expression (Bernard et al., 2003; Guss et al., 2013).

In the larva, *sd* expression has been well characterized in the wing and haltere discs. By the third instar, *sd* is expressed throughout the wing pouch as well as in aspects of the hinge and notum

(Campbell et al., 1992); this overlaps significantly with both Vg in the wing pouch as well as Tgi, which is expressed ubiquitously throughout the entire disc (Koontz et al., 2013). It is also expressed at relatively lower levels in both the leg and eye discs (Campbell et al., 1992; Guss et al., 2013). A subset of larval VNC cells also co-express *sd* and *vg*, the neuroblast 1-2 descendants as well as the ventral unpaired median motor neurons (Guss et al., 2008; Guss et al., 2013; Landgraf et al., 2003) although whether they also overlap with *Tgi* expression is as yet unclear. In the adult, *sd* is expressed along with *vg* in the flight muscles (Bernard et al., 2003; Bernard et al., 2009). It is also required for proper central nervous system development (Garg et al., 2007).

Sd was originally identified as a wing-specific protein, not a myogenic factor (Campbell et al., 1991; Campbell et al., 1992). Loss of *sd* expression results in poorly developed adult wings with phenotypes ranging from scalloping of the margins to a majority loss of the wing blade, depending on the degree of gene dysfunction or loss (Campbell et al., 1992). The partnership between Vg and Sd is required for later differentiation by driving expression of key fate specification genes including *cut* (*ct*), *knirps* (*kni*), and *senseless* (*sens*) (Blochlinger et al., 1991; Ludlow et al., 1996; Srivastava and Bell, 2003).

As inferred by the name of its target MCAT motif, Sd is a key transcription factor in myogenic fate specification. In *Drosophila*, Sd and Vg form a non-obligate tripartite complex with the muscle-defining transcription factor Mef2 to promote embryonic somatic muscle differentiation (Deng et al., 2009; Deng et al., 2010). Vg and Sd interaction is important at both the protein and DNA level, as Sd also acts as a scaffold for recruitment of p38 MAPK for Vg phosphorylation

that is necessary for proper late-stage muscle differentiation (Pimmett et al., 2017). This function is also conserved in humans and mice. Sd is also important for specification of the cardiac muscle program during embryogenesis. Much of the initial investigation into MCAT elements was performed on the chicken cardiac Troponin-C promoter (Mar and Ordahl, 1988; Mar et al., 1988; Stewart et al., 1994), and further research has shown both Sd and its mammalian orthologues are necessary in *Drosophila*, mice, and human cardiac muscle (Chen et al., 1994; Deng et al., 2009; Stewart et al., 1994; Stewart et al., 1998).

In mammals, the expansion of the TEAD family to four genes is reflected in a complex expression pattern extending from the earliest developmental stages through to adult tissues. TEAD1 and TEAD3 are detectable in unfertilized mouse oocytes, while TEAD2 mRNA is already apparent at the two cell stage (Kaneko et al., 1997). As the embryo develops, TEAD proteins are required for the trophectoderm to form, as well as cardiac and skeletal muscle, the notochord and neural crest cells (Anbanandam et al., 2006; Milewski et al., 2004; Qiu et al., 2011; Sawada et al., 2008; Yagi et al., 2007), indicating some conservation between *Drosophila* and mice in terms of expression. There is some degree of functional redundancy between TEAD1 and TEAD2 (Sawada et al., 2008), although a complete study of redundancy between the four genes has yet to be completed.

1.6 Development of the Adult Wing

Vg and Sd were both originally named based on the mutant phenotype in the adult *Drosophila* wing (Gruneberg, 1929; Morgan and Bridges, 1919). The system of wing development in

Drosophila has been used for examining developmental and homeostatic regulatory mechanisms due to several convenient or unique features. The adult *Drosophila* wing is derived from the embryonic ectoderm and is a highly stereotyped structure with precise architecture and well-understood developmental processes. Although the wing is a complex structure, adult laboratory *Drosophila* strains do not require them for survival or reproduction. The wing is an ideal system for experimentation for several reasons: they are dispensable, easily manipulated with genetic tools, widely studied and provide an easily visible phenotype.

Imaginal discs are clusters of cells set aside during embryogenesis that are later used during the larval aspect of the life cycle to develop into specific adult structures (**Figure 1.3**). There is a total of 19 imaginal discs in the *Drosophila* larvae: bilateral pairs of clyprolabral, labral, eye-antenna, dorsal prothoracic, wing, haltere, and first, second and third leg discs, along with a single genital disc.

The larval wing disc is largely comprised of a columnar epithelial monolayer that will go on to form much of the adult wing, along with a small population of myoblasts and few tracheal and neural cells. It is bordered by a peripodial membrane of squamous cells that contributes very little to the adult wing. The larval wing disc is an excellent model for fate acquisition and implementation, as the epithelial monolayer is easy to image both in terms of gross structure as well as individual cell dynamics across development. The adult wing is also easily examined for defects with low-power magnification and is generally dispensable for most aspects of the adult lifecycle.

Tissue patterning, the process of defining regions of presumptive fate from a cellular field to generate complex structures, begins early in the embryo. The wing disc is specified during embryogenesis at the intersection of stripes of Wg and Decapentaplegic (Dpp) expression in the ectoderm, positioned dorsally to the leg disc in the second thoracic compartment (Cohen et al., 1993). Initial isolation of wing progenitor cells comes from a small cluster of approximately 22-24 ectodermal cells marked by Vg expression on each side of the T2 segment of the embryo (Bate and Arias, 1991; Cohen et al., 1993; Meise and Janning, 1993). At 9-10h AEL, the presumptive wing cells begin to invaginate from the ectoderm in the ventral half of the embryo. By stage 15 of embryogenesis, approximately 11.5-13h AEL, the presumptive wing cells can be identified by expression of Vg protein (Cohen et al., 1993). As the egg hatches into the first instar larva at approximately 24h AEL, the wing imaginal disc is comprised of 38 cells (Madhavan and Schneiderman, 1977). These cells begin to rapidly proliferate halfway through the first instar stage and continue through the second and third instar until the late third instar disc is approximately 50 000 cells (Martin, 1982).

One of the challenges of using the larval wing disc as a model is the patterning of a three-dimensional adult structure on a two-dimensional plane. The wing disc is defined by radial patterning, where the centre of the disc comprises the wing blade and the more proximal adult structures such as the hinge and notum are organized at the periphery of the disc (**Figure 1.4**). The initial signals that control patterning in the wing disc define the boundary between the wing and notum/body wall regions. This is accomplished by induction of *wingless* (*wg*) expression during the second instar larval stage (Garcia-Bellido et al., 1973; Morata and Lawrence, 1977), which separates the tissue into wg^+ presumptive wing cells and wg^- notum cells. *wg* is considered

the hierarchical master of wing fate, as complete loss of *wg* expression results in a fate transformation of the entire wing into notum (Morata and Lawrence, 1977), while ectopic expression causes the notum to become a wing (Ng et al., 1996).

To further refine a future wing blade/pouch region separate from the hinge, the disc must be able to coordinate two separate organizing centres at the anterior/posterior (A/P) boundary and the dorsal/ventral (D/V) boundary. While the precise mechanism behind these organizing centres is unclear, the A/P boundary is established first, demarcated by *engrailed* (*en*) expression in the posterior compartment. Subsequently, the D/V boundary is established via expression of the dorsal-specific protein *apterous* (*ap*), which can be seen in the first instar larval wing disc (Nienhaus et al., 2012).

The formation of the D/V boundary by *ap* drives the expression of the Notch (*N*) pathway ligands *delta* (*Dl*) and *serrate* (*ser*), as well as the effector *fringe* (*fng*) specifically at the D/V boundary (Diaz-Benjumea and Cohen, 1993; Klein and Martinez Arias, 1998; Williams et al., 1994). As Notch signaling is cell-cell contact-mediated, this activation is restricted to a small region that overlaps with the ventrally-restricted expression of *wg*. *N* and *wg* together activate the expression of *vg* via Suppressor of Hairless (*Su(H)*) activation of the *vg* margin enhancer (*vgME*) (Kim et al., 1996). Vg is a transcriptional co-factor and the key wing blade identity gene in the wing disc, as misexpression of Vg in other non-wing tissues causes a fate conversion to wing (Simmonds et al., 1998), and its expression eventually marks all cells of wing blade fate. *vg* expression driven by the *vgME* at the D/V boundary overlaps with a region of high *sd*

expression, the partner transcription factor necessary for Vg activity (Guss et al., 2013; Simmonds et al., 1998; Williams et al., 1991).

Activation of the *vgME* drives the initiation of a feed-forward circuit of Vg auto-activation (Klein and Martinez Arias, 1999). Vg and Wg expression from the D/V boundary, as well as expression of Dpp from a stripe at the A/P boundary, collaborate to activate a second *vg* regulatory element, the quadrant enhancer (*vgQE*), during the third larval instar (Zecca and Struhl, 2007a), that activates an as-yet unknown signal to expand the presumptive wing pouch (**Figure 1.5**). Both the *vgME* and the *vgQE* are self-reinforcing; expression of exogenous Vg causes activation of both enhancers *in vivo*, and the TEA domain of Sd has been shown to bind directly to DNA sequences within the *vgQE* (Halder et al., 1998). Wg and Dpp are diffusible morphogens, the combination of these two signals as well as the unknown Vg-responsive element allows for the non-autonomous expansion of Vg expression (Kim et al., 1997; Zecca and Struhl, 2007b; Zecca et al., 1995). It has been proposed that the Hippo pathway may partially mediate the unknown Vg-responsive factor (Zecca and Struhl, 2007b), as high Vg expression drives expression of the Hippo pathway gene *four-jointed* (*fj*) and represses *Dachsous* (*Ds*) (Cho and Irvine, 2004; Zecca and Struhl, 2010). The inverse gradients of Fj and Ds enable a high level of *yorkie* (*yki*) expression at the interface. Yki is a transcriptional co-regulator that also functions through Sd at the wing blade primordium (Goulev et al., 2008; Wu et al., 2008). Interestingly, Yki is known to compete with Vg for Sd interaction (Li et al., 2015a). Ectopic expression of Vg may then cause a titration of Sd away from Yki to bind Vg, shifting the balance of proliferation versus differentiation signal and stopping the recruitment of cells into the wing blade, resulting in smaller adult wings.

Beyond the edges of the wing blade region is tissue fated to become the wing hinge. The hinge region is refined during the third instar larval stage by restricting expression of the key transcription factors *homothorax* (*hth*) and *teashirt* (*tsh*). Together Hth and Tsh repress the wing pouch fate by inhibition of the *vgQE* (Kim et al., 1996). Interestingly, although Hth and Tsh inhibit Vg expression, there is still a non-autonomous requirement for Vg and Sd in hinge development that is unclear (Liu et al., 2000).

1.7 Vestigial-like Genes and Cancer

vg and its related orthologues are involved in cancers of several different tissue origins. Upregulation of *VGLL1* is noted specifically in triple negative-like basal breast carcinoma of both sporadic and hereditary *BRCA1* mutation origins, and is associated with reduced patient survival (Castilla et al., 2014). *VGLL2* fusion events are strongly associated with spindle cell rhabdomyosarcoma (SRMS) in children, particularly with the *CITED2* and *NCOA2* genes; a small study indicated 7 of 11 SRMS cases had *VGLL2* fusions or mutations (Alaggio et al., 2016). The same study also found of the remaining three cases, two of them had *TEAD1* fusion events; this presents a strong case for a causative relationship between a *TEAD* and *VGLL* complex with SRMS.

Of the *vg/VGLL1-3* subfamily of Vestigial-like genes, *VGLL3* has been more extensively studied across a range of cancers. In several types soft tissue sarcomas, including undifferentiated sarcomas, pleiomorphic rhabdomyosarcoma, dedifferentiated and well-differentiated

liposarcomas, and leiomyosarcoma, *VGLL3* is amplified and overexpressed along with another TEAD-binding protein and downstream Hippo pathway effector, the Yki orthologue *Yes-associated protein-1* (*YAP1*; Hélias-Rodzewicz et al., 2009). When *VGLL3* expression is knocked down in soft tissue sarcoma cell lines, cells display diminished proliferation and migration, suggesting that this amplification may play a role in invasion and metastasis (Hélias-Rodzewicz et al., 2009). This same amplification was also commonly noted in myxoinflammatory fibroblastic sarcoma and hemosiderotic fibrolipomatous tumours (Antonescu et al., 2011; Hélias-Rodzewicz et al., 2009). Conversely in epithelial ovarian cancer, *VGLL3* expression may function as a tumor suppressor. Low to absent expression of *VGLL3* was identified in malignant tumor biopsies compared to healthy controls and benign tumor samples, and expression of *VGLL3* in OV-90 human ovarian cancer cells is significantly diminished (Cody et al., 2009; Gambaro et al., 2013). Coincident with its role in ovarian cancer, *VGLL3* has also been implicated in female-biased autoimmune disorders where genes regulated by *VGLL3* were strongly associated with diseases such as lupus, Sjögren's syndrome, and scleroderma (Liang et al., 2016). Prostate cancer is associated with a *VGLL3* oncogenic signature, where low expression of *VGLL3* along with *IGFBP3* and *F3* in prostate cancer biopsies correlate to an aggressive form with a median survival time of 3.23 years, and relatively higher expression of all three genes correlated to a less aggressive prostate cancer with a median survival time of 9.85 years (Peng et al., 2014).

Tgi/VGLL4 subfamily genes are broadly considered tumor suppressors and have had the most progress made with pharmacologic interventions for various types of cancer out of all the Vestigial-like genes. A mutagenesis screen in mice identified *VGLL4* mutation as a driver of

pancreatic cancer, and associated mutations in the human gene with significantly poorer survival (Mann et al., 2012). Subsequently *VGLL4* mutations or expression level changes were associated with gastric, lung, colorectal, and esophageal cancer (Jiang et al., 2015; Jiao et al., 2014; Jiao et al., 2017; Li et al., 2015; Zhang et al., 2014). Interference with YAP1-TEAD binding using a VGLL4-mimicking peptide however showed a protective and anti-proliferative effect in human MCG-803 gastric cancer cells as well as *in vivo* mouse gastric tumours (Jiao et al., 2014). This caused a reduction in YAP1-responsive gene expression, indicating a likely competitive inhibition of the YAP1-TEAD transcriptional complex, a theory borne out with several other studies (Liu-Chittenden et al., 2012; Zhang et al., 2014). This may be achieved both using pharmacologic disruption, as well as deubiquitination of the endogenous protein and VGLL4-mediated sequestration of Inhibitor of Apoptosis (IAP) family proteins in the cell nucleus (Jin et al., 2011; Zhang et al., 2016).

1.8 Cancer Stem Cell Hypothesis and Differentiation Therapy

One of the mysteries of cancer progression is how tumors are initiated and propagated within normal tissue. One theory building substantial evidence is the cancer stem cell (CSC) hypothesis. The CSC hypothesis states that tumors are heterogeneous in genotype, and a small pool of stem-like cells (CSCs) divide to produce daughter cells that make up the bulk of a tumor (Sell, 2004; Tannishtha et al., 2001). CSCs share many similarities with normal stem cells, in that they are a self-renewing population capable of asymmetric division to produce daughter cells that become a tumor mass, but differ from both typical stem cells and bulk tumor cells in that they have undergone an epithelial-to-mesenchymal (EMT) transition. They are also resistant to traditional

cancer therapeutics, through combinations of upregulated DNA damage responses, infrequent cell cycling, improved drug efflux, and better resistance to reactive oxygen species (Ffrench et al., 2017; Kurtova et al., 2015; Somasagara et al., 2017; Song et al., 2017; Wu et al., 2017). Because they can divide asymmetrically, CSC daughter cells are able to undergo rapid proliferation and generate a cancerous mass without compromising the integrity of the CSCs themselves, which can remain resident in tissue even after traditional cancer treatments halt or remove the tumor itself (Kreso et al., 2013). The quiescence and reduced vulnerability to traditional therapeutics means that CSCs may remain to induce relapse in patients.

One of the hallmarks of CSCs is the mis-activation of developmental signaling pathways such as the Wnt, Hippo and Notch pathways (Clevers, 2011; Tannishtha et al., 2001). During development, activation of the Wnt pathway is required for promoting cell division in multiple tissues (Giraldez and Cohen, 2003; Heallen et al., 2011; Hu et al., 2004; Reya et al., 2003); re-activation of this pathway is a key component of proliferation in several types of cancers, and attenuation of its activity is able to significantly diminish the hyperproliferative phenotype of cancer cells *in vitro* (Kansara et al., 2009; Ordóñez-Morán et al., 2015; Wang et al., 2015). Similarly, the Hippo signaling pathway is key in organ size specification and terminal differentiation by repressing cell division and permitting apoptosis (Boone et al., 2016; Lee et al., 2010; Peng et al., 2009; Shen et al., 2015). Dysregulation of this pathway is prevalent in several cancers, including gastric cancer, breast cancer, and lung cancer, and is frequently associated with poorer prognosis (Jang et al., 2017; Lamar et al., 2012; Zhang et al., 2014).

Cancers associated with changes in VGLL family gene expression or function link several of the traits of the CSC hypothesis. Two recent studies have examined the broader Hippo signaling pathway and disruption of the VGLL-TEAD interaction as a potential therapeutic target for differentiation therapy. The initial study done in a mouse cancer model (Jiao et al., 2014) showed that injection of a VGLL4-mimicking peptide caused a strong inhibition of tumor growth both *in vivo* and *in vitro* using gastric cancer cell culture models when compared to the control by preventing the interaction between YAP and TEAD4, and that this inhibition is mediated through the TDU domains of VGLL4 necessary for interaction with TEAD family proteins. This inhibition was also extended to include a range of *in vivo* induced tumors, including HeLa, HCT116, A549, MGC-803 and MCF-7 derived masses, and that the degree of tumor growth inhibition correlated to the expression profile of VGLL4 in the original cell line. The second study (Jiao et al., 2017) presented a significant downregulation of VGLL4 in clinical colorectal cancer cells, and this loss of expression was associated with poorer prognosis and shorter patient survival time. However, colorectal carcinoma disease progression was significantly inhibited in mice treated with a VGLL4-mimicking peptide, likely due to disrupting a TEAD4-TCF4 complex that would otherwise co-regulate both the Hippo and Wnt signaling pathways. Both studies indicated that cells treated with the VGLL4-mimicking peptide lost traits associated with the CSC phenotype; cells had a lower proliferation rate, became less motile, and were more susceptible to apoptosis. Conversely, overexpression of VGLL4 in human embryonic stem cells causes a significant decrease in cell death and increase in colony formation from dissociated single cells in culture (Tajonar et al., 2013).

Because of the intrinsic complexity and crosstalk between the Hippo signaling pathway and other pathways, directly targeting upstream components of the pathway to force differentiation of cancer cells is likely not feasible. However, because the Vestigial-like family is a known downstream regulator of TEAD family transcription factors with few other regulatory partners, and because interfering with the VGLL-TEAD interaction has already been shown to promote various outcomes mentioned above that indicate differentiation therapy is a viable option, investigating further the link between VGLLs and TEADs is a necessary component of developing potential targeted therapies such as the VGLL4-mimicking peptide discussed above. Relative levels of TEAD and VGLL proteins have also shown some prognostic value, which could also lead to better molecular diagnostic methodologies as well as improving treatment selection for patients. By understanding the link between VGLLs and developmental programming, it will be possible to develop future strategies to understand and treat several types of human diseases.

1.9 Summary

In this thesis, I establish the role of Vg phosphorylation in regulating development of the adult *Drosophila* wing and embryonic somatic musculature (Pimmett et al., 2017). Vg is phosphorylated by p38 MAPK on Ser-215, and this phosphorylation is dependent on the presence of Sd. Vg phosphorylation affects anterior/posterior fate specification in the developing wing disc and altering phosphorylation via a non-phosphorylatable or a phosphomimetic mutant results in mis-specification of the anterior and posterior margins respectively.

Further, the role of the recently identified second VGLL family gene in *Drosophila*, *Tgi*, was examined. Tgi has substantial regions of homology to human VGLL4 as well as other model system orthologues, particularly in the TONDU domain sequences. I propose a competitive model to describe interactions between the Vestigial-like proteins and Sd, as even though Tgi and Vg are able to co-immunoprecipitate with Sd, they do not form complexes together. Overexpression of Tgi in the Vg domain causes a decrease in wing surface area and wing cupping from loss of ventral cells that is dependent on the relative level of Vg expression. Expression of Tgi also causes nuclear exclusion of Vg in live *Drosophila* Kc167 cells, and both developmentally- and cell cycle-related target genes of Sd are cross-regulated when Sd is overexpressed with either Vg or Tgi. Finally, I propose some potential mechanisms for how a competitive binding model may be implemented at the cellular level.

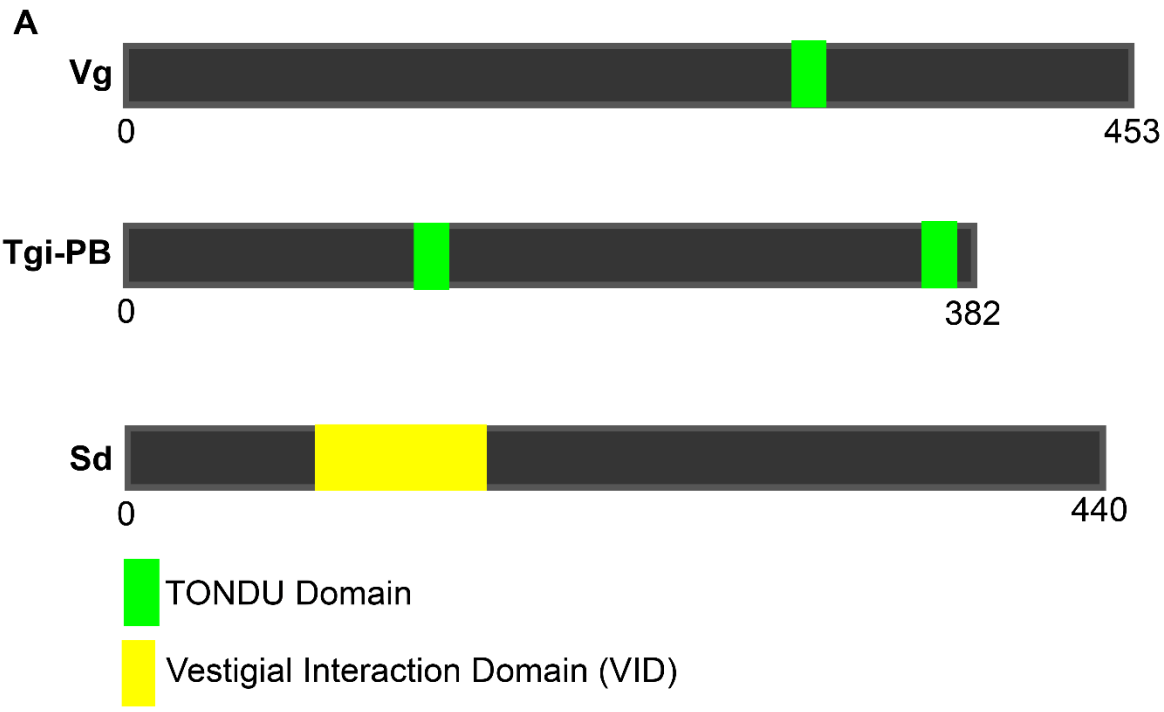
A
Vg
0
453
Tgi-PB
0
382
Sd
0
440
TONDU Domain
Vestigial Interaction Domain (VID)

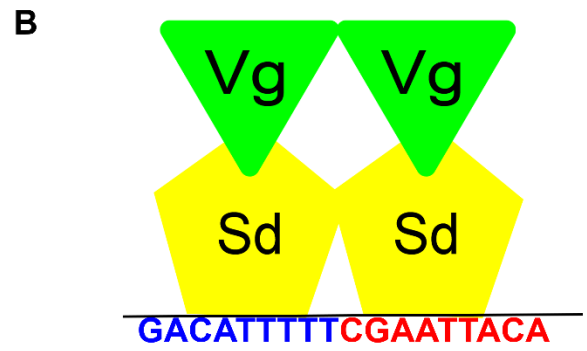
B
Vg
Vg
Sd
Sd
GACATTTTTCGAATTACA

Figure 1.1: A diagram of the *Drosophila* VGLL and TEAD family proteins. A) Vg and Tgi contain a common TONDU domain (green), although Vg has a single domain while two are present in Tgi. Sd has a single Vestigial Interaction Domain, or VID (yellow). B) The coordinate heterotetrameric binding of Vg and Tgi to the *cut* promoter requires the coordination of two Vg and two Sd proteins. The binding sequences of Sd (Guss et al., 2001) are shown for each protein in blue and red. Note that there is divergence from the canonical MCAT motif.

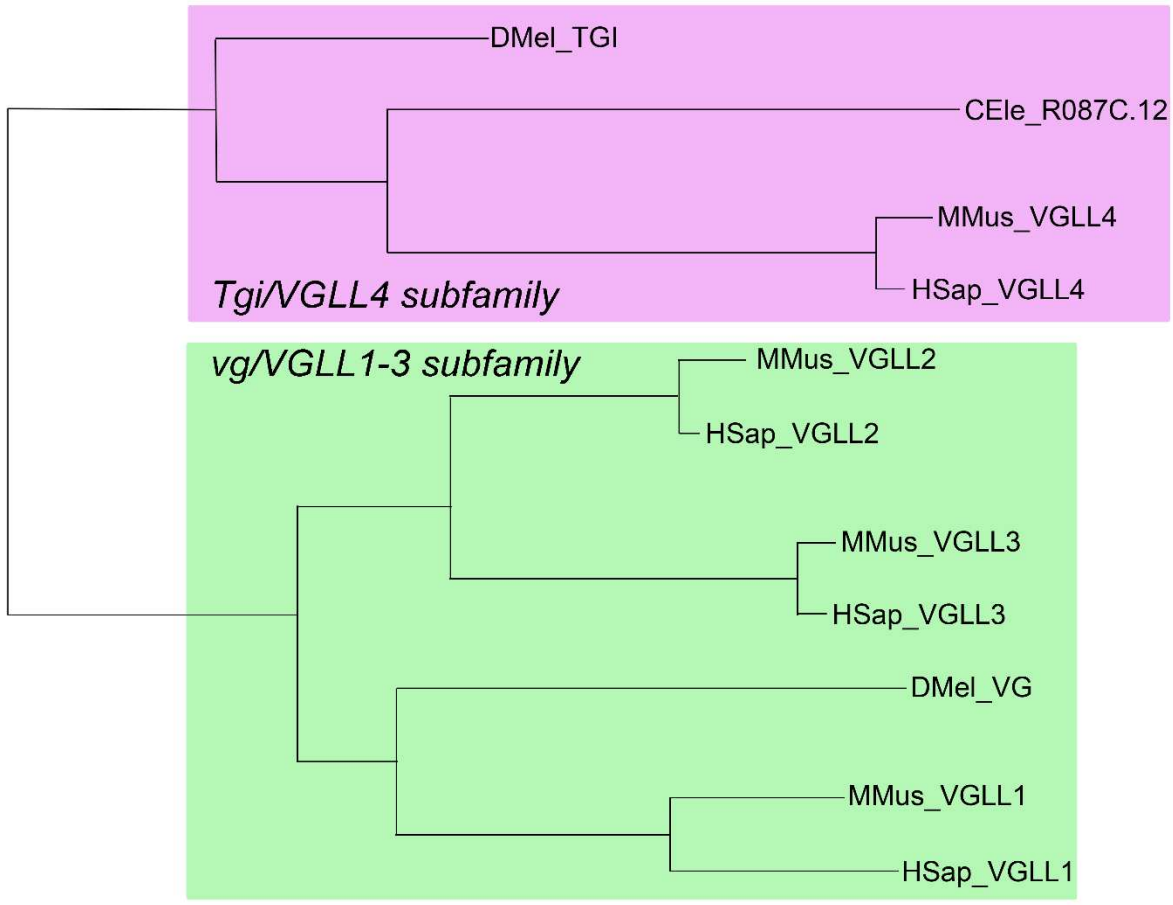
DMel_TGI
CEle_R087C.12
MMus_VGLL4
HSap_VGLL4
Tgi/VGLL4 subfamily
vg/VGLL1-3 subfamily
MMus_VGLL2
HSap_VGLL2
MMus_VGLL3
HSap_VGLL3
DMel_VG
MMus_VGLL1
HSap_VGLL1

Figure 1.2: A phylogenetic tree showing the evolution of the human (HSap), mouse (MMus), *Drosophila* (DMel) and *C. elegans* (CEle) VGLL family proteins. The Tgi/VGLL4 subfamily is clustered in the upper portion, while the Vg/VGLL1-3 family clusters as a collective subfamily in the lower portion. The phylogenetic tree was constructed using BIONJ (Gascuel, 1997).

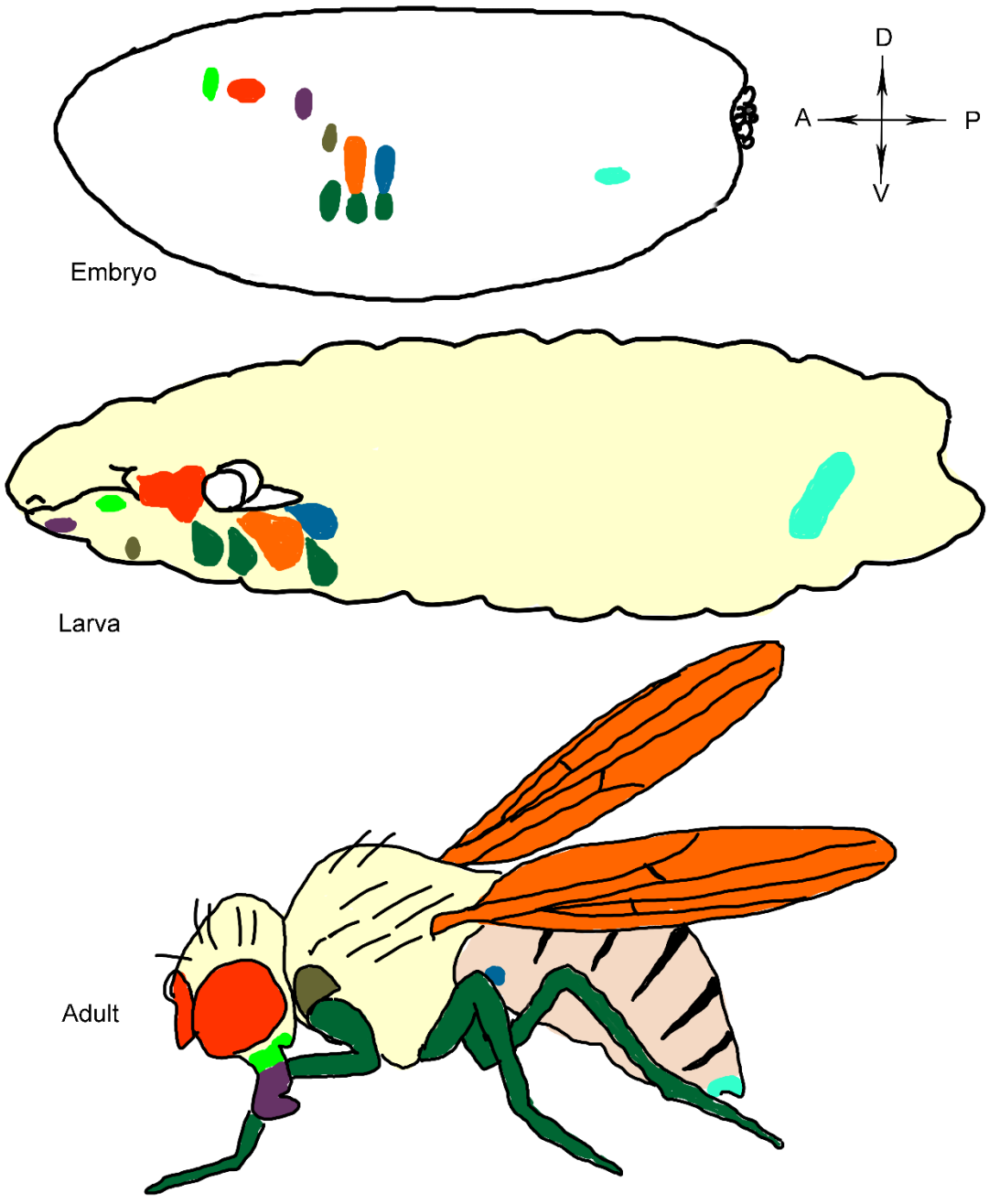
D
A
P
V
Embryo
Larva
Adult

Figure 1.3: Adult structures in *Drosophila* are specified during embryogenesis. Clusters of cells in the embryo are fated to become specific adult structures and set aside for later expansion during the larval stage. After hatching, larvae undergo rapid cell proliferation and further specification of adult structures in cell clusters called imaginal discs. During pupariation, these discs further expand and differentiate to form the adult structures. Adult structure colours are represented in the larvae and embryo. Cell clusters fated to become wings are labelled in orange. Original design from Beira and Paro, 2016.

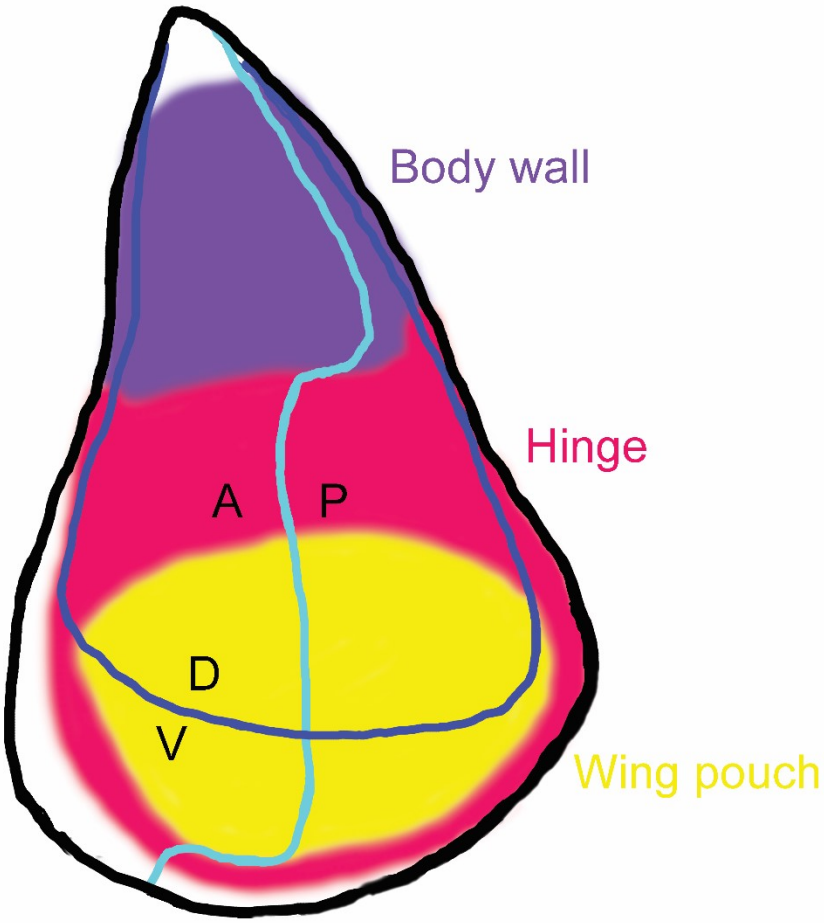
Body wall
Hinge
A
P
D
V
Wing pouch

Figure 1.4: The third instar larval wing imaginal disc is specified in fields. The body wall adjoins the fly thorax (purple). The hinge forms a flexible structure necessary for flight (pink). The wing pouch becomes the blade of the adult wing (yellow). The anterior/posterior boundary is demarcated in light blue and the dorsal/ventral boundary in dark blue.

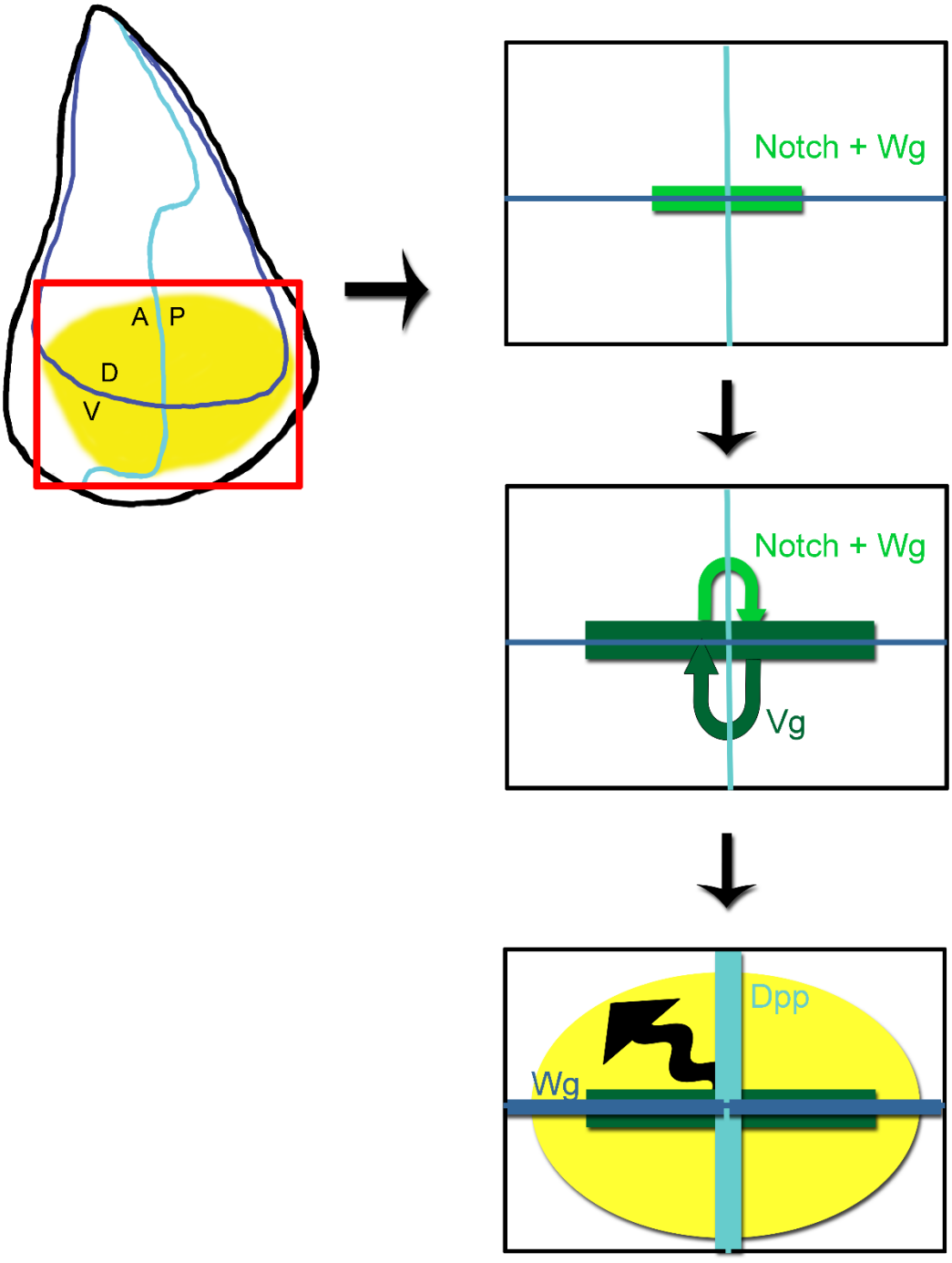
A
P
D
V
Notch + Wg
Notch + Wg
Vg
Dpp
Wg

Figure 1.5: Enhancers of *vestigial* in the wing pouch (yellow) form a feed-forward circuit. Induction of Notch and wingless signalling at the nexus of the dorsal/ventral and anterior/posterior boundary induces expression of *vg* at the *vgME*. Vg, N and Wg synergistically reinforce the expression of *vg* at the *vgME*. *vg* also combines with the expression of *wg* from the dorsal/ventral boundary and *decapentaplegic* at the anterior/posterior boundary as well as unknown factors to expand the domain of *vg* expression by auto-activation of the *vgQE*. This domain expands to define the complete wing pouch region.

Chapter 2: Phosphorylation of Vestigial is Necessary for Proper Tissue Differentiation

Portions of this chapter were previously published as:

Pimmett, V. L., Deng, H., Haskins, J. A., Mercier, R. J., LaPointe, P. and Simmonds, A. J. (2017). The activity of the Drosophila Vestigial protein is modified by Scalloped-dependent phosphorylation. *Dev. Biol.* **425**, 58–69.

2.1 Introduction

Drosophila tissue development is a complex process relying on the activity of "selector genes" at specific points in defined sub-populations of cells that narrow the fate of a group of cells from a broad, general fate to a specific identity that is then maintained throughout development (Hariharan, 2015). Selector genes most frequently encode transcriptional regulators such as transcription factors and co-factors that stipulate fate by driving a specific program of target gene expression resulting in terminal differentiation of the tissue. *vg* is a key selector gene involved in differentiation of the wing blade from the wing imaginal disc (Williams et al., 1991; Williams et al., 1994). *vg* is necessary for both specification and proliferation in the larval imaginal wing disc, as homozygous loss of the gene causes a complete absence of the adult wing, variable loss of wing structure with hypomorphic alleles dependent on the strength of the hypomorph, and transdifferentiation of non-wing ectoderm into a wing fate when the gene is expressed ectopically (Green, 1945; Kim et al., 1996; Silber, 1980; Simmonds et al., 1997; Simmonds et al., 1998; Williams et al., 1991).

More recently, the functional importance of *vg* has been demonstrated in tissues outside the wing. In the developing embryonic mesoderm, Vg acts as a regulator of late stage muscle differentiation. Loss of *vg* causes a weakened muscle phenotype in the embryo, with poor attachment of the muscle to tendon cells and absence of ventral lateral (VL) muscles (Deng et al., 2009; Deng et al., 2010). In the adult, Notch-dependent Vg expression is also required for correct specification of the adult indirect flight muscles (IFMs). Reduction of Vg via hemizygous vg^{null} allele expression causes a fate transition to a direct flight muscle (DFM)-like fate and apoptotic degradation of the muscle fibre (Bernard et al., 2003; Bernard et al., 2009).

One of the mechanisms found to control protein function and activity is post-translational modification of the existing peptide. There are a large variety of post-translational modifications that have been identified so far and with wide-ranging effects. These modifications include attachment of macromolecular structures such as carbohydrate moieties via glycosylation, lipid groups by cholesterylation, and covalent linkage of small peptides by sumoylation (Ciepla et al., 2015; Monribot-Villanueva et al., 2017; Smith et al., 2012; Walski et al., 2017). Also common and important to cellular function and proper tissue development are phosphorylation or dephosphorylation of target proteins (Oliva and Hassan, 2017; Zhao et al., 2017).

Many of the kinases present in *Drosophila* are conserved in humans and other mammals, including but not limited to cyclin-dependent kinases (CDKs), mitogen-activated protein kinases(MAPKs), and receptor tyrosine kinases (RTKs) (Ashton-Beaucage and Therrien, 2017; Fry et al., 2017; Ishidate et al., 2014; Morrison et al., 2000). The p38 MAPK signaling pathway is required for the development of the wing through regulation of the Transforming Growth

Factor-β/Decapentaplegic (TGF-β/DPP) pathway downstream of the receptor *thickvein* (*tkv*) (Adachi-Yamada et al., 1999). Further, increasing the activity of Tkv by ectopic expression of a constitutively active mutant increased the levels of active p38, and blocking the activity of p38 attenuated the phenotype in the adult wing caused by ectopic constitutively active Tkv (Adachi-Yamada et al., 1999). p38 MAPK also regulates the Activating transcription factor-2 (ATF-2) protein; while ectopic expression of a dominant negative p38b allele using the *MS1096*-GAL4 driver had no effect on wing size or shape, ectopic expression of a dominant negative ATF-2 in the wing disc using the same driver resulted in smaller wings with disrupted veins, and the phenotype was enhanced by co-expression of the dominant negative p38 allele (Sano et al., 2005).

Another signaling pathway that relies on phosphorylation to regulate its activity is the Hippo signaling pathway (**Figure 2.1**). The core of the Hippo signaling pathway is comprised of a kinase cascade that relies on the phosphorylation status of Yki to direct target gene expression (reviewed in Pfleger, 2017). When the signaling pathway is inactive, Yki is phosphorylated on Serine 168 and either sequestered in the cytoplasm by the 14-3-3 protein or targeted for degradation (Oh and Irvine, 2008; Pfleger, 2017; Ren et al., 2010). Activation of the pathway results in formation of a Yki/Sd nuclear complex that can activate transcription of target genes (Wu et al., 2008; Zhang et al., 2008). One of the most studied roles of Sd is as an effector transcription factor for the Hippo signaling pathway (reviewed in Lin et al., 2017b; Wu et al., 2008; Zhang et al., 2008). Sd and TEAD1-4 have recently been identified to be a target of active regulation by post-translational modification as well (Lin et al., 2017b). TEAD1 is targeted in cardiomyocytes and choriocarcinoma cells by both Protein Kinase A and Protein Kinase C

respectively for phosphorylation, both of which have functional consequences for protein function and gene expression (Gupta et al., 2000; Jiang et al., 2001). TEAD1, TEAD2, TEAD3, and TEAD4 as well as Sd are lipidated through addition of a palmitoyl group to a conserved cysteine residue (Chan et al., 2016; Noland et al., 2016). Surprisingly, palmitoylation of TEAD1 was required for interaction with the Yki orthologues YAP1 and *Transcriptional coactivator with PDZ-binding motif* (TAZ), but not for TEAD1/VGLL4 binding (Chan et al., 2016).

The VGLL family proteins are also modified post-translationally. Vg is a known target of sumoylation, and although the specific residue where the SUMO covalent linkage is made is unclear, blocking this by downregulation of the E3 ligase Ubc9 reduces Vg-dependent activation of a *vgQE* luciferase reporter in S2 cells (Takanaka and Courey, 2005). Sumoylation of transcription factors is strongly increased relative to the general protein pool in human cells (Filtz et al., 2014). Paradoxically, sumoylation is associated with both increased transcriptional repression by some transcription factors and chromatin-associated proteins, and increased transcriptional activation by others, as evidenced by the necessity of sumoylation on DNMT1 for DNA methylation and condensation of heterochromatin as well as the enhanced RNA polymerase II recruitment to constitutively active promoters with sumoylated proteins (Cubeñas-Potts and Matunis, 2013; Lee and Muller, 2009; Rosonina et al., 2010).

In the mammalian VGLL family, there is some evidence that VGLL2 is phosphorylated by casein kinase II on Ser-96 (Teng et al., 2008), but the functional relevance of this is unknown. VGLL4 is acetylated on Lys-224 in the first TONDU domain, although this residue is not conserved in *Drosophila* (Lin et al., 2016). Importantly, this acetylation reduces the ability of

VGLL4 to interact with TEAD1 in cardiomyocytes, and blockage of VGLL4 acetylation by mutation decreases cardiomyocyte proliferation *in vivo* (Lin et al., 2016). VGLL4 is also phosphorylated by cyclin-dependent kinase 1, and is a target of the de-ubiquitinating enzyme Ubiquitin-specific protease 11 which interacts with VGLL4 at the amino terminus and stabilizes the protein (Zeng et al., 2017; Zhang et al., 2016).

In this chapter, evidence is provided for Vg post-translational modification via Ser-215 phosphorylation. This residue is a possible target of p38 MAPK, and its phosphorylation is dependent on interaction between Vg and Sd. *In vivo*, both pseudo-phosphorylation and phosphorylation blockage at this residue result in fate changes in the adult wing. The requirement for Vg phosphorylation is partially maintained in the embryonic muscle, demonstrating both the similarities and differences inherent in repurposing of transcriptional regulators across different germ layers and tissues.

2.2 Results

Vestigial is Phosphorylated on Serine 215

Seven deletion mutants were made within Vg, each removing approximately 50 amino acids and leaving the TONDU domain intact (VgΔ1- VgΔ7, **Figure 2.2**). These were transfected into *Drosophila* Schneider-2 (S2) cells, both with and without the presence of Sd. Western blots of these lysates showed that in most cases, co-transfection of the Vg deletion mutant with Sd resulted in higher molecular weight bands (Pimmett et al., 2017). However, the VgΔ5 mutant had only a single band both with and without co-transfection of Sd (Pimmett et al., 2017). Within the VgΔ5 region, there are 11 serine, 2 threonine and 1 lysine residue, with a consensus MAPK site at Serine-215 (S215) (**Figure 2.3A**). Analysis of both the full-length Vg peptide (**Figure 2.3B**) as well as the VgΔ5 deletion region (**Figure 2.3C**) by kinase prediction software indicated that S215 was the most likely target for phosphorylation and was a likely target of the MAPK pathway. Mutagenesis of S215 to either the non-phosphorylatable alanine (Vg^{S215A}) or the pseudo-phosphorylated glutamic acid (Vg^{S215E}) followed with co-transfection in S2 cells with Sd showed that the Vg^{S215A} mutant was unable to recapitulate the higher molecular weight bands of wild type Vg, while the Vg^{S215E} mutant showed increased post-translational modification consistent with the wild type Vg (**Figure 2.3D**).

To confirm the effect of co-expression of Sd on Vg post-translational modification, two-dimensional gel electrophoresis followed by immunoblotting was performed on transiently transfected S2 cell lysates and probed with anti-Vg antibody. Lysates of 6xMyc-Vg transfected

cells resolved into three distinct isoforms with the same molecular mass but different isoelectric points (**Figure 2.4A**). Treatment of 6xMyc-Vg lysate with λ-phosphatase caused a collapse of isoforms into one single position with the same predicted size and isoelectric point of unmodified Vg (**Figure 2.4B**). Co-transfection with 6xMyc-Vg and GFP-Sd (**Figure 2.4C**) resulted in the three same molecular weight isoforms with different isoelectric points as in **Figure 2.4A**. Similarly to Figure 2.3B, treatment of the co-transfected lysate with λ-phosphatase also caused a collapse of isoforms into a single point (**Figure 2.4D**). Analysis of the relative proportions of each of the three positions showed that co-transfection with 6xMyc-Vg and GFP-Sd caused an increase in phosphorylated Vg isoforms compared to 6xMyc-Vg lysate alone (**Figure 2.4E**). The same results were shown using an anti-Myc antibody (not shown). Since λ-phosphatase treatment reduced both single transfected and co-transfected Vg to a single point, sumoylation of Vg (Takanaka and Courey, 2005) was examined via co-transfection with 3xFLAG-SUMO (**Figure 2.4F**). Interestingly, all Vg isoforms seem to be relatively equally sumoylated, indicating that the pool of un-sumoylated Vg is below the detection limit of a two-dimensional Western blot.

Phosphorylation of Vestigial affects wing development

To investigate whether S215 phosphorylation affects Vg function, we developed transgenic *Drosophila* expressing either a 3xHA-Vg^{S215A} or 3xHA-Vg^{S215E} transgene under the control of the UAS promoter. These transgenes were expressed using a synthetic GAL4 driver that contains two Vg enhancer elements, the *vgME* and *vgQE* (*vg(M+Q)*:GAL4). Together these enhancers recapitulates the majority of the *vg* expression pattern in the wing blade, with *vgME* driving

expression along the wing imaginal disc dorsal/ventral boundary during the third larval instar and *vgQE* driving expression in the wing pouch (**Figure 1.4**). During larval development, these enhancers are self-activated by Vg in a feed-forward loop to delineate wing fate across the entire blade region of the wing disc (Kim et al., 1996; Williams et al., 1994; Zecca and Struhl, 2007a).

Expression of either Vg^{S215A} or Vg^{S215E} in a wild type w^{1118} background alone had no phenotypic effect on the adult wing (data not shown), indicating there was no dominant effect created by hyperphosphorylation or blocked phosphorylation at Vg^{S215}. A rescue experiment was designed to test the effect of altered Vg phosphorylation in the presence of insufficient endogenous Vg. The vg^{null} allele of Vg, a mutant allele derived from P-element mutagenesis with an eight exon deletion in the *vg* gene, is largely pupal lethal when homozygous, with a few adult escapers. These escapers have extremely reduced larval wing discs with adults having very small wings with no definable features relative to a wild type adult wing, suggesting a failure in differentiation, proliferation, or both (Delanoue et al., 2004; Paumard-Rigal et al., 1998). The homozygous vg^{null} phenotype can be rescued by expression of 3xHA-Vg under the control of the *Vg(M+Q)*:GAL4 driver (**Figure 2.5B**), although the wings are slightly diminished in size. Expression of the 3xHA-Vg^{S215A} transgene in the same conditions partially rescues the vg^{null} phenotype (**Figure 2.5C**), but shows clipping of the lateral wing margin that appears similar to the weak loss of function alleles of *sd* or *vg* (Campbell et al., 1992; Williams et al., 1991). The anterior margin of the wing also had partial loss of the sensory bristles, and patchy replacement by the finer bristles of the posterior margin (**Figure 2.5C'**). Conversely, rescue of the vg^{null} phenotype using 3xHA-Vg^{S215E} largely restored wing size as well as maintained anterior sensory bristle structure (**Figure 2.5D**), but instead showed partial duplication of the posterior bristles

(**Figure 2.5D'**). Collectively this indicates that phosphorylation of Vg is required to maintain anterior vs posterior margin identity. To ensure this was not a function of Vg expression levels, qPCR testing of wing discs indicated a similar level of Vg expression in all three rescue experiments (**Figure 2.5E**). The *vgQE* has been shown to be bound by and regulated by the Vg/Sd complex (Halder and Carroll, 2001; Halder et al., 1998) , so a dual-luciferase assay was performed in S2 cells to examine whether or not Vg phosphorylation affected the ability of Vg and Sd to regulate the *vgQE*. It showed that while wild type Vg and Sd could significantly upregulate the *vgQE* compared to Vg alone, the activation of the *vgQE* was attenuated when Vg^{S215A} or Vg^{S215E} was expressed with or without co-transfection with Sd (**Figure 2.5F**).

Sensory bristles in the adult wing are derived from sensory organ precursor (SOP) cells in the larval wing disc. These cells are located along the dorsal/ventral margin of the third instar wing disc. Subsets of these cells are identifiable by expression of the pro-neural Vg/Sd target genes *cut* (*ct*) and *achaete* (*ac*) (Skeath and Carroll, 1991; Skeath and Carroll, 1994). Specification of SOPs requires the expression of Sd (Morcillo et al., 1996; Srivastava and Bell, 2003) but as yet there is no functionally identified role for Vg in this process. To examine SOP cell specification, third instar larval wing discs from the wing rescue experiments were examined using anti-*ct*. In wild type wing discs, Ct^+ cells are expressed in a row along the dorsal/ventral margin in the wing pouch (**Figure 2.6A**). Expression of the 3xHA-Vg transgene using *vg(M+Q)*:GAL4 in a homozygous vg^{null} background causes restoration of the disc at a reduced size, along with reappearance of the Ct-positive cells along the margin (**Figure 2.6B**). The same rescue performed with the 3xHA-Vg^{S215A} transgene also results in restoration of the disc at a diminished size, but few Ct^+ cells are observed along the dorsal/ventral margin, consistent with the loss of

sensory bristles in the adult wing (**Figure 2.6C**). The expression pattern of the Vg transgene is also altered compared to other transgenes expressed from the same GAL4 driver. Cells immediately proximal to the dorsal/ventral margin are not Vg-positive (anti-HA), and there appears to be a reduced amount of Vg in the disc compared to wild type. This may indicate that non-phosphorylated Vg may be unable to activate the feed-forward mechanism required to sustain the enhancers driving GAL4 expression, or that the Vg^{S215A} protein is destabilized and targeted for degradation. Expression of 3xHA-Vg^{S215E} in the same rescue background is also able to restore the disc, and the number and position of Ct-positive cells is largely normal with occasional small gaps (**Figure 2.6D**). This collectively suggests that Vg phosphorylation has an effect on the ability to drive a pro-neural SOP cell fate and the ability to sustain the Vg margin enhancer (Halder et al., 1998), but not the Vg/Sd-mediated cell proliferation in the rest of the disc induced by the Vg quadrant enhancer (Zecca and Struhl, 2007a).

Embryonic muscle specification also required Vg phosphorylation at Ser-215

While best studied in the wing, Vg also plays a role in the specification of the embryonic somatic musculature. The *Drosophila* somatic musculature is comprised of a repeating pattern of 30 individual muscles per abdominal hemisegment, and is analogous to human skeletal muscle (**Figure 2.7**). This muscle pattern is maintained after hatching and through the larval stages (reviewed in Dobi et al., 2015). This provides an interesting context to study what aspects of Vg function are conserved between different tissues and germ layers, as the musculature is derived from the mesodermal layer instead of the ectoderm like wing tissue. The musculature also forms a stereotypical and regularly repeating pattern, making the observation of subtle or infrequent

phenotypes easier to examine (**Figure 2.8A**). As with the wing tissue, expression of either the 3xHA-Vg^{S215A} or 3xHA-Vg^{S215E} transgenes under the control of a muscle-specific Mef2:GAL4 driver caused no observable phenotypic differences in comparison to the wild type embryonic musculature.

Embryos that are homozygous for vg^{null} have significantly reduced viability, as well as muscle contraction defects, weak attachment between the myotubes and tendon cells, and occasional loss of the VL2 muscle (Deng et al., 2009). When the 3xHA-Vg^{S215A} transgene was expressed using the Mef2:GAL4 driver in a homozygous vg^{null} background (**Figure 2.8B**), partial rescue was achieved with weak attachments in the VL muscles and some muscles absent entirely (**Figure 2.8B'**). The ventral musculature also showed rounding defects (**Figure 2.8B"**). This is a similar phenotype to the *rhea*-sensitized vg^{null} embryo (Deng et al., 2010). *Rhea*-sensitized embryos are deficient in talin, a βPS integrin-interacting protein needed for interactions between the muscle and tendon cells (Brown et al., 2002). The vg^{null} allele shows defects in muscle-tendon interaction in a *rhea*-sensitized background, while expression of a Vg^{S215A} allele shows similar defects even without reduction of tailin, indicating a stronger phenotype than vg^{null} alone.

Expression of the 3xHA-Vg^{S215E} transgene using Mef2:GAL4 in the homozygous vg^{null} background also was able to rescue the vg^{null} phenotype to a substantially greater extent (**Figure 2.8C**). No significant rounding or detachment phenotypes (**Figure 2.8C', C"**) were present in the lateral or ventral musculature. This indicates collectively that phosphorylation of Vg is a requirement for proper muscle differentiation at both the early (muscle founding) and late

(muscle attachment and positioning) stages, and blocking phosphorylation inhibits terminal differentiation.

p38β is required for Vestigial phosphorylation

Kinase prediction software (Xue et al., 2011) indicated that the most likely position within the VgΔ5 region, as well as the entire Vg peptide, to be phosphorylated was at Ser-215; further, this position was most likely the target of the p38 MAPK pathway (**Figure 2.3**). Ser-215 is within a canonical MAPK consensus sequence of Pro-Asp-Ser-Pro (Davis, 1993). To test whether p38 MAPK had an effect on Vg phosphorylation, S2 cells were transfected with 3xHA-Vg and 3xFLAG-Sd, and treated with the pan-p38 MAPK inhibitor SB203580 (Han et al., 1998). Phosphorylation of Vg was inhibited by SB203580 (**Figure 2.9A**), as increasing concentrations of SB203580 caused a diminished presence of the heaviest molecular weight bands. This was Sd-dependent, as treatment of cells without Sd showed no difference in Vg banding. 3xFLAG-p38β and 6xMyc-Sd co-immunoprecipitated in S2 cells, indicating that this could be the kinase responsible for phosphorylation of Vg (**Figure 2.9B**). However, expression of RNAi against p38β in the wing disc using the *Vg(M+Q)*:GAL4 driver did not result in any differences in wing structure (**Figure 2.9C**), possibly because the level of knockdown was insufficient to produce noticeable effect or there was compensatory phosphorylation by p38a (**Figure 2.9D,E**). Expression of a dominant negative p38β isoform however did result in a similar lateral clipping phenotype as the wings observed in the Vg^{S215A} mutant rescue wings (Adachi-Yamada et al., 1999).

2.3 Discussion

There is a well-established role for Vg as an identity gene for wing development. Because of the ability to enforce a new fate on non-wing tissue (Simmonds et al., 1998), regulation of Vg activity must necessarily be tightly controlled to ensure proper fate specification during development. Regulation of a specific gene product can and does occur at multiple levels; mechanisms such as epigenetic chromatin modification, combinatorial transcriptional control, RNA interference and sequestration, and protein modification are all employed to ensure that proteins are available when, where and in the proper amount that the cell requires for development. Post-translational modifications in particular have a long history of providing fine-tuned control over activity and expression levels (Lomelí and Vázquez, 2011; Talamillo et al., 2008; Tootle and Rebay, 2005). Here phosphorylation of Ser-215 is established in regulating the function of Vg, and the functional consequences of alterations in Ser-215 phosphorylation are shown.

Previous to this, the only known post-translational modification of Vg was sumoylation (Takanaka and Courey, 2005). Sumoylation of Vg was established based on a mass spectrometry screen of sumoylated *Drosophila* proteins, and addition of SUMO residues to Vg by the E3 ligase Ubc9 was shown to be required for activation of a *vgQE*-fused luciferase reporter in S2 cells. However, the position of the SUMO conjugated residue is unclear. There are 5 lysines within the Vg peptide that could possibly be used for SUMO covalent linkage. Of these, Takanaka and Courey established that it was not K180, and mutants for the sumoylation pathway in wings did not show a sensory bristle phenotype. Further, our lab has also shown that K257

was also not sumoylated as mutation of the residue to arginine did not result in loss of the SUMO modifier.

The second post-translational modification established here is phosphorylation of Ser215. Deletion of amino acids 197-258 (VgΔ5) resulted in a loss of both higher molecular weight bands present after co-transfection of Vg and Sd in S2 cells, leaving only one at the predicted Vg molecular weight. Further, examination of Vg for sumoylation showed that all isoforms of Vg are sumoylated, and treatment of cell lysate with λ-phosphatase resulted in only a single point instead of a sumoylated and non-sumoylated position. This indicates that sumoylation of Vg does not appear to be dependent on initial phosphorylation. None of the 5 lysine residues are within a canonical phosphorylation-dependent sumoylation motif (Mohideen et al., 2009), which further supports this hypothesis. However, the fact that neither the Vg^{S215A} or Vg^{S215E} isoforms were able to fully recapitulate activation of the Vg quadrant enhancer in a luciferase assay suggests that these modifications may play a different or more subtle role. One potential function may be to keep Vg in a 'poised' state of pre-activation, so that rapid phosphorylation or dephosphorylation can be used to sharply and quickly adjust Vg function as time and development continue. Priming of proteins has been corroborated across multiple species and tissues, including in the *Drosophila* embryo and mammalian T cells (Bevington et al., 2017; Sun et al., 2015a). Phospho-turnover can be very dynamic, and relatively less taxing on cellular resources than continual degradation and translation of new protein across a broader timespan (reviewed in Prabakaran et al., 2012). Alternatively, assembly of an activating complex may require a change in Vg phosphorylation and not just a simplistic binary yes/no. By preventing Vg from being phosphorylated or dephosphorylated in a dynamic manner by expressing only

phosphomimetic and non-phosphorylatable Vg mutants, formation of a complex dependent on dynamic modification may be prevented.

Within the VgΔ5 region, Ser-215 was identified as a candidate site for phosphorylation by the MAPK pathway. 3xHA-tagged mutant forms with non-phosphorylatable (vg^{S215A}) and phosphomimetic (vg^{S215E}) Vg coding sequence were placed under UAS control to investigate the functional role of Vg phosphorylation *in vivo*. While expression of 3xHA-Vg^{S215A} or 3xHA-Vg^{S215E} using *Vg(M+Q)*:GAL4 in a wild type background did not have a dominant effect over endogenous Vg, rescue experiments using mutant Vg to compensate for a homozygous vg^{null} background showed that phosphorylation of Vg is key to proper specification of the adult wing, especially in establishing anterior versus posterior margin identity. Rescue with the vg^{S215A} allele was able to re-establish wing fate with minor clipping of the lateral margin, but could not fully promote pro-neural gene activation, resulting in loss of sensory bristles on the anterior margin. Conversely, the vg^{S215E} allele was able to properly establish anterior margin but caused bristle duplication along the posterior margin. Tracing the sensory bristle precursor cells to the third instar larval wing disc, the vg^{S215A} allele was not able to promote expression of the SOP marker Ct, whereas the vg^{S215E} allele could.

Interestingly, the vg^{S215A} allele was unable to sustain expression along the dorsal/ventral boundary where the *vgME* is normally active in the third instar (Klein and Martinez Arias, 1999). In normal wing discs, induction of the *vgME* at the dorsal/ventral boundary by Wg (Williams et al., 1994) drives the Vg-dependent induction of its own quadrant enhancer (Kim et al., 1996), both of which are also initiated at a low level by basal expression from the priming enhancer

(Zecca and Struhl, 2007b). The feed-forward nature of the Vg enhancer system is not cell-autonomous (Zecca and Struhl, 2007a). Decoupling of these enhancers by altering the phosphorylation status of Vg is a novel aspect of this regulatory network that indicates a method for positional and temporal control that is more nuanced than a simple on/off mechanism. By altering relative levels of Vg phosphorylation, the wing disc may be able to control input into the circuit in a more graded manner. Combined with the concept of a 'poised' state for Vg via sumoylation, this fine-grained control of activity is more complex than previously demonstrated.

Overexpression of either the Vg^{S215A} and Vg^{S215E} mutants resulted in wing discs smaller than wild type, indicating increased apoptosis and/or diminished proliferation. Vg and Sd both play a role in managing the balance between proliferation and differentiation. Absence of Vg blocks proliferation of the third instar wing pouch by affecting the cell cycle, while truncated Vg proteins alter the levels of *Death-associated inhibitor of apoptosis-1* (*diap1*) expression (Delanoue et al., 2004; Legent et al., 2006; Van de Bor et al., 1999; Williams et al., 1994). Sd also controls cell cycle re-entry and progression through interactions with dE2F1 and Yki (Meserve and Duronio, 2015; Shu and Deng, 2017; Zhang et al., 2017a). Phosphorylation of Vg may interfere with either proliferation or apoptosis, or both, by interfering with the stability of the Vg protein or Vg/Sd complexes, or by changing the regulation of pro-apoptotic or cell cycle repressor targets.

Transcription factors are often repurposed in different contexts during *Drosophila* development. In mammalian systems, this repurposing can be eliminated in part by the existence of multiple overlapping and/or semi-redundant developmental regulatory genes with differential expression

patterns. In *Drosophila* embryogenesis, Vg and Sd are repurposed for specification of the VL1-4, LL1, and DA1-3 somatic muscles (Bataillé et al., 2010; Deng et al., 2009; Deng et al., 2010). Loss of Vg in the embryonic musculature leads to weak muscle attachments, muscle rounding, poor motility and absence of the VL2 muscle. Rescuing the homozygous vg^{null} phenotype using either the vg^{S215A} or vg^{S215E} transgenes had a differential effect on the degree of rescue observed. In the vg^{S215A} rescue embryos, muscle attachment weakness was still apparent in the ventral muscles, and in some cases the VL muscles were entirely absent. This can be contrasted to rescue performed using the vg^{S215E} transgene, which restored an essentially wild type musculature pattern with no defects in attachment or absent muscles. This indicates a requirement for Vg phosphorylation in muscle development that differs from wing development in that dephosphorylation of Vg may not be necessary for proper gene regulation. The requirement for Vg sumoylation, and thus its function as a priming mechanism as proposed for wing development, is still unknown and a potential area for future research.

Finally, p38β was identified as the kinase potentially responsible for Ser-215 phosphorylation. Previous studies have shown some degree of compensatory overlap and redundancy between p38a/Mpk2 and p38β in *Drosophila* (Chen et al., 2010), as loss of either gene individually showed no phenotype but loss of both genes results in larval/pupal lethality with few escapers. Sd interacts with p38β as shown by co-immunoprecipitation, which then posits a model where Sd acts as a scaffold for p38β/Vg interaction in addition to its role as the partner transcription factor for Vg. A p38 MAPK family protein interaction map has been performed in S2 cells via mass spectrometry, but did not pull down either Vg or Sd as interacting partners (Belozerov et al., 2014); this is not particularly surprising as endogenous Sd expression is low and Vg virtually

absent in this cell line (Cherbas et al., 2011). One of the challenges of examining p38-mediated phosphorylation of Vg pharmacologically using SB203580 is that the drug may be able to inhibit other kinases at a lower level (Cuenda et al., 1995; Davies et al., 2000). This could potentially be resolved by the use of dsRNA-mediated knockdown of the p38 MAPKs to reduce function. Alternatively, co-transfection of a known dominant negative form of p38β could also be used to examine the role of the specific kinase but would require careful evaluation of the pleiotropic effects of the dominant negative isoform on cell viability and function.

The Hippo signaling pathway has recently been found to be regulated by p38β-mediated phosphorylation of Ajuba, which modulates the F-actin accumulation in the cell and alters Yki activity resulting in changes in *Diap1* regulation (Huang et al., 2016). TEADs in mice are also regulated by interaction with p38 MAP kinases that regulate shuttling between the nucleus and cytoplasm while cells are under stress (Lin et al., 2017a). It is possible that the interaction between Sd, Vg and p38 may regulate the downstream effects of the Hippo pathway. Sd is a key transcription factor that mediates the signaling pathway output in conjunction with the co-factor Yki (Goulev et al., 2008; Wu et al., 2008). However, Yki and Vg compete for Sd binding (Li et al., 2015a). If Vg binding to Sd is sequestering it from Yki, then destabilization of Vg itself or the Vg/Sd interaction by changes in Vg phosphorylation could affect the amount of available Sd that Yki is able to interact with. Thus, whether or not Vg phosphorylation affects Hippo pathway signaling output is an interesting area for future research.

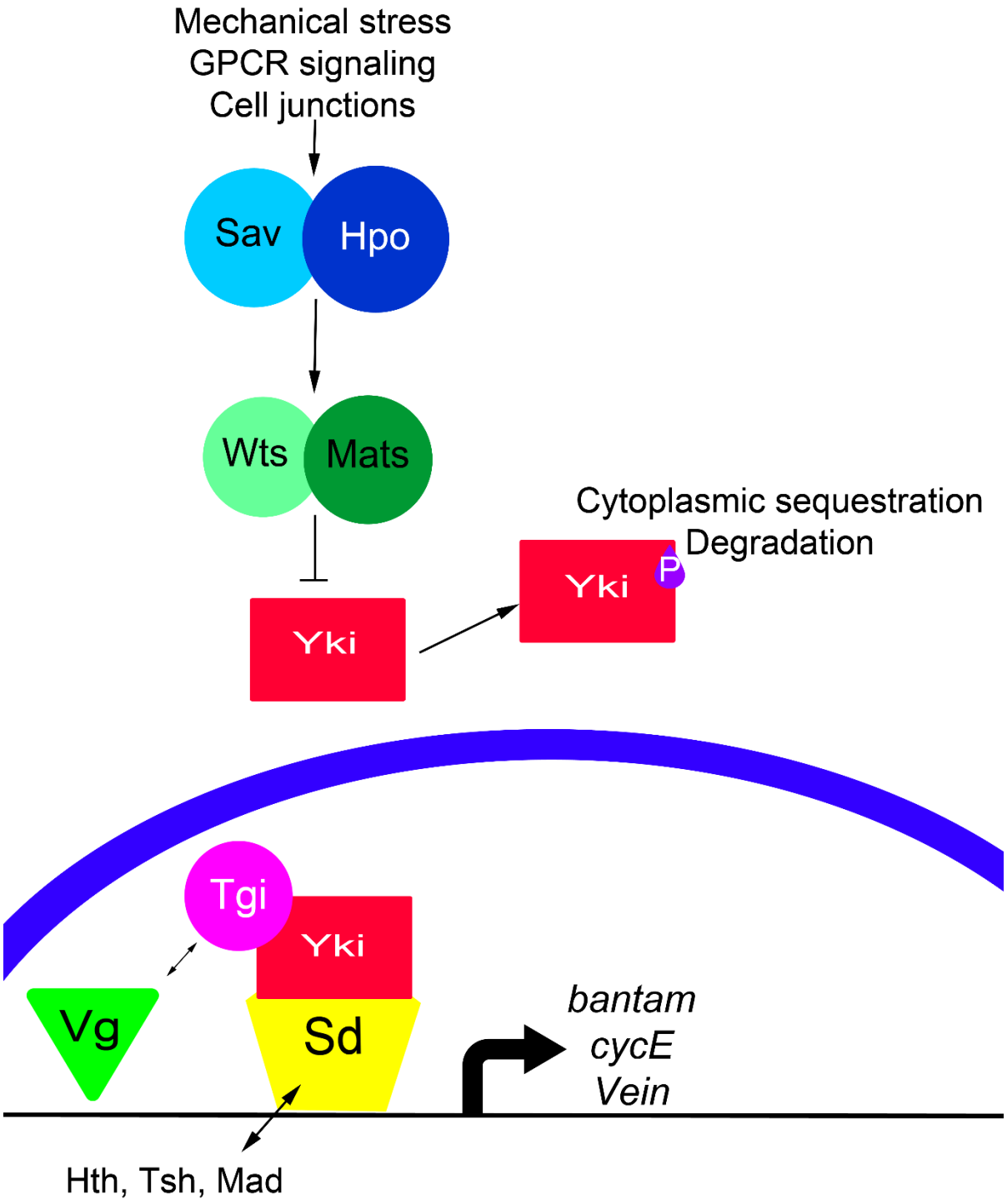
Mechanical stress
GPCR signaling
Cell junctions
Sav
Hpo
Wts
Mats
Cytoplasmic sequestration
Degradation
Yki
P
Yki
Tgi
Yki
Vg
Sd
bantam
cycE
Vein
Hth, Tsh, Mad

Figure 2.1: A schematic of the core *Drosophila* Hippo signaling pathway. When the Hippo signaling pathway is on, Hpo phosphorylates Sav, which results in phosphorylation of Wts and Mats, and subsequent phosphorylation of Yki. Phospho-Yki can then either be sequestered in the cytoplasm or targeted for proteasomal degradation. When the pathway is off, Yki is instead targeted to the nucleus where it associated with a number of transcription factors such as Sd, Hth, Tsh and Mad. Yki and Sd are able to induce expression of a number of pro-proliferative and anti-apoptotic genes. Yki and Tgi compete for Sd binding to alter Sd target gene expression.

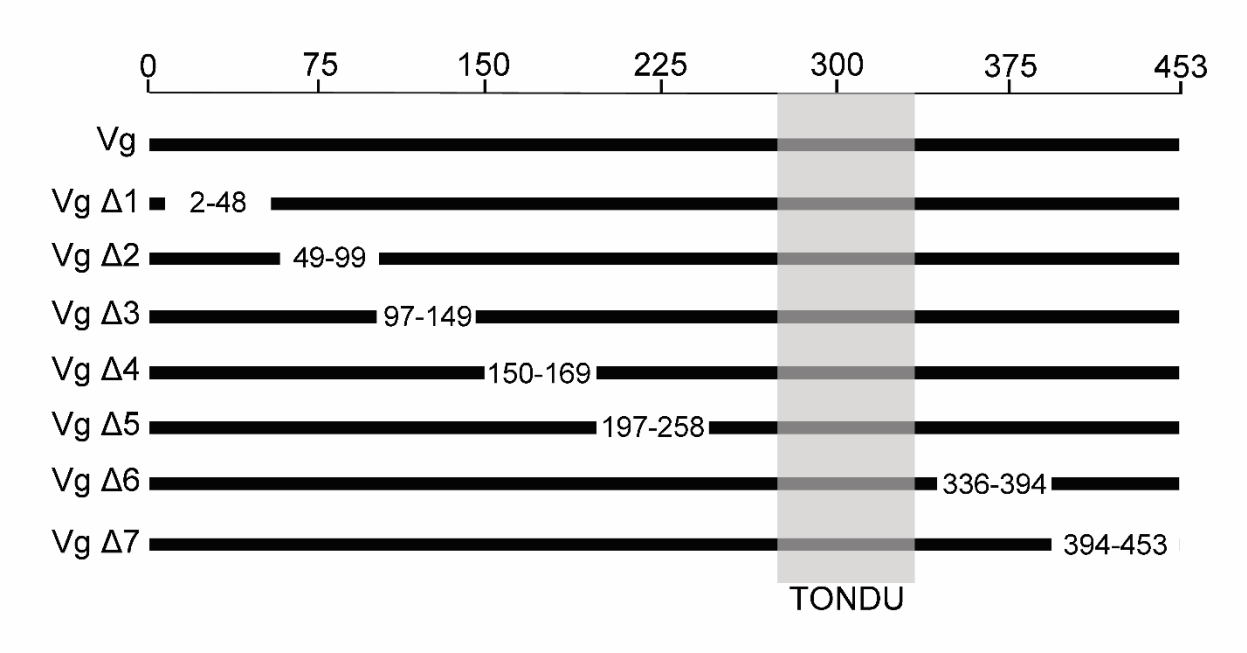
0
75
150
225
300
375
453
Vg
Vg Δ1
2-48
Vg Δ2
49-99
Vg Δ3
97-149
Vg Δ4
150-169
Vg Δ5
197-258
Vg Δ6
336-394
Vg Δ7
394-453
TONDU

Figure 2.2: A schematic showing the location of Vg deletions within the protein. Numbers within each row indicate the position of deleted amino acids. The labelled grey bar represents the TONDU domain necessary for interaction with Sd.

A

GSQQHQHHNESSCSSGPDSPRHA

197 Vg^{S215A} Vg^{S215E}

A E

HSHSHPLHGGGGATGGPSSAGGT

GSGGGDGGGTGAIPKN

258

B

Predicted Sites

Position	Code	Kinase	Peptide
82	S	CAMK	VAAAAHNSAAAAVAV
95	S	CAMK	AVAANQASSSGGIGG
4	S	CK1	****MAVSCPEVMYG
215	S	CMGC	SCSSGPDSPRHAHSH
322	S	CMGC	KDSKESSSPMSNRNF
129	S	STE	SNVVPGSSSVGSVGL
149	S	STE	LSGAAGHSLHSSHRT
156	T	STE	SLHSSHRTHAHSLAH
160	S	STE	SHRTHAHSLAHAHTH
166	T	STE	HSLAHAHTHPHSHTH

C

Predicted Sites

Position	Code	Kinase	Peptide
41	S	CAMK	GGATGGPSSAGGTGS
2	S	CK1	******GSQQHQHHN
19	S	CMGC	SCSSGPDSPRHAHSH
25	S	STE	DSPRHAHSHSHPLHG
27	S	STE	PRHAHSHSHPLHGGG
12	S	AGC/DMPK	HQHHNESSCSSGPDS
56	T	AGC/GRK	GGGDGGGTGAIPKN*
12	S	AGC/NDR	HQHHNESSCSSGPDS
27	S	AGC/NDR	PRHAHSHSHPLHGGG
19	S	AGC/PDK1	SCSSGPDSPRHAHSH

D

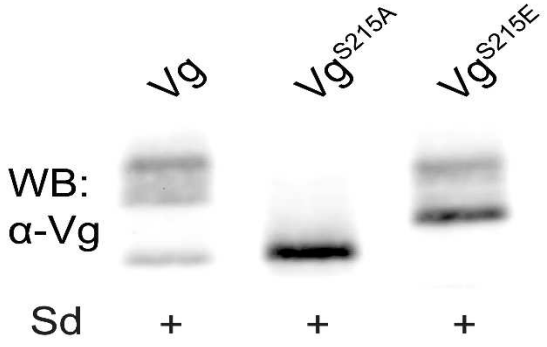

Figure 2.3: A) Amino acid sequence of the VgΔ5 deletion region indicated in Figure 2.2. The canonical MAPK target motif is indicated in blue with Ser-215 labelled in red. B) Top 10 predicted phosphorylation sites predicted across full Vg peptide with highest likelihood kinase family. GPS 3.0 kinase prediction software indicated Ser-215 (highlighted) as a likely site of post-translational modification by MAPK family kinases. The CMGC kinase group includes cyclin-dependent kinases, CDK-like kinases, casein kinase 2, CLK kinases, DYRK kinases, glycogen synthase kinases, mitogen-activated protein kinases, RCK kinases and SR-rich protein kinases (Morrison et al., 2000). C) Top 10 predicted phosphorylation sites for VgΔ5 amino acid sequence with highest likelihood kinase family. Ser-215 is listed as position 19. D) Western blot of S2 cell lysate co-transfected with with Sd and either wild type Vg, a non-phosphorylatable mutant (Vg^{S215A}) or a phosphomimetic mutant (Vg^{S215E}).

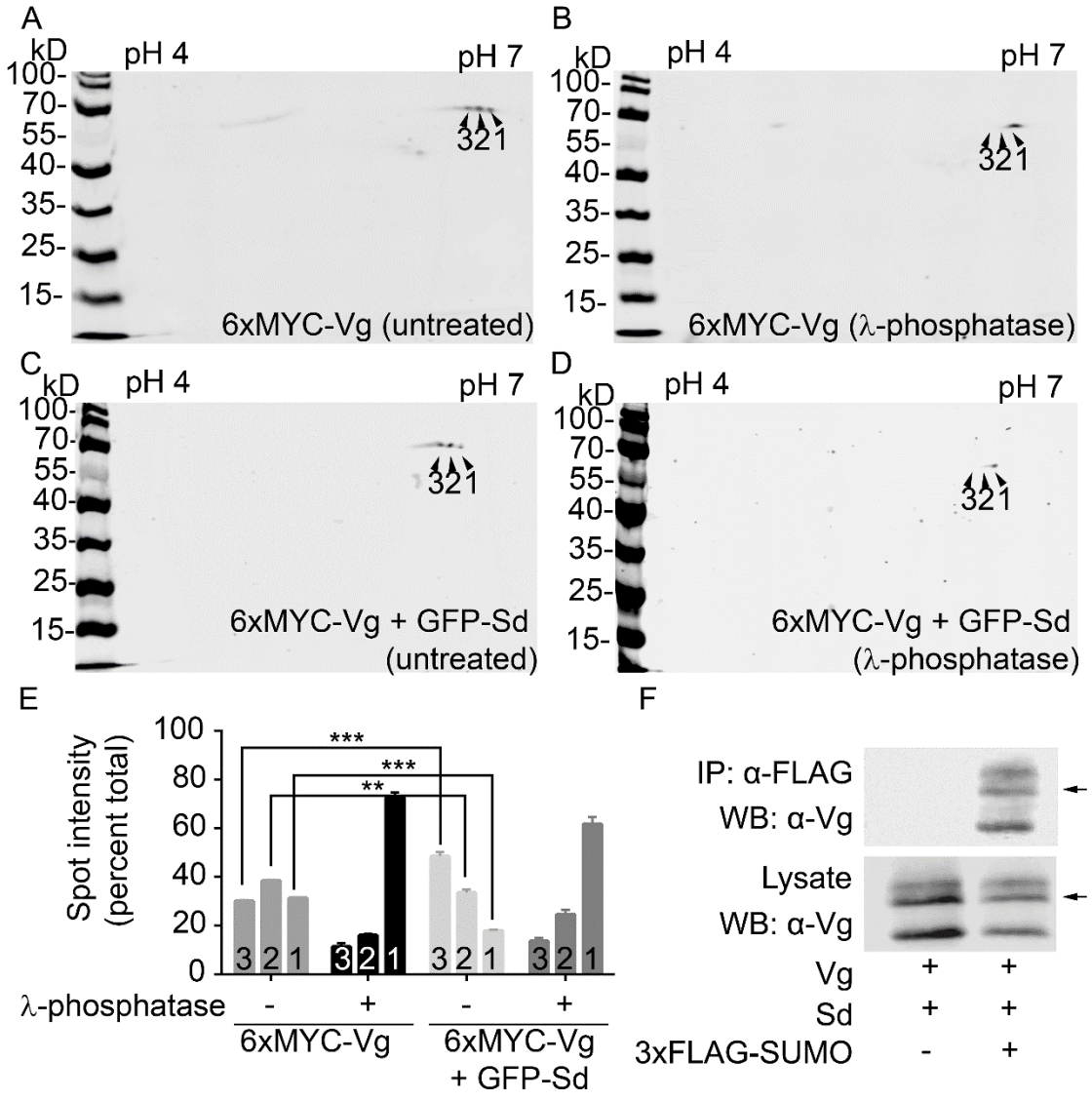
A
kD
pH 4
pH 7
100-
70-
55-
40-
35-
25-
15-
321
6xMYC-Vg (untreated)
B
kD
pH 4
pH 7
100-
70-
55-
40-
35-
25-
15-
321
6xMYC-Vg (λ-phosphatase)
C
kD
pH 4
pH 7
100-
70-
55-
40-
35-
25-
15-
321
6xMYC-Vg + GFP-Sd
(untreated)
D
kD
pH 4
pH 7
100-
70-
55-
40-
35-
25-
15-
321
6xMYC-Vg + GFP-Sd
(λ-phosphatase)
E
Spot intensity
(percent total)
100
80
60
40
20
0
***
***
**
3 2 1
3 2 1
3 2 1
3 2 1
λ-phosphatase
-
+
-
+
6xMYC-Vg
6xMYC-Vg
+ GFP-Sd
F
IP: α-FLAG
WB: α-Vg
Lysate
WB: α-Vg
Vg
+
+
Sd
+
+
3xFLAG-SUMO
-
+

Figure 2.4: Vg phosphorylation is dependent on Sd. A) 2-dimensional gel electrophoresis of S2 cell lysate transfected with 6xMyc-Vg shows three distinct isoforms (arrows 1-3). B) Treatment of 6xMyc-Vg lysate with λ-phosphatase causes collapse of three isoforms to one. C) Co-expression of 6xMyc-Vg and GFP-Sd in S2 cells shows three isoforms of Vg. D) Treatment of of 6xMyc-Vg and GFP-Sd lysate with λ-phosphatase again results in a single isoform. E) Quantification of intensity at each of three positions in 2-dimensional gel electrophoresis immunoblot shows that co-transfection of 6xMyc-Vg with GFP-Sd results in a shift in position intensity to the left (Position 3) compared to transfection of 6xMyc-Vg alone. Treatment with λ-phosphatase causes collapse to Position 1, indicating lower pI positions are the result of phosphorylation. F) All isoforms of Vg are sumoylated, as immunoprecipitation of Vg followed by anti-Vg Western blot shows all forms are linked to 3xFLAG-SUMO. N = 3 for all two-dimensional gel electrophoresis immunoblots and quantifications.

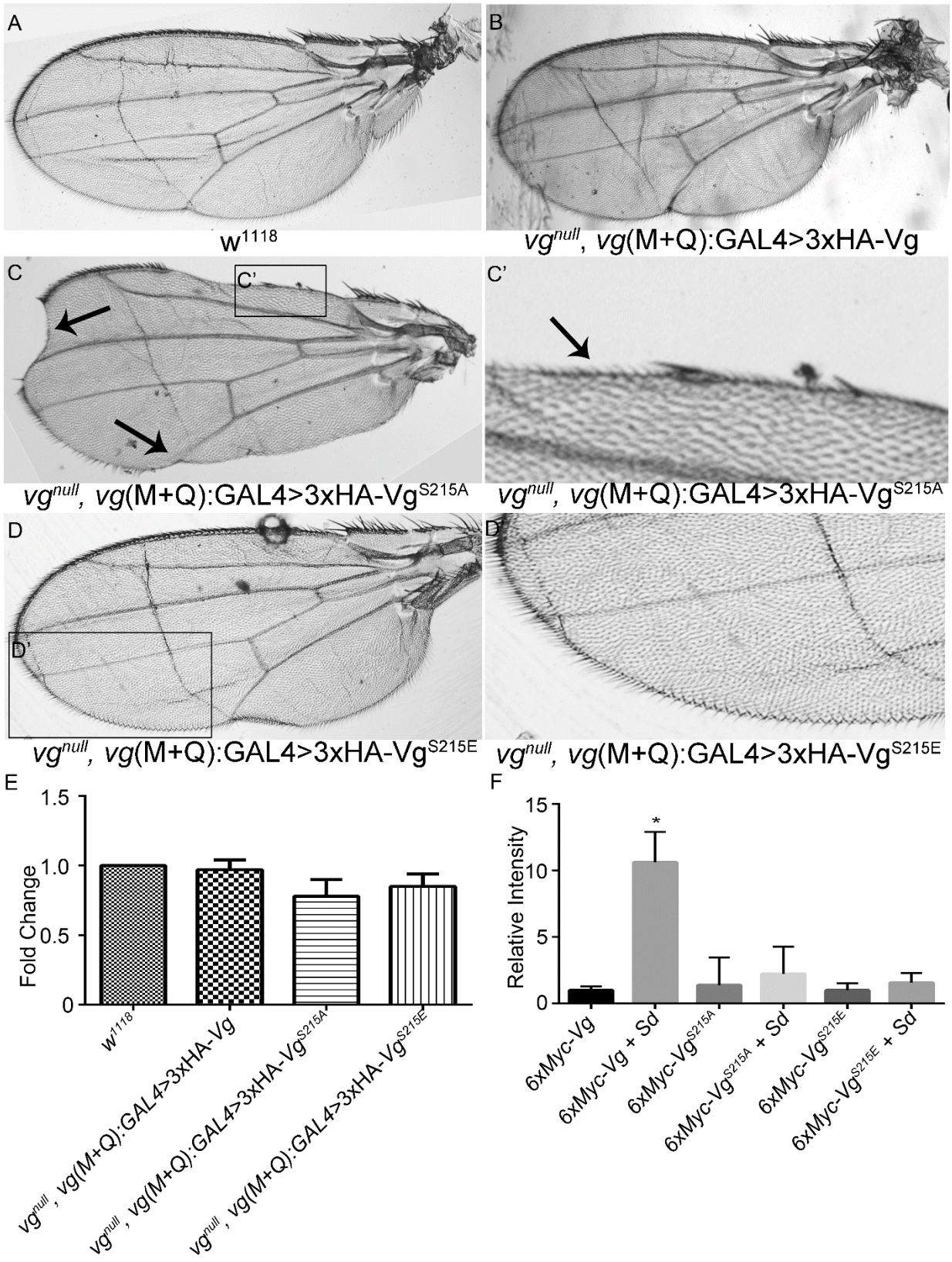
A
w1118
B
vgnull, vg(M+Q):GAL4>3xHA-Vg
C
C'
vgnull, vg(M+Q):GAL4>3xHA-VgS215A
C'
vgnull, vg(M+Q):GAL4>3xHA-VgS215A
D
D'
vgnull, vg(M+Q):GAL4>3xHA-VgS215E
D'
vgnull, vg(M+Q):GAL4>3xHA-VgS215E
E
Fold Change
1.5
1.0
0.5
0
w1118
vgnull, vg(M+Q):GAL4>3xHA-Vg
vgnull, vg(M+Q):GAL4>3xHA-VgS215A
vgnull, vg(M+Q):GAL4>3xHA-VgS215E
F
Relative Intensity
15
10
5
0
*
6xMyc-Vg
6xMyc-Vg + Sd
6xMyc-VgS215A
6xMyc-VgS215A + Sd
6xMyc-VgS215E
6xMyc-VgS215E + Sd

Figure 2.5: Phosphorylation at Ser-215 affects rescue of the wing development of a vg^{null} mutation by a mutant transgene. A) A wild type wing showing the normal wing structure. B) Expression of UAS-3xHA-Vg under the control of the *vg(M+Q)*-GAL4 driver expressing at the margin and quadrant enhancer-controlled domains leads to rescue of the adult wing including both anterior and posterior margins. C) Expression of a 3xHA-Vg^{S215A} transgene only partially rescues the homozygous vg^{null} phenotype. The resulting wing shows clipping of the lateral margin and slight L5 vein reduction (arrows), and loss of anterior margin sensory bristles (C'). D) Expression of the 3xHA-Vg^{S215E} transgene in a homozygous vg^{null} background also partially rescues the wing although duplication of the posterior margin bristles is often seen (D'). E) qPCR measurement of mRNA isolated from dissected wing discs of the genotypes shown in A-D show the UAS-Vg, UAS-Vg^{S215A} and UAS-Vg^{S215E} transgenes are expressed at similar levels. (N = 3 independent biological replicates) F) Activation of the *vgQE* in S2 cells by Vg, Vg^{S215A} and Vg^{S215E} with and without co-expression of Sd. (N = 3 independent biological replicates)

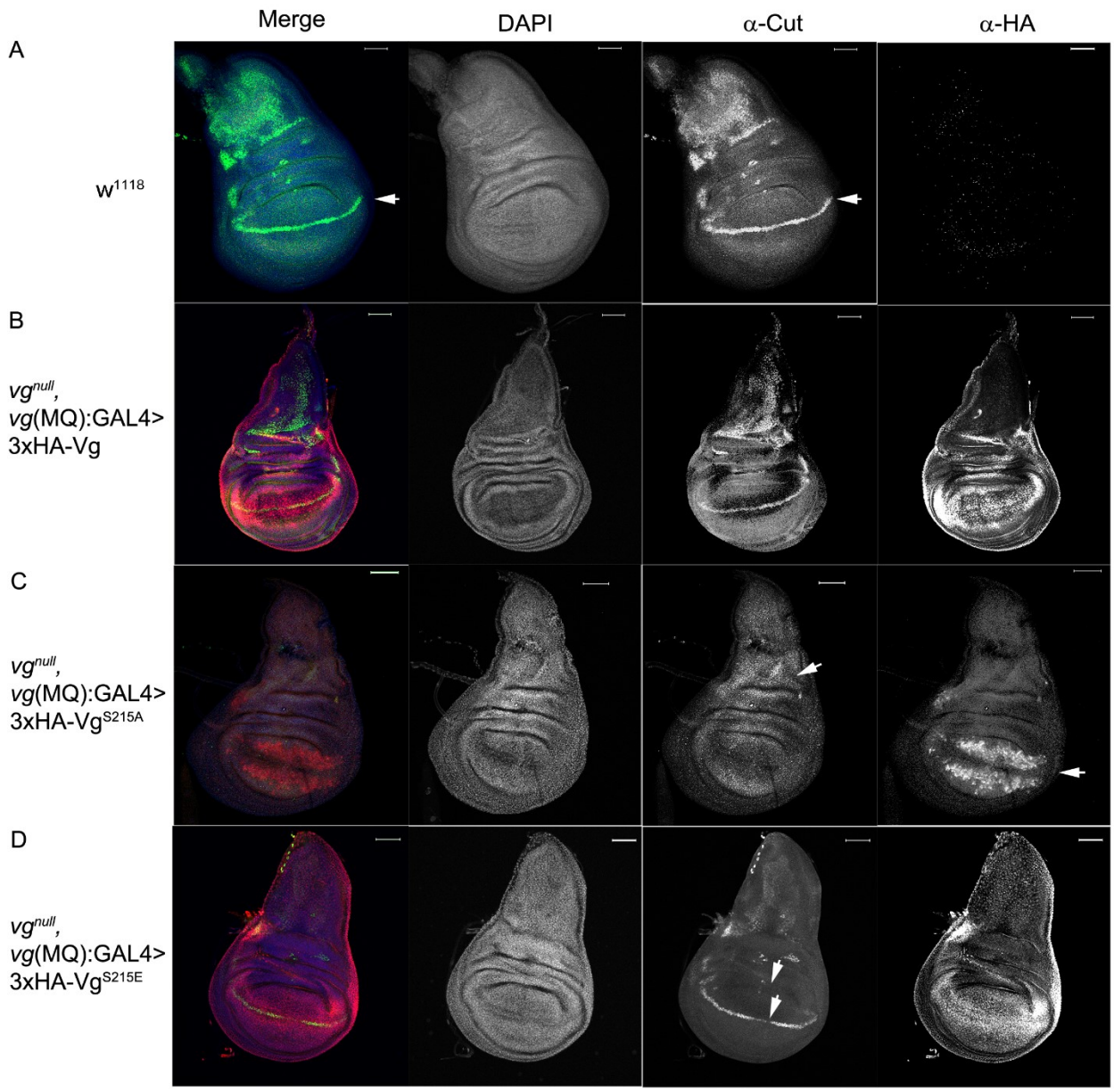
Merge
DAPI
α-Cut
α-HA
A
w1118
B
vgnull,
vg(MQ):GAL4>
3xHA-Vg
C
vgnull,
vg(MQ):GAL4>
3xHA-VgS215A
D
vgnull,
vg(MQ):GAL4>
3xHA-VgS215E

Figure 2.6: Phosphorylation of Vg215 is necessary for wing imaginal disc growth and differentiation. Scale bar is 50μm. A) A wild type late third instar larval wing disc showing normal expression of Cut (Ct). The row of Ct positive cells along the dorsal/ventral margin marks sensory organ precursors fated to become sensory bristles (arrow). B) Inducing expression of a 3xHA-Vg transgene along the wing margin via *vg(M+Q)*-GAL4 in a vg^{null} background produces a wing disc with slightly reduced size compared to wild type but with Ct^{+} cells similar to wild type. C) Expression of a 3xHA-Vg^{S215A} transgene via *vg(M+Q)*-GAL4 in a vg^{null} background leads to a reduced disc size compared to wild type and a reduction in Ct^{+} cells (arrow). Cells at the dorsal/ventral boundary do not sustain HA-Vg^{S215A} expression (arrow) D) Expression of a 3xHA-Vg^{S215E} transgene via *vg(M+Q)*-GAL4 in a vg^{null} background largely restores the overall size of the wing disc and the pattern of Ct^{+} cells is similar to wild type with some gaps at the dorsal/ventral border (arrow). Some ectopic Ct^{+} cells are seen adjacent to this region in the wing pouch (arrow).

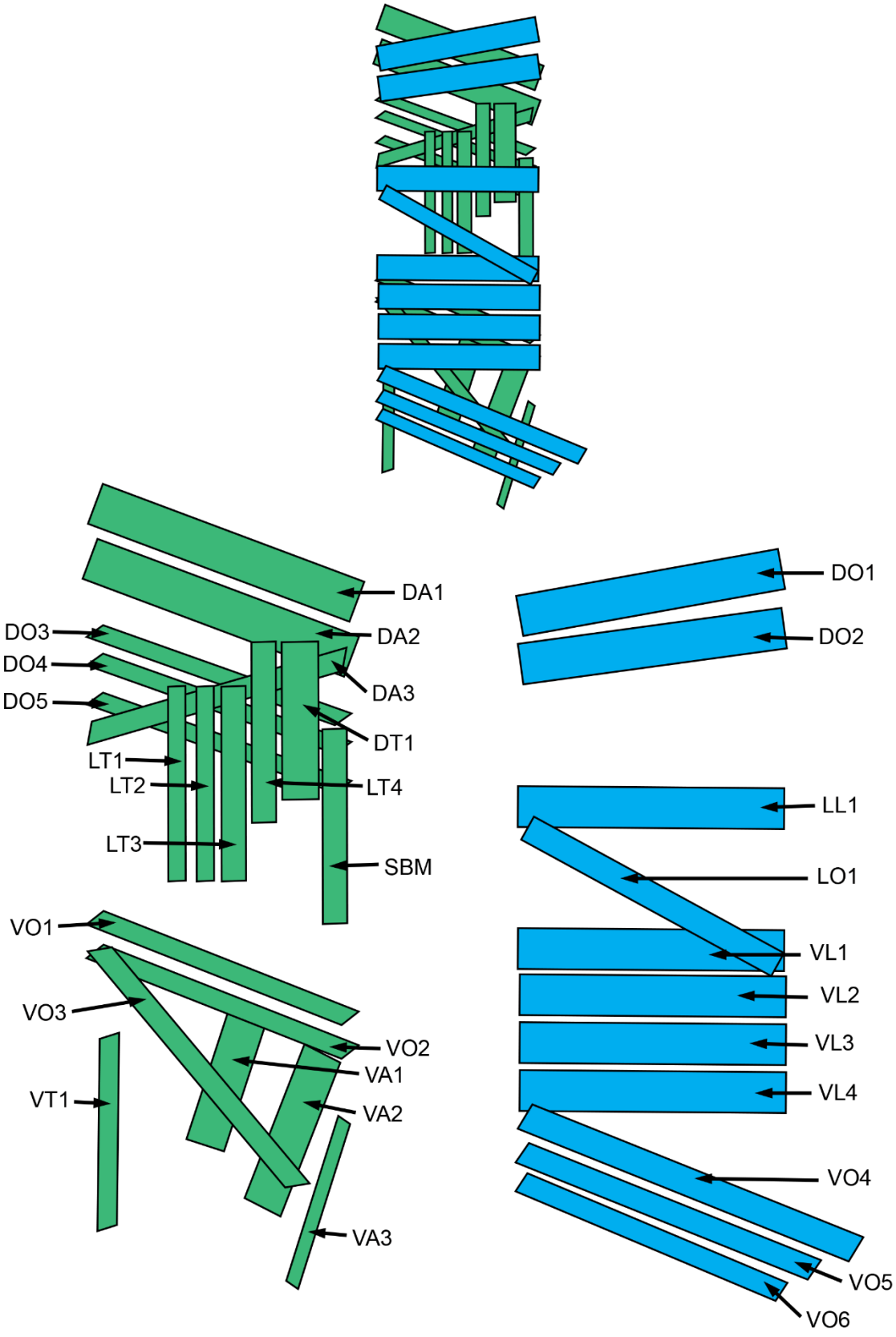
DA1
DO3
DA2
DO4
DA3
DO5
DT1
LT1
LT2
LT4
LT3
SBM
VO1
VO3
VO2
VA1
VT1
VA2
VA3
DO1
DO2
LL1
LO1
VL1
VL2
VL3
VL4
VO4
VO5
VO6

Figure 2.7: The embryonic somatic musculature is a pattern of 30 muscles per hemisegment that repeats along the length of the embryo. The majority of the muscles are named according first to their position (D – dorsal; L – lateral; V – ventral) and then to the angle of orientation (O – oblique; L – longitudinal; T – transverse; A – acute). The exception to the naming convention is the segment border muscle (SBM). The top figure shows the full muscle pattern, and the lower two are separated for clarity of naming. Original design adapted from Dobi et al., 2015.

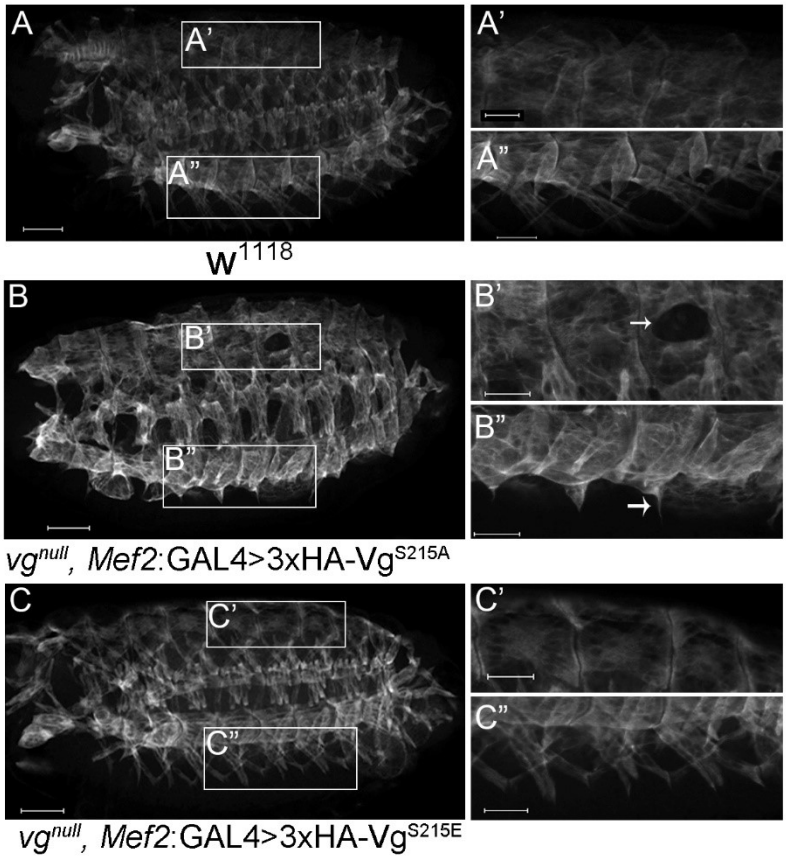
A
A'
A"
A'
A"
w1118
B
B'
B"
B'
B"
vgnull, Mef2:GAL4>3xHA-VgS215A
C
C'
C"
C'
C"
vgnull, Mef2:GAL4>3xHA-VgS215E

Figure 2.8: Phosphorylation at Ser-215 is required for muscle differentiation in embryos. Whole embryo scale bars are 40 μm and inset scale bars are 20 μm. A) An example of the pattern of somatic muscles in a wild type embryo. Close-up views of dorsal and ventral muscles are shown in A' and A'' respectively. B) Expression of 3xHA-Vg^{S215A} in a homozygous *vg^{null}* embryo leads to muscle defects at both the dorsal (B') and ventral (B") regions as shown by absent muscles in the dorsal musculature (B', arrow) and ventral musculature with weak and misdirected attachments (B", arrows). C) Expression of 3xHA-Vg^{S215E} rescues Vg function in terms of directing muscle attachment in a *vg^{null}* embryo. The attachment points and positioning of the dorsal (C') and ventral (C") muscles are comparable to wild type.

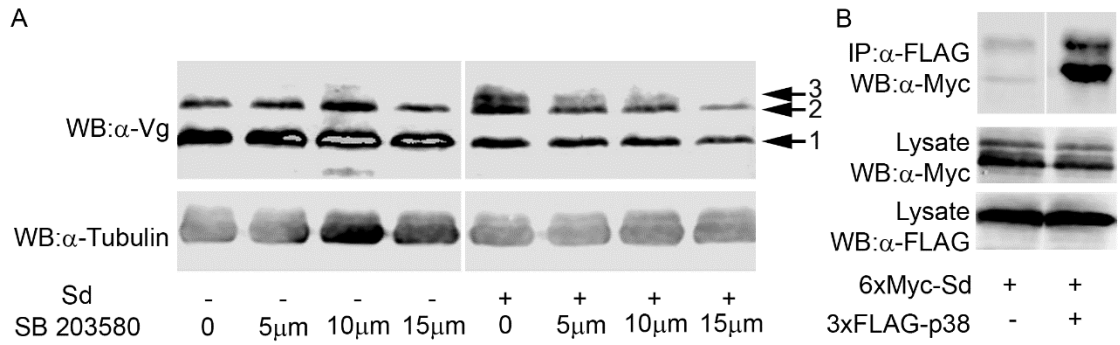

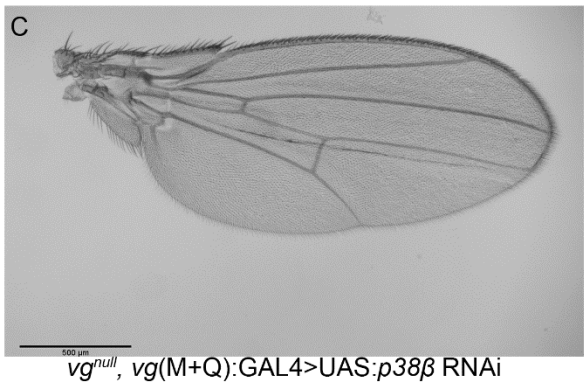

vg^{null}, *vg*(M+Q):GAL4>UAS:*p38β* RNAi

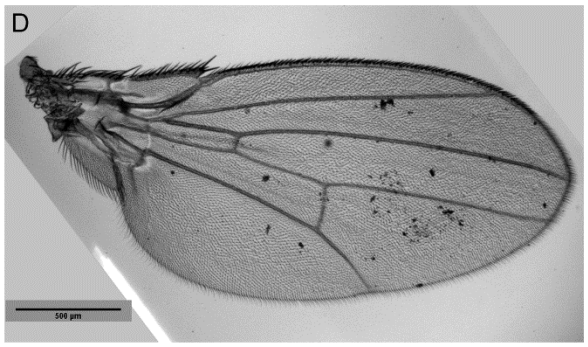

vg^{null}, *vg*(M+Q):GAL4>UAS:*mpk2* RNAi

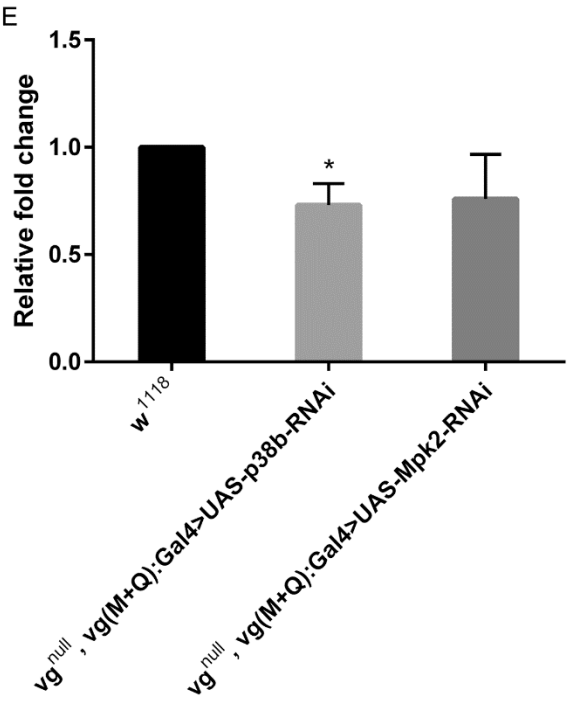

Figure 2.9: Pan-p38 MAPK inhibition by SB 203580 reduces Sd-directed Vg phosphorylation. A) S2 cell lysates co-transfected with Vg and Sd and treated with the pan-p38 MAPK inhibitor SB 203580 show a dose-dependent decrease in intensity of the λ-phosphatase-sensitive Vg uppermost band. B) 6xMyc-Sd and 3xFLAG-p38β can co-immunoprecipitate together. C) Knockdown of p38β by RNAi did not result in altered wings. D) Knockdown of *Mpk2/p38α* did not result in altered wings. E) qPCR quantitation of RNAi-mediated knockdown of *p38β* and *Mpk2* in third instar larval wing discs. * indicates $p<0.05$, with N = 4 independent biological replicates.

Chapter 3: Tondu domain-containing Growth Inhibitor is an inhibitor of Vestigial in *Drosophila* wing development

3.1 Introduction

Maintaining the balance between cell growth and differentiation during tissue development is a complex process requiring coordinated input from several signaling pathways. Dysregulation of this process can lead to cancer in the case of hyperproliferation, and misspecified tissue or developmental failure in the case of precocious differentiation (Aiello and Stanger, 2016; De Craene and Berx, 2013).

A key signaling pathway involved in regulation of tissue size and fate in most metazoans is the Hippo signaling pathway (**Figure 2.1**, reviewed in Irvine and Harvey, 2015). The core kinase cascade regulating this pathway culminates with phosphoregulation of the transcriptional co-regulator Yki (Huang et al., 2005). Unphosphorylated Yki is able to translocate to the nucleus, where it interacts with a host of transcription factors such as Sd (Wu et al., 2008), Homothorax (Hth; Peng et al., 2009) and Cabut (Cbt; Ruiz-Romero et al., 2015). The Yki/Sd complex regulates expression of target genes such as *diap1*, *Cyclin E* (*cycE*) and the miRNA *bantam* (Shu and Deng, 2017; Slattery et al., 2013; Zhang et al., 2008). The cells where these interactions occur are frequently tissue- and temporally-restricted, providing a control mechanism for cell-fate selection during development. In particular, Sd is required for proper formation of the adult *Drosophila* wing (Campbell et al., 1992); the progressive decrease in Sd function results in increasingly strong phenotypes, ranging from scalloping of the wing margin in a weak *sd* mutant

to loss of the wing blade entirely with a strong *sd* mutant (Campbell et al., 1992; Srivastava et al., 2004). Interestingly, Yki requires co-expression of Sd only in the developing wing disc (Goulev et al., 2008; Wu et al., 2008), but is dispensable for directing expression of Yki target genes in other imaginal discs. In this model, the default regulatory function of Sd is thought to be repressive when not bound to Yki, and binding of Yki to the C-terminus of Sd is linked to activation of target genes (Koontz et al., 2013; Wu et al., 2008).

A function for Sd in the wing imaginal disc was established prior to the identification of Yki, based on its interaction with Vg (Simmonds et al., 1998; Williams et al., 1991). Vg binds to the C-terminus region of Sd via its TONDU (TDU) domain (Halder et al., 1998; Paumard-Rigal et al., 1998; Simmonds et al., 1998; Vaudin et al., 1999). This interaction alters the DNA motif preference of Sd from a single Sd binding motif to a paired binding motif requiring formation of a 2xSd+2xVg protein complex for coordinate gene regulation (Halder and Carroll, 2001). Together this exclusion mechanism may fine-tune gene expression in the developing wing disc. Vg and Sd are able to form co-complexes with other transcriptional regulators as well, such as a tripartite complex with Myocyte enhancing factor-2 (Mef2), to direct terminal fate acquisition in a subset of the body wall muscles (Deng et al., 2009; Deng et al., 2010). Loss of the Vg/Sd/Mef2 complex leads to poor attachment of myotubes at the myotendinous junction and embryonic lethality.

Tgi, the second Vestigial-like family member gene in *Drosophila*, and related *VGLL4* subfamily genes are broadly considered tumor suppressors (Li et al., 2015c; Zhang et al., 2014; Zhang et al., 2017b). *VGLL4* mutation or expression level changes in humans is associated with gastric,

lung, colorectal, and esophageal cancer (Jiang et al., 2015; Jiao et al., 2014; Jiao et al., 2017; Li et al., 2015; Zhang et al., 2014). While comparatively little is known about the function of Tgi during *Drosophila* development, studies of mouse VGLL4 suggests it is critical during regulation of tissue growth and development (Lin et al., 2016; Shen et al., 2015). Tgi is thought to be expressed throughout the imaginal wing disc at a low level as well as in the ovaries and eye imaginal discs based on *in situ* hybridization (Koontz et al., 2013; Li et al., 2015a). This domain of expression overlaps with the restricted domain of cells expressing Vg in the wing disc. Tgi also plays a role in adult *Drosophila* heart function, where overexpression of Tgi can attenuate Raf-driven cardiac hypertrophy through a Sd-dependent mechanism (Yu et al., 2015). The function of Tgi in the wing disc has been found to be absolutely dependent on the presence of TDU domains (Guo et al., 2013), which is similar to the role of Vg as an intrinsically Sd-dependent co-factor (MacKay et al., 2003; Simmonds et al., 1998; Srivastava et al., 2002). Since both proteins require an interaction with the same domain of Sd to direct transcriptional regulation, this leads to the hypothesis that there is a competitive interaction between Vg and Tgi for Sd binding.

Here, it is established that although Vg and Tgi are both able to bind Sd, they do not form a co-complex with each other *in vitro*. *In vivo*, changing the relative levels and expression patterns of Vg, Sd and Tgi indicate that there is a dose-dependent response in size and fate determination of the adult wing, and that size and structural effects are established at least as early as the third instar wing disc. In Kc167 cells, Vg/Sd and Tgi/Sd complexes are both nuclear, but co-expression of fluorescently-tagged Vg and Tgi result in a nuclear accumulation of Tgi and cytoplasmic localization of Vg. qPCR analysis of Kc167 cells showed that co-transfection of Sd

and Tgi caused a significant increase in *vg* expression, and that overexpression of Vg/Sd or Tgi/Sd *in vitro* resulted in differential regulation of Sd target genes. Taken collectively, this supports the hypothesis that Vg and Tgi are competing for Sd binding in order to direct development of the *Drosophila* wing.

2.2 Results

Tgi is an evolutionarily conserved protein

Analysis of both Tgi isoforms (Tgi-PA and Tgi-PB) using MAFFT (Kuraku et al., 2013) showed conservation of Tgi at the protein level (**Figure 3.1**). This conservation is seen in across *Danio rerio* VGLL4L and VGLL4B, *Caenorhabditis elegans* R08C7.12, human VGLL4, and mouse VGLL4 orthologues. Tgi shows a substantial degree of conservation with its orthologous genes, particularly the Tgi-PB isoform. This is especially captured in the TONDU-2 domain at the C-terminus of the protein, which shows a very high degree of conservation. Tgi-PB was chosen for this study based on the higher degree of conservation, as well as other groups that have reported the *Tgi-RA* and *Tgi-RB* mRNA transcripts have similar expression patterns as shown by *in situ* hybridization in larval tissues and thus chosen to analyze the PB isoform (Koontz et al., 2013).

Tgi Interacts with Scalloped but not Vestigial

It is well established that Vg and Sd are able to form a co-complex through the TONDU domain of Vg (Simmonds et al., 1998). Tgi has also been shown to interact with Sd and Yki (Guo et al., 2013; Koontz et al., 2013). The ability of Vg to interact with Tgi was tested by co-transfection of 6xMyc-Vg with 3xFLAG-Tgi into Kc167 cells (**Figure 3.2**), followed by co-immunoprecipitation to look for formation of complexes. While a 6xMyc-Vg/3xHA-Sd interaction was preserved in Kc167 cells, as well as the 3-FLAG-Tgi/3xHA-Sd interaction, 6xMyc-Vg was unable to co-immunoprecipitate with 3xFLAG-Tgi. As Vg is known to form

heterotetramers with Sd for DNA binding, and that the Vg-Vg homotypic interaction is mediated through domains outside the TONDU domain (Halder and Carroll, 2001), the lack of a co-complex containing both Vg and Tgi indicates a possible mechanism for Sd regulation via titration of available Sd protein between Vg and Tgi.

Altering Relative Tgi Levels Affects Wing Development

If Vg and Tgi are competing for available Sd protein in the cell, then changes in the relative expression levels of Vg and Tgi would cause phenotypic consequences in tissues where both are expressed. Previous research has shown that Tgi is expressed ubiquitously and at a low level in the larval wing disc (Koontz et al., 2013), where Vg and Sd are known to play an important role in specifying wing fate. To investigate this, a system was developed in the *Drosophila* wing to test changes in the relative levels of Tgi and Vg using the *vg(M+Q)*:GAL4 driver line. This is a synthetic driver combining sequences from the *VgME*, which expresses at the dorsoventral margin, and the *VgQE*, which drives expression through the wing pouch region. We also developed a line for overexpression of the Tgi-PB coding sequence doubly tagged with 3xFLAG and 6xMyc (denoted FM-Tgi).

When FM-Tgi is overexpressed using the *vg(M+Q)*:GAL4 driver, a *vg*-dose-dependent response is observed in both size and development of the wing. Compared to a wing from a w^{1118} fly (**Figure 3.3A**), overexpression of FM-Tgi in a $vg^{+/+}$ background causes adult wings to be approximately 40% smaller than wild type and cupped downwards, with 18% displaying a shortened L5 vein that fails to connect with the posterior margin (**Figure 3.3B)**. To increase the

imbalance between Vg and Tgi expression further, a hemizygous vg^{null} allele was incorporated into the genetic background of the *vg(M+Q)*:GAL4>UAS:FM-Tgi cross. The vg^{null} allele has no Vg expression due to a loss of multiple exons (Paumard-Rigal et al., 1998), and a homozygous adult escaper will have very little to no functional wing tissue. In a hemizygous vg^{null} background, overexpression of Tgi under the *vg(M+Q)*:GAL4 driver results in wings on average 70% smaller than the $vg^{+/+}$ wings. There were a range of phenotypes within this genetic cross, with some wings retaining a general wing-like phenotype (**Figure 3.3C**), but with substantial downward cupping as well as short L5 veins and occasional absence of the posterior crossvein as well (**Figure 3.3C, arrows**). The short L5 vein and absend posterior crossvein phenotype is very similar to wings from flies carrying mutations in the TGF-β/BMP pathway, especially *dpp* and *glass-bottom boat* (*gbb*) (Bangi and Wharton, 2006; Khalsa et al., 1998). Dpp signaling from the anterior/posterior boundary is required to activate the *vgQE* and expand the wing pouch domain (Kim et al., 1996; Kim et al., 1997), so this phenotype may indicate that the Dpp signal is affected in some manner. At the most affected end of the phenotypic spectrum, the wing was largely comprised of semi-differentiated tissue with occasional small numbers of bristles of indeterminate origin (**Figure 3.3D**). The entire phenotypic range demonstrated substantial cupping and blistering reminiscent of integrin-ECM interaction failures (Dominguez-Gimenez et al., 2007). To test whether this phenotype is dependent on endogenous expression or loss of *vg*, Tgi was overexpressed using a *tsh*:GAL4 driver. *tsh* expression overlaps in the early second instar wing disc with endogenous *vg* expression, but the fields of *vg* and *tsh* expression become opposing, as repression of *tsh* expression is required for induction of the wing pouch (Wu and Cohen, 2002). If the effect of Tgi overexpression is dependent on Vg, overexpression of Tgi in cells not expressing *vg* should result in no significant change to the wing. This is the phenotype

shown in *tsh*:GAL4>UAS:FM-Tgi wings, which have neither a change in wing area nor any appreciable changes in differentiation (**Figure 3.3E**). The wing area change was quantified for analysis, which showed a *vg* dose-dependent response to *Tgi* overexpression, but no significant change when *Tgi* was overexpressed outside the *vg* domain (**Figure 3.3F**).

Another phenotype resulting from overexpression of Tgi in the *vg(M+Q):*GAL4 domain is cupping of the wing. Cupping is caused by an imbalance in the relative volumes of the dorsal and ventral regions of the wing disc. During pupariation, the wing blade evaginates from the dorsal/ventral margin into a bilayered structure that inflates after the adult emerges. If the available tissue volume for the dorsal and ventral planes of the adult wing are unequal due to inhibited proliferation or diminished cell death, tension between the two surfaces will cause cupping. The boundary of the dorsal/ventral region is composed of a band of *wg*-expressing cells across the centre of the presumptive wing blade. When *Tgi* is overexpressed using *vg(M+Q):*GAL4 in a $vg^{null/+}$ hemizygous background, there is a strong loss of ventral disc volume, as well as a decrease in the ratio of total disc volume to ventral segment volume. As the imaginal discs proceed through pupariation, histolysis and formation of the adult wing structures, the imbalance between dorsal and ventral tissue results in the cupping observed in the adult wing. To determine the source of the cupping from overexpression of FM-Tgi via the *vg(M+Q)*:GAL4 driver, third instar larval wing discs were analyzed for size and tissue compartment volume (**Figure 3.4**). Compared to wild type discs (upper panel), ectopic expression of FM-Tgi in a $vg^{null/+}$ background (lower panel) had both smaller total disc volume as well as a relatively smaller ventral compartment volume. This disparity explains both the significantly smaller size of wing as well as the cupping observed in **Figure 3.3B-D**.

Overexpression of Tgi using *Tgi*:GAL4 also results in a slightly smaller wing in comparison to wildtype (**Figure 3.5A)**, although with no observable differentiation defects (**Figure 3.5B,D**), consistent with the proposed role of Tgi as a tumor suppressor causing diminished proliferation. However, overexpression of HA-Vg using *Tgi*:GAL4 causes loss of the anterior and posterior margins as well as an overall size reduction of the adult wing (**Figure 3.5C,D**). The phenotype is similar to a sd^{EXT4} or sd^{1} mutant wing (Paumard-Rigal et al., 1998); both of these alleles are *sd* hypomorphic mutations. Overexpression of HA-Vg in the Tgi domain, which comprises the entirety of the wing disc, mimicking an *sd* insufficiency seems to support the idea that Vg and Tgi compete for Sd binding, and titration of available Sd into complexes with ectopic Vg would alter expression of genes responsive to a Tgi/Sd complex. Overexpression of HA-Vg does not affect the posterior crossvein or the L5 vein, unlike overexpression of Tgi in the Vg domain. This indicates a possible fate decision point during development, where the option for cells to become vein or margin may be decided by relative levels of Vg and Tgi expression. Overexpression of FM-Sd using the *Tgi*:GAL4 driver results in a larval lethality phenotype very similar to a $Tgi^{-/-}$ larvae (Koontz et al., 2013). Compared to a wild type larvae (**Figure 3.5E**), the *Tgi*:GAL4>UAS:HA-Sd larvae are smaller, and die in first and second instar, with very rare escapers to early third instar and no pupae ever observed (**Figure 3.5F**). The wing imaginal discs are often not present at the second instar, and the phenotype is 100% lethal prior to pupariation with most larval death occurring in second instar.

Finally, the effect of Tgi overexpression in the Sd domain was examined. Compared to a wild type wing (**Figure 3.6A**), *sd*:GAL4>UAS:FM-Tgi expression resulted in necrotic tissue that was

extremely poorly differentiated and very fragile (**Figure 3.6B**). This cross only resulted in female adults, and no male was ever observed. The expression of a dsRNA line targeting *Tgi* mRNA (UAS:*Tgi* TRiP) under the control of the *sd*:GAL4 driver line had no effect on differentiation (**Figure 3.6C**). The degree of knockdown was measured at 10-30% using qPCR, which may partially explain this lack of response. Wing area was quantified (**Figure 3.6D**), which showed a significant reduction in size for the *sd*:GAL4>UAS:FM-Tgi wing but not for the *sd*:GAL4>UAS:*Tgi* RNAi wings.

Vg and Tgi compete for transport into the nucleus

If Vg and Tgi are competing to bind Sd for transport into the nucleus, then cells with an insufficient amount of Sd expressed would preferentially transport one co-factor into the nucleus over the other. KC167 cells were co-transfected with plasmids encoding GFP- or RFP-labelled constructs to determine if nuclear transport was affected by the presence of both Vg and Tgi. Individual transfection of GFP-Sd, RFP-Vg and GFP-Tgi resulted in a nuclear localization for GFP-Sd, which has an NLS, as well as RFP-Tgi, and cytoplasmic punctae for RFP-Vg (**Figure 3.7A-C**). While neither Vg nor Tgi have a canonical nuclear localization signal (NLS) and both proteins are too large for passive diffusion into the nucleus, a general cytoplasmic localization was expected; the nuclear localization of GFP-Tgi is possibly a result of low-level expression of endogenous Sd in Kc167 cells (Cherbas et al., 2011), or potentially a non-canonical NLS within the peptide. When either Vg or Tgi were transfected alongside fluorescently-labelled Sd, both proteins were present in the nucleus of the cell (**Figure 3.7D-D", E-E"**). Sd has previously been shown to be necessary for Vg nuclear transport via an internal NLS located immediately next to

the DNA-binding domain (Halder et al., 1998; Magico and Bell, 2011). However, when Vg and Tgi were co-transfected into Kc167 cells, there was a preferential localization of Tgi into the nucleus and exclusion of Vg into the cytoplasm where it formed large aggregates (**Figure 3.7F-F"**). This posits a second possible mechanism for differential regulation of Tgi/Sd versus Vg/Sd target genes that does not rely on transcription factor binding site variations.

A negative feedback loop is established by Tgi and Sd

Titration of available Sd by Vg and Tgi by necessity would rely on a careful balance of the amount of Vg and Tgi in the cell. However, there would need to be a mechanism in place to alter the relative levels between Vg and Tgi in order to drive differential gene expression. Vg is well known to drive its own expression via a Vg/Sd-dependent feed-forward loop in the *vgQE* (Zecca and Struhl, 2007a) that expands the domain of Vg in the wing pouch. Because Tgi is expressed ubiquitously throughout the wing disc (Koontz et al., 2013), the use of exclusive domains of expression is not possible. Another possibility is the use of genetic control via the implementation of another feedback loop. Kc167 cells were co-transfected with either 6xMyc-Vg and 3xHA-Sd, 3xFLAG-Tgi and 3xHA-Sd, or 3xFLAG-Tgi and 6xMyc-Vg, and the resulting mRNA was analyzed by qPCR to determine if exogenously increased expression of either pair of genes affected expression of the third. Co-expression of Vg and Sd did not significantly alter expression of Tgi mRNA, and neither did co-expression of Tgi and Vg change the level of Sd mRNA (**Figure 3.8A**). However, co-expression of Tgi and Sd caused a significant increase in the level of Vg mRNA expressed in Kc167 cells. The increase in Vg resulting from high levels of Tgi and Sd co-expression may institute a negative feedback loop that allows for

the expansion of the field of Vg-expressing cells in the wing disc, which then reinforces itself via activation of a Vg enhancer.

Next, the expression of known Sd target genes in the wing were examined to determine if there was a differential regulation when Sd was co-expressed with either Vg or Tgi in Kc167 cells. Interestingly, this differential regulation was found for some but not all target genes, and for both differentiation-related and cell cycle-related targets (**Figure 3.8B**). *achaete* (*ac*), *spalt-major* (*salm*), *blistered* (*bs*) and *serrate* (*ser*) are Sd targets in the wing disc, and mediate different aspects of differentiation (Couso et al., 1995; Gómez-Skarmeta et al., 1995; Halder and Carroll, 2001; Halder et al., 1998). Salm is particularly interesting in the context of Tgi overexpression, as it is required to transduce the Dpp signal during development (Akiyama and Gibson, 2015; Bosch et al., 2017; Organista et al., 2015), which may help to explain the L5 vein shortening phenotype that is similar to a *dpp* or *gbb* mutant. *dE2F2* encodes an E2F family transcription factor that negatively regulates the G1/S-phase cell cycle transition (Korenjak et al., 2004). Sd is known to physically interact with dE2F1, a paralog of dE2F2, but there has yet to be any indication that Sd and dE2F2 share that interaction (Zhang et al., 2017a).

2.3 Discussion

While the function of Vg has been explored to a considerable extent in the past near-century since its original discovery (Morgan and Bridges, 1919), examination of its paralogue Tgi is in relatively early stages. This is some of the first evidence that Tgi has an important functional role to play during wing development. Balancing the relative levels of Tgi and Vg in the larval wing disc is required for cell survival and fate specification. Prior to this, Tgi was shown to interact with Sd and Yki in the larval wing and eye-antenna discs as well as the adult heart, where its ability to attenuate the overgrowth phenotype caused by ectopic expression of Yki requires expression of Sd (Guo et al., 2013; Koontz et al., 2013; Yu et al., 2015). Tgi also affects the differentiation of germ cells in the ovary, where it is again dependent on Sd for function (Li et al., 2015a).

The evidence for a competitive relationship between Vg and Tgi for Sd binding is exemplified by showing that both Vg and Tgi are able to co-immunoprecipitate with Sd, but do not co-immunoprecipitate with each other (**Figure 3.2**). There is previous evidence to indicate that Vg is able to form multipartite co-complexes with other proteins, as it was able to form a non-obligate complex with Sd and Mef2 (Deng et al., 2009), and has been shown to form a co-complex with Yki as well (Li et al., 2015a). Tgi has also previously been shown to interact with Sd and with Yki, but not both simultaneously (Koontz et al., 2013). Because both Vg and Tgi bind to the VID of Sd via their TONDU domains, the most simple theory is that one protein is displacing the other from interacting with Sd (Guo et al., 2013; Koontz et al., 2013; Simmonds et al., 1998). It was intriguing to see that there was no co-immunoprecipitation of Vg and Tgi. Vg and Sd are known to form multimeric complexes when bound to DNA, so there was potential for

the formation of larger co-complexes incorporating all three (Halder and Carroll, 2001). This may imply that the binding partner of Sd is the key to a repression/activation switch on specific genes, or to alternative gene targeting between Vg/Sd and Tgi/Sd complexes.

Examining the effect of altered Vg and Tgi levels *in vivo* showed that there is a dose-dependent response to increased Tgi and decreased Vg expression in the wing (**Figure 3.3**). Overexpression of Tgi using the *vg(M+Q)*:GAL4 driver caused a decrease in wing size, as well as cupping and shortening of the L5 vein. This effect was stronger in the hemizygous vg^{null} background, where only half of the normal expression level of Vg is maintained. When the difference between Vg and Tgi was maximized while still maintaining the potential for wing growth, the resulting wings were significantly smaller, ranging from slightly reduced in comparison to the *vg(M+Q)*:GAL4>UAS:FM-Tgi genotype to a largely undifferentiated structure with a significantly reduced tissue size. The $vg^{null/+}$, *vg(M+Q)*:GAL4>UAS:FM-Tgi wings also had shortening of the L5 vein as well as occasional loss of the posterior crossvein. The vg^{null} allele in the heterozygous state ($vg^{null/+}$) alone is insufficient to cause size or fate differences in the adult wing, indicating that half of normal Vg levels is enough to meet the necessary threshold to drive normal wing development. Escaper adults with homozygous vg^{null} phenotype have no wings whatsoever (Paumard-Rigal et al., 1998). The ectopic expression of Tgi is sufficient to antagonize normal Vg expression, and the stronger phenotypes resulting from reducing Vg expression in addition to providing ectopic Tgi shows that there is some degree of antagonism between both proteins. Further, the effect of Tgi overexpression seems to be dependent on Vg, as overexpression of Tgi outside the wing pouch using *tsh*:GAL4 had no observable effect on any wing structures. Sd is expressed both across the wing pouch as well as in parts of the hinge and

notum regions of the disc (Campbell et al., 1992; Guss et al., 2013), but there were no apparent defects in these regions. Tgi function then may be restricted to the wing pouch and not the entire disc, even though *Tgi* mRNA is ubiquitously expressed throughout the disc (Koontz et al., 2013).

Shortening of the L5 vein as well as loss of the posterior crossvein is frequently seen with TGF-β/BMP pathway mutations, especially *dpp* and *gbb* (Bangi and Wharton, 2006; Khalsa et al., 1998; Ray and Wharton, 2001; Serpe et al., 2005). The L2-L5 wing veins are specified sequentially in narrow fields running parallel to the anterior/posterior border in the wing pouch, with the L2 vein at the most anterior position and the L5 vein furthest to the posterior edge of the disc (Shimmi et al., 2014). The posterior crossvein is entirely formed from cells in the ventral portion of the wing disc (Díaz-Benjumea et al., 1989). Although the link between Vg and Dpp in the wing has been extensively studied, the interplay between TGF-β signaling and the Hippo pathway has not been examined in detail. During larval wing disc development, Dpp secreted from the anterior/posterior boundary results in activation of the *vgQE* via binding of the transcription factor Mad (Basler and Struhl, 1994; Kim et al., 1997). Loss of Mad blocks the expression of Vg by both being unable to directly activate Vg expression as well as mediating Wg signaling which is required for propagation of the Vg-inducing signal in the wing pouch (Eivers et al., 2009; Kim et al., 1997). In the ovary, Yki and Hh collectively work to inhibit BMP signaling through Dpp and Gbb (Huang et al., 2017), where Tgi and Sd are proposed to mediate default repression in absence of Yki (Koontz et al., 2013; Li et al., 2015a). It is possible that high Tgi expression in the wing disc is also repressing TGF-β signaling in areas where the concentration of Dpp diffused from the boundary is lowest, leading to shortened or absent wing veins, whereas Vg may be permitting or promoting this signal as a mechanism to recruit cells

into the wing pouch field. It also may explain why the posterior crossvein is absent, as there is a strong reduction in ventral compartment volume in the wing disc. What this theory does not explain is why the L2 vein was not also shortened, as it is roughly equidistant from the anterior/posterior boundary as L5 is but is entirely within the anterior domain. It could be informative to examine the effect of Tgi overexpression on Dpp pathway activity *in vivo* in the wing disc, possibly via a *Dad*-GFP reporter (Hamaratoglu et al., 2011) or through the expression of Dpp target genes such as *omb* and *sal*.

The loss of anterior compartment cells in the third instar wing disc (**Figure 3.4)** results in cupping in *vg(M+Q)*:GAL4>UAS:FM-Tgi and $vg^{null/+}$, *vg(M+Q)*:GAL4>UAS:FM-Tgi wings. Cupping is the result of an unequal amount of material available to form the dorsal and ventral surfaces of the wing during pupariation – a shortage of ventral cells results in a downward cupping effect as demonstrated with the adult wings listed. It is difficult to determine what causes the loss of ventral cells, as this could be due to either reduced cell proliferation or increased cell death within this domain. Other groups have shown that a decrease in Tgi expression results in diminished expression of a *diap1* reporter (Koontz et al., 2013). As reduced *diap1* expression is associated with relief of the inhibition on apoptosis (Hay et al., 1995), increased cell death may account for the loss of ventral compartment cells. On the other hand, knockdown of VGLL4 via *MiR-222* results in increased proliferation in gastric cancer, and a MiR-130 inhibition of VGLL4 in bladder cancer also caused increased proliferation, indicating that Tgi may also have some function in controlling cell cycle as well (Li et al., 2015c; Liu et al., 2018).

Another challenge in understanding the function of Tgi during development is the complete absence of known *cis*-regulatory elements controlling spatiotemporal expression of the gene. Recently a *Tgi*:GAL4 line derived from an insertion in the second intron has been released from the inSITE Enhancer Trap Project (**Figure 3.5**) (Gohl et al., 2011). The position of this element is curious in that Vg is also known for its internal enhancer sequences in the second and fourth introns (Guss et al., 2001; Kim et al., 1996; Williams et al., 1994). Although the *cis*-regulatory element controlling expression of GAL4 has yet to be fully defined in the *Tgi*:GAL4 enhancer trap line, the line itself is expresses ubiquitously throughout the wing disc. Overexpression of Tgi in its own domain resulted in wings that were smaller than wild type but had no observable differentiation defects. Smaller wings are also consistent with the concept of Tgi as a tumor suppressor. Overexpression of Vg in the same domain resulted in smaller wings as well, but also defects in anterior and posterior margin differentiation similar to but stronger than that caused by the rescue of vg^{null} wings by pseudo-phosphorylated Vg^{S215A} in Chapter 2. These wings resemble the phenotype of sd^{1} or sd^{EXT4} mutants (Anand et al., 1990; Campbell et al., 1991; Campbell et al., 1992; Paumard-Rigal et al., 1998), both of which are hypomorphic *sd* alleles. The fact that an overexpression of Vg causes a phenotype similar to an insufficient amount of Sd implies that at some point during development Tgi must associate preferentially over Vg with Sd in order to implement the proper genetic programming for formation of the wing. Proper spatiotemporal expression of Vg is also shown to be necessary for formation of the margin, reinforcing what was demonstrated in Chapter 2. It is impossible to tell if the L5 vein defect is corrected here in comparison to the *vg*:GAL4>UAS-FM-Tgi and $vg^{null/+}$, *vg*:GAL4>UAS-FM-Tgi genotypes, since there is no posterior margin for the vein to connect with. Remarkably, the overexpression of Sd in the Tgi domain results in a phenotype very similar to the $Tgi^{-/-}$ phenotype with weakly

motile larvae that die in first and second instar, and some very rare small third instar escapers with no pupae or adults. These larvae are also very poorly differentiated upon dissection, with very little in terms of identifiable morphological structures. While two null alleles of Tgi have been published, one is difficult to obtain (Guo et al., 2013) and the other is unstable (Koontz et al., 2013), possibly owing to a requirement for sufficient Tgi expression to reach adulthood as well as a confirmed necessity of Tgi in the adult ovary for proper function (Li et al., 2015a). The recapitulation of this phenotype by overexpression of Sd, and presumably higher association and activity of the Tgi/Sd complex, is a likely result of both reduction in cell number as well as poor tissue differentiation causing larvae to be unable to reach the checkpoints at the end of first or second instar and instead die of necrosis.

It is interesting to note that overexpression of Tgi using the s*d*:GAL4 driver also results in poorly differentiated and necrotic wing tissue from escaper adults (**Figure 3.6**). Escapers are also always female. The phenotype is consistent with the idea that Tgi is acting as a tumor suppressor, similar to the proposed function of VGLL4 in mammals (Zhang et al., 2014; Zhang et al., 2017b). It is interesting to note that this does not seem to affect the notum at all and instead is restricted to the wing blade itself. However, this may be a survivorship bias issue, as more strongly affected individuals may be part of the majority that do not survive to the end of pupariation. The fact that expression of an anti-*Tgi* RNAi (s*d*:GAL4>UAS:Tgi RNAi) did not cause a difference in wing size or fate has several potential explanations. First, the degree of knockdown ranged from 10-30%, which is not particularly strong. This may indicate that the degree of *Tgi* knockdown is simply insufficient to result in a phenotype. A RNAi screen in the notum showed that knockdown of *Tgi* caused a colour defect (Mummery-Widmer et al., 2009),

but this phenotype was not replicable using an independent RNAi line, leading to the possibility that the phenotype resulted from a second-site mutation or off-target effect. Another conceivable explanation is that loss of Tgi is unable to cause a size outgrowth of the wing simply because the wing area is maximized already. Mutations causing larger wings are comparatively far rarer than mutations causing smaller or absent wings, even though outgrowth of the wing disc itself is frequently seen; mutation of the cell adhesion protein *echinoid* (*ed*) is able to result in non-uniform increases in wing size, but also ectopic vein tissue not present with Tgi knockdown (Bai et al., 2001).

There are several potential solutions to the challenge of developing a *Tgi* knockdown system *in vivo*. One option would be design of a stronger RNAi line that targets both isoforms of *Tgi* or simply has a more effective target sequence than the currently available lines. Engineering a new RNAi line is technologically simple but in practice requires a large amount of validation and consideration of off-target effects. Alternatively, incorporation of increased *dicer-2* (*dcr-2*) expression with the currently existing RNAi line could hopefully strengthen the effect of the knockdown by increasing the capacity to process dsRNA at the cellular level. Another alternative is a very recent development in *Drosophila*, which is the ability to activate CRISPR/Cas9-mediated gene knock-in or knockout conditionally in cell subsets (Jia et al., 2018; Lee et al., 2018; Port et al., 2014). This technique relies on conditional expression of the Cas9 protein using the UAS/GAL4 system coupled to tissue-specific promoters, combined with ubiquitous expression of a sgRNA targeting the gene of interest using the U6:3 promoter. This system will then only be able to activate sgRNA-mediated genome editing in the tissues where Cas9 is conditionally expressed. The benefit to this system is that the spatial and temporal control of

Cas9 can separate the effects of gene knockout into different compartments. *Tgi*$^{-/-}$ flies have complete larval lethality, so the effect of *Tgi* knockout in the wings alone can't be examined because no adult wings ever form. Restricting *Tgi* knockout to only the wing discs, or even regions within the disc, isolates the pleiotropic effects of the currently available mutant. This system does have several caveats (Peng et al., 2016). There would need to be a way to monitor whether none, one or two alleles of the gene have been targeted in knockout tissues. Additionally, the CRISPR/Cas9 system relies on DNA repair systems incorrectly repairing the DNA. This system is imperfect, and repairs are not necessarily identical in all cells; some may contain deletions of large regions, others a small number of mutant bases, and some might be repaired correctly. This mosaicism is also compounded by off-target effects of sgRNAs, although targeted engineering of Cas9 variants combined with careful sgRNA sequence selection can reduce this considerably.

The mechanistic aspect of the Tgi/Vg competition for Sd is interesting in that both Vg and Tgi are competing for the same domain on Sd instead of competing for separate binding domains that prevent co-binding due to steric hindrance. Two non-exclusive possibilities exist to explain where or how Vg and Tgi compete. The first possibility is a competition for Sd as it iss pre-bound to the DNA. This would propose that both Vg and Tgi are transported into the nucleus by Sd, or another unknown factor capable of transporting Tgi into the nucleus as Sd has been shown to be required for Vg transport (Halder et al., 1998; Simmonds et al., 1998). Sd would then be essentially poised to undertake repressive or activating function depending on whether Tgi or Vg is bound to the Vestigial interaction domain (VID) of Sd. The second possibility, presupposing that the limiting factor is the availability of unbound Sd, is that competition for Sd binding at the

VID takes place in the cytoplasm, where unbound Sd would preferentially associate with either Tgi or Vg for active transport into the nucleus. If this scenario were the case, the subcellular localization of Vg and Tgi when co-expressed with Sd should be broadly exclusionary such that one remains majority cytoplasmically and the other is transported into the nucleus. Co-expression of Sd and either Vg or Tgi in Kc167 cells shows that both Vg/Sd and Tgi/Sd complexes can enter the nucleus, while expression of either Vg or Tgi alone causes a majority cytoplasmic accumulation, which is unsurprising as Kc167 cells express relatively low levels of endogenous Sd (Cherbas et al., 2011). However, when both Vg and Tgi are co-transfected into Kc167 cells without addition of exogenous Sd, Tgi accumulates in the nucleus while Vg is more strongly cytoplasmic. This does not preclude competition at the DNA level, however, as there is still some level of Vg in the nucleus and Tgi in the cytoplasm. The concept of competition for Sd binding in general has been previously demonstrated, and the model proposed here is certainly simplified in comparison to the biological reality. Sd has been shown to bind a number of other proteins, including Yki (Goulev et al., 2008), Vg (Simmonds et al., 1998), Mask (Sidor et al., 2013), and dE2F1 (Zhang et al., 2017a). It has also been shown that Yki is able to competitively interfere with Vg binding to Sd, likely through a steric hindrance due to the proximal positioning of the VID and PPxY motifs required for Yki interaction (Li et al., 2015a; Salah and Aqeilan, 2011). Tgi is also able to bind Yki via three PPxY motifs (Koontz et al., 2013), which leaves open an interesting question on how Yki affects the formation of Vg/Sd and Tgi/Sd complexes.

Because both Vg/Sd and Tgi/Sd complexes are required to form *in vivo* during development, as shown in this chapter and by many other groups, there must therefore be some means of regulating which co-factor Sd is interacting with. There are several potential options, all of which

may be responsible in part. One alternative is that post-translational modification of any one or more of the three proteins may cause a conformational change or quaternary structure change that affects the ability of Vg, Tgi or Sd to form a specific complex (**Figure 3.9A**). In Chapter 2, post-translational modification of Vg at Ser-215 was demonstrated (Pimmett et al., 2017), and although it doesn't entirely attenuate the ability of Vg to associate with Sd since the wing blade is able to form, phosphorylation may affect the relative stability of the complex. Vg is also necessarily sumoylated at an unidentified residue, and blocking sumoylation results in the inability of Vg to activate the *vgQE in vitro* (Takanaka and Courey, 2005). All TEAD proteins in humans, as well as Sd in *Drosophila*, are palmitoylated (Chan et al., 2016; Noland et al., 2016); palmitoylation of TEADs is not necessary for binding of VGLL4 and does not affect nuclear localization, but is required for formation of complexes between TEADs and the Yki orthologues YAP1 and TAZ (Chan et al., 2016). VGLL4 in mice is post-translationally modified by acetylation at Lys-225, which inhibits the formation of TEAD1/VGLL4 complexes in the cardiac muscle (Lin et al., 2016). It is also targeted for phosphorylation by cyclin-dependent kinase 1 (CDK1) in mice; interestingly, blocking phosphorylation at four mitotically key residues increased the stability of the VGLL4/TEAD1 complex (Zeng et al., 2017).

A second alternative is that one co-factor can outcompete the other based on a relative increase in abundance resulting in increased frequency of stochastic interactions initiating formation of a co-complex (**Figure 3.9B**). This appears to be partially the case with Vg and Tgi. While co-expression of Vg and Tgi does not alter Sd mRNA expression in Kc167 cells, and co-expression of Vg and Sd does not alter the levels of *Tgi* mRNA, co-expression of Tgi and Sd results in an 84-fold increase in the level of *vg* mRNA. This essentially forms a negative feedback loop

wherein Tgi suppresses its own interaction with Sd by increasing the level of its competitor. The existence of negative feedback loops in *Drosophila* is well understood, as they are a component of several key systems such as the circadian clock (Mendoza-Viveros et al., 2017; Sivachenko et al., 2013). Sd is able to bind to both the *vgME* and the *VgQE*, where previous to this it was known to interact with Vg (Guss et al., 2001; Kim et al., 1996; Williams et al., 1994). A Tgi/Sd complex may be able to co-opt this to upregulate Vg expression to initiate a wave of recruitment of putative wing blade cells in the wing pouch. However, this enhancer also requires the cooperative activity of other signals such as Dpp and Wg (Kim et al., 1996; Kim et al., 1997).

Competition between Vg and Tgi for Sd binding could occur in either the cytoplasm or the nucleus (**Figure 3.9C**). This adds a further layer of complexity to the model. There are two key aspects to the Vg/Sd interaction that enables the complex to function; first Sd is required to bring Vg into the nucleus, and secondly Vg is required by Sd to appropriately target the *cis*-regulatory elements of specific genes and recruit the transcriptional machinery for target gene expression (Halder and Carroll, 2001; MacKay et al., 2003; Magico and Bell, 2011). Whether or not Sd is also required to bring Tgi into the nucleus is not known and a priority for future research, but is likely based on the absence of any identified type of NLS within the Tgi peptide. If it is the case that Sd is required for nuclear transport of both Tgi and Vg, then one mechanism for regulatory control of Sd is through preferential nuclear transport. This theory implies that the interaction with Sd for shuttling to the nucleus is the limiting factor for which Vestigial-like protein is able to form a functional transcriptional complex with the DNA. Some support for this theory lies in the live cell imaging wherein co-transfection of fluorescently tagged Tgi and Vg results in a nuclear localization of Tgi and cytoplasmic sequestration of Vg. Further experiments will be

required to determine whether or not Tgi requires Sd for nuclear localization, and whether or not there is a difference in binding affinity between Vg and Tgi for the VID of Sd.

A second competitive mechanism is the substitution of Vestigial-like proteins on Sd at the site of the DNA itself (**Figure 3.9D**). This model posits Sd as a potentiator of transcription, and the actual activation or repression of a target gene is dependent on which binding partner is partnered with Sd. Analysis of mRNA expression of known Sd target genes showed that there is a degree of cross-regulation between Vg/Sd and Tgi/Sd complexes, which lends some credence to this model as well. Curiously, it was not a uniform suppression or enhancement of transcription response – some targets had increased expression and others were repressed. To investigate this in more detail, it would be interesting to look at the degree of overlap between Vg/Sd- and Tgi/Sd-bound *cis*-regulatory elements and compare the mRNA expression from those particular genes under each condition.

Differential gene regulation by Vg/Sd and Tgi/Sd complexes is a deceptively complex level of control for fate determination. Examination of some known Sd target genes indicated that at least a subset of these are differentially regulated by Vg/Sd compared to Tgi/Sd in Kc167 cells. It is unclear what separates those genes differentially regulated by either complex. As Kc167 cells are not a wing-derived cell line, it may simply be that some of the target genes require other transcriptional regulators not present in the cell line for any noticeable activation or cross-regulation. It is interesting that targets are not collectively repressed or activated by one complex over the other, which is a departure from the existing literature confoundingly describing both Vg/Sd and Tgi/Sd as repressive complexes (Deng et al., 2009; Koontz et al., 2013). The

biological reality appears to be more complicated than simple activation versus repression, and the causes of this behaviour is certainly worthy of further examination.

```
DMel_TGI-PA     ---MALRLDYRCLLDAFEDYYYHKEIQRLVAETAGGATATSPASSASSASSTASISSASC
DMel_TGI-PB     ---METALD-----------------------------------------------------
HSap_VGLL4      ---METPL--------------D---------------------------------------
MMus_VGLL4      MLFMKMDLLN-----------YQ---------------------------------------
DRer_VGLL4L     -----MAVTN-----------FH---------------------------------------
DRer_VGLL4B     MLFTKMDLLN-----------YQ---------------------------------------
CEle_R08C7.12   -------MAS-----------PHAE-------------------------------------
                       :
DMel_TGI-PA     SSGPSTSSIVSSAASSHGSLAQVATARAAAALADQQALASQRAMFYNVQHPQQLEQLHAL
DMel_TGI-PB     --------VLSRAATM-----------------------------------------------
HSap_VGLL4      --------VLSR---------------------------------------------------
MMus_VGLL4      --------YLDK---------------------------------------------------
DRer_VGLL4L     --------YITR---------------------------------------------------
DRer_VGLL4B     --------YLDK---------------------------------------------------
CEle_R08C7.12   --NDMVPEMIDH-----------------------------------------------------
                         :
DMel_TGI-PA     QAESGNQQMHPQANADPNASSMANSLLWQPWRDLQQAAAMHHQLYRQQQQQLQLHSEMRA
DMel_TGI-PB     ------VQNNP-------------------------------------------SEMRA
HSap_VGLL4      ------------------------------------------------------------
MMus_VGLL4      ------------------------------------------------------------
DRer_VGLL4L     ------------------------------------------------------------
DRer_VGLL4B     ------------------------------------------------------------
CEle_R08C7.12   ------------------------------------------------------------

DMel_TGI-PA     TSKVLTTTKWRRERRQRSAGYQPHEAGNSERERERERDREDRDMDSPIDMSVTTGALKQR
DMel_TGI-PB     TSKVLTTTKWRRERRQRSAGYQPHEAGNSERERERERDREDRDMDSPIDMSVTTGALKQR
HSap_VGLL4      ------------------------------------------AASLVHADDEKREAALR
MMus_VGLL4      -----------------------------------------MNNNIGVLCYEGEASLR
DRer_VGLL4L     ----------------------------------------MSSGFKVYILEGQPNLR
DRer_VGLL4B     -----------------------------------------MNNNIGILCYEGDAALR
CEle_R08C7.12   --RHLQMWKWLHSR-------SGARGNTSETSFESSVSVSTNSFDFSADMSRSIDSSSSR
                                                                        *
```

```
DMel_TGI-PA     ASPPPPYREPLPGTNYAANSRPSVITQAPPKREPPEQAHSTDMAMCDIDEHFRRSLGENY
DMel_TGI-PB     ASPPPPYREPLPGTNYAANSRPSVITQAPPKREPPEQAHSTDMAMCDIDEHFRRSLGENY
HSap_VGLL4      GE---PRMQTLPVASALSSHRTGPPPISPSKRKFSMEPGDEDL---DCDNDHVSKMSRIF
MMus_VGLL4      GE---PRMQTLPVASALSSHRTGPPPISPSKRKFSMEPGDKDL---DCENDHVSKMSRIF
DRer_VGLL4L     SE---------DRFRHMTSDRVRMRPAHPMKRKHSSDRGR------TLEERRERALSKCV
DRer_VGLL4B     GE---SRMQSL--SSAVSNHRTGPPPISPSKRKHSAEQADDDI---DCNSEHVAKMSRLF
CEle_R08C7.12   MLPSPITNFVTPSSSFSSHQMHDIYSLAASYLQAPPPPYTPTTAFHPHNAHQLLLLHNMT
                                :       .  .   : .             :      : .

DMel_TGI-PA     AALFAKKSPTPTPTPTPSPSGTPKQQVSPLAYGLPSSTSTAASQHYQQQRSPLAKSGWVI
DMel_TGI-PB     AALFAKKSPTPTPTPTPSPSGTPKQQVSPLAYGLPSSTSTAASQHYQQQRSPLAKSGWVI
HSap_VGLL4      NPHLNKTANGDCRR---DPRER---SRSPIERAVAPTMSLHGSHLY------TSLPSLGL
MMus_VGLL4      SPHLNKTVNGDCRR---DPRER---SRSPIERAAAPAVSLHGGHLY------ASLPSL-M
DRer_VGLL4L     ANSARRSSGFSIPE---SPTSTWSPTASPTHLIPSPVFS-----------------SPVM
DRer_VGLL4B     AAQLGKPANGDYRK---DPRER---SRSPIERMAAPSMSLVGGH-H------LYMPSLAL
CEle_R08C7.12   AAVQTPEDPDIDVVGLADTTNLVSLNDKEDEEKLDQTTESEESDRISI--------STTE
                              ..       .         .                .

DMel_TGI-PA     LEPESLQPE---LPPPQEEPLPLSLA-LHRTQTPPSPPPSATGSAPALPTAVSQVMEAAV
DMel_TGI-PB     LEPESLQPE---LPPPQEEPLPLSLA-LHRTQTPPSPPPSATGSAPALPTAVSQVMEAAV
HSap_VGLL4      EQPLALTKN--SLDASRPAGLSPTLTPGERQQNRPS------------------VITCAS
MMus_VGLL4      EQPLALTKN--SSDTGRSA--------VERQQNRPS------------------VITCAS
DRer_VGLL4L     DEPLALIKK---PRPEPEKTESQNKA-TTQIQMRPS------------------VITCVS
DRer_VGLL4B     DQPLALTKN---MDSSRSMGISPTASPVERQQNRPS------------------VITCAP
CEle_R08C7.12   ECPLDLTFKPTSLDSPTSSTFIP---------LRPS------------------VII---
                  *  *  :     .                    **                  *:

DMel_TGI-PA     AGRRILDTPHHTPPRYNTPPPPPPAYGIAGTTVVAPTLTPTPTPNPTPSQIPTPTPSMPA
DMel_TGI-PB     AGRRILDTPHHTPPRYNTPPPPPPAYGIAGTTVVAPTLTPTPTPNPTPSQIPTPTPSMPA
HSap_VGLL4      AGARNCNLSHCPIAHSGCAAPGPASY------------------RRPPSAATTCDPV---
MMus_VGLL4      AGARNCNLSHCPIAHSGCSAPGSASY------------------RRPPSATATCDPV---
DRer_VGLL4L     SASRSTKQDCCN--HSTAVSKHSYDH-----------------------------------
DRer_VGLL4B     ANNRNCNLSHCTGSHNGCSPGLNASY------------------RRASNSNTACDPV---
CEle_R08C7.12   -------DHHIPKPHT-----------------------------------------------
                              :
```

```
DMel_TGI-PA     IIRVKAEPGLAAVAASSTQTPPASPTSSTNISIFTKTEASVDDHFAKALGETW-KKLQGG
DMel_TGI-PB     IIRVKAEPGLAAVAASSTQTPPASPTSSTNISIFTKTEASVDDHFAKALGETW-KKLQGG
HSap_VGLL4      -----VEEHFRRSLGKNYKEPEPAPNS-------VSITGSVDDHFAKALGDTW-LQIKAA
MMus_VGLL4      -----VEEHFRRSLGKNYKEPEPAPNS-------VSITGSVDDHFAKALGDTW-LQIKAA
DRer_VGLL4L     -----VEEHFQRSLGINYHR------A-------TSISVSVDDHFAKALGDKW-LQLKAS
DRer_VGLL4B     -----IEEHFRRSLGKNYKEPEPVTNS-------VSITGSVDDHFAKALGETW-LQIKA-
CEle_R08C7.12   --------SVRRSMSSVSSS------A-------SSTQEEVAAHFRRSLSGKWPKRCKVN
                         .    .           :        .   .*  ** ::*. .*  : :

DMel_TGI-PA     HKE-------------------------------------------------------
DMel_TGI-PB     HKE-------------------------------------------------------
HSap_VGLL4      KDGASSSPESASRRGQPASPSAHMVSHSHSPSVV-----S--------------------
MMus_VGLL4      KDSASSSPESASRRGQPASPTAHMVSHSHSPSVV-----S--------------------
DRer_VGLL4L     SSSCHSSSSSSS-SSPPSSP-TFIHSPGYSPKRARKDSSSPTTTTP-------NFWSD--
DRer_VGLL4B     -KGGSSSPD--------ASPNTHMVNHNHSPSLV-----S--------------------
CEle_R08C7.12   SEEARNSPLRRRPSFNTHTSVSSLSVHSVSPT--------PPVTSSAQTIIVNNHCSDTT

                 .

DMel_TGI-PA     -------------------------
DMel_TGI-PB     -------------------------
HSap_VGLL4      -------------------------
MMus_VGLL4      -------------------------
DRer_VGLL4L     -------------------------K
DRer_VGLL4B     -------------------------
CEle_R08C7.12   LSVADHFRRALLGKGLFDFQRKSNK
```

Figure 3.1: Tgi is an evolutionarily conserved protein homologous to humans as well as other model systems. MAFFT (Kuraku et al., 2013) alignment of the *Drosophila* TGI-PA and TGI-PB isoforms, as well as the human (HSap), mouse (MMus), *Danio rerio* (DRer), and *Caenorhabditis elegans* (CEle) protein sequences show substantial regions of homology. Outlined are two TONDU domains (TONDU-1 in blue and TONDU-2 in yellow) necessary for interaction with Scalloped (Guo et al., 2013; Koontz et al., 2013).

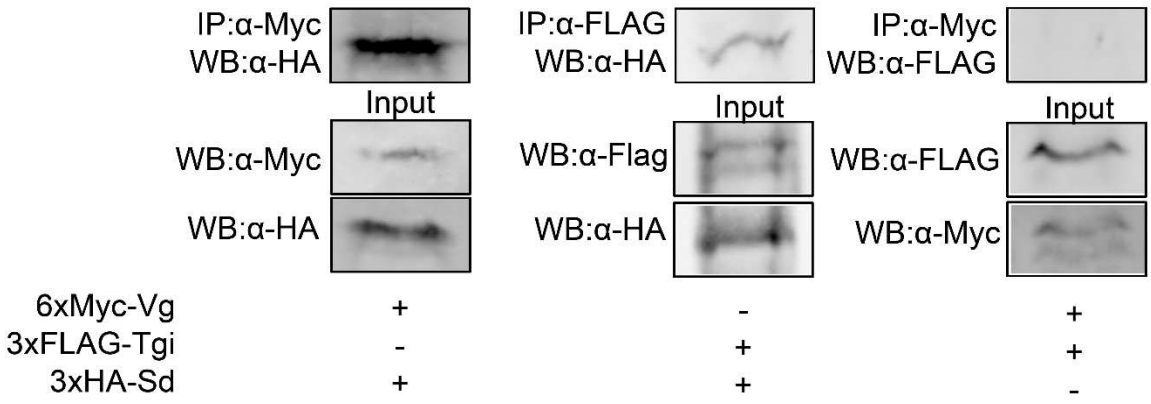
IP:α-Myc
WB:α-HA
Input
WB:α-Myc
WB:α-HA
IP:α-FLAG
WB:α-HA
Input
WB:α-Flag
WB:α-HA
IP:α-Myc
WB:α-FLAG
Input
WB:α-FLAG
WB:α-Myc
6xMyc-Vg + - +
3xFLAG-Tgi - + +
3xHA-Sd + + -

Figure 3.2: Vestigial and Tgi do not form co-complexes. Co-immunoprecipitation of Kc167 cell lysates transfected with indicated constructs show that 6xMyc-Vg and 3xHA-Sd form a co-complex (left), and 3xFLAG-Tgi and 3xHA-Sd also form a co-complex (centre). However, 6xMyc-Vg and 3xFLAG-Tgi are unable to co-immunoprecipitate together (right), indicating a mutual exclusion from protein complexes.

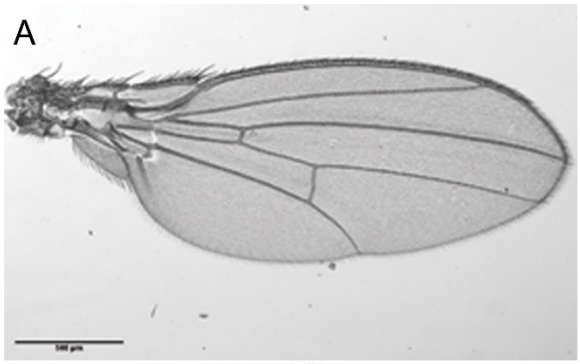

w^{1118}

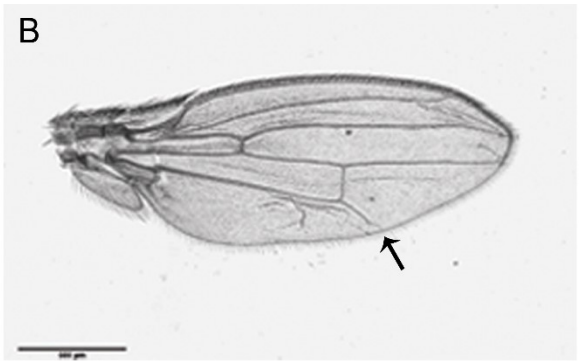

vg(M+Q):GAL4>UAS:FM-Tgi

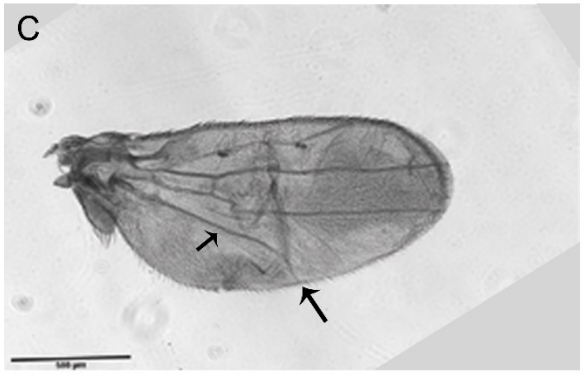

$vg^{null/+}$, *vg(M+Q)*:GAL4>UAS:FM-Tgi

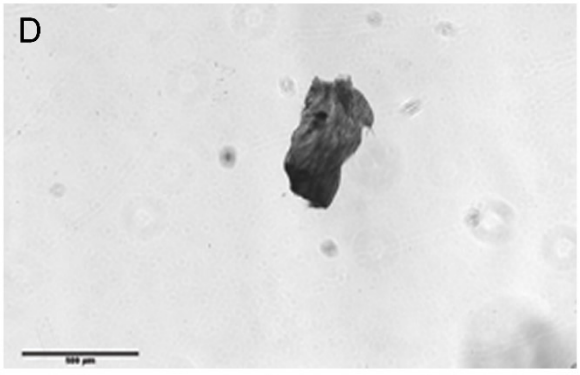

$vg^{null/+}$, *vg(M+Q)*:GAL4>UAS:FM-Tgi

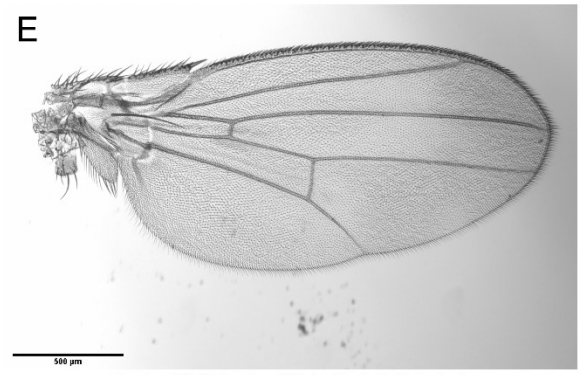

tsh:GAL4>UAS:FM-Tgi

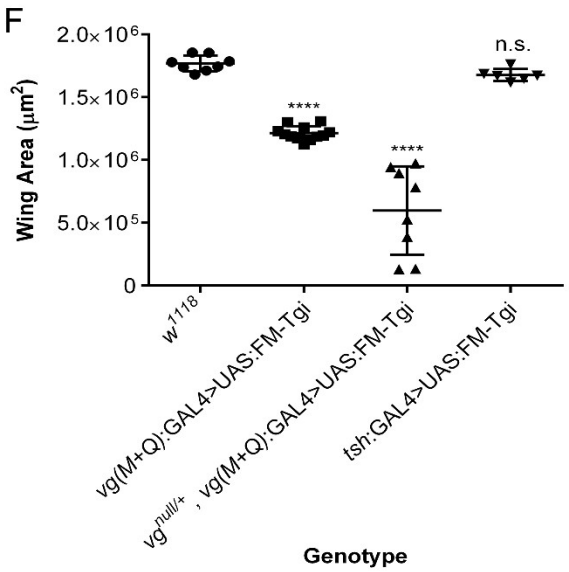

Figure 3.3: Altering levels of Tgi and Vg relative to each other results in defects in the adult wing. A) a w^{1118} adult wing demonstrating normal size and structure. N = 8 independent biological replicates, n ≥ 5 per replicate. B) Increased levels of Tgi in the domain of Vg cause shrinking of the wing volume, wing cupping, and shortening of the L5 vein (arrow). N = 12 independent biological replicates, n ≥ 4 for each replicate. C and D) Increased *Tgi* expression combined with hemizygous reduced *vg* expression results in a smaller wing, increased wing cupping, loss of the posterior crossvein (C; left arrow) shortening of the L5 vein (C; right arrow). Panel D shows strongest affected phenotype with minimal identifiable wing structures. N = 8 independent biological replicates with n ≥ 5 for each replicate. E) Overexpression of *Tgi* under the control of a *tsh:*GAL4 driver showed no significant difference in wing size or differentiation. N = 6 independent biological replicates with n ≥ 4 for each replicate. F) Wing area diminishes in a dose-dependent manner based on relative increase in *Tgi* expression coupled with decrease in v*g* expression. Scale bar for wings indicates 500 μm and **** indicates $p<0.001$.

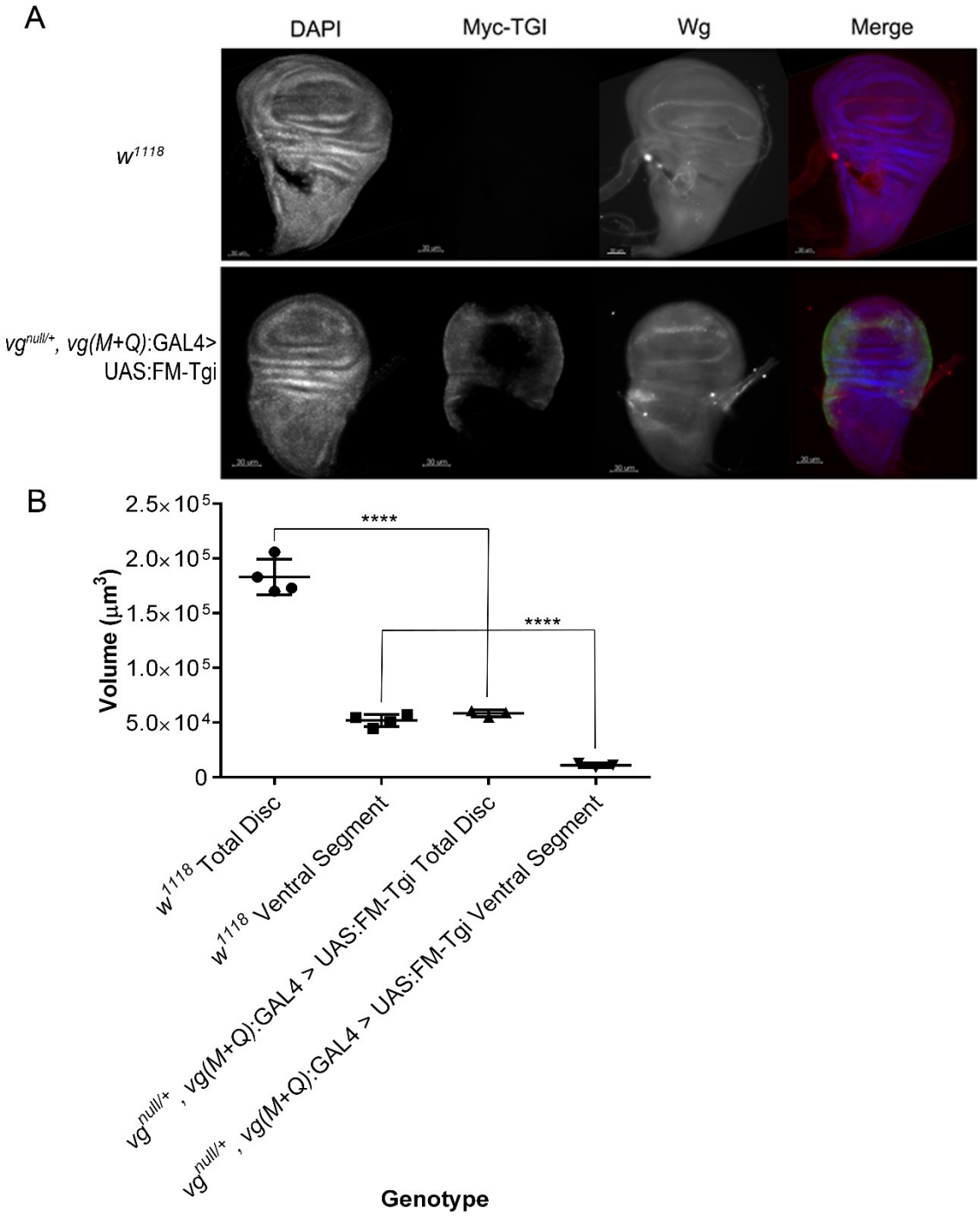
A
DAPI
Myc-TGI
Wg
Merge
w1118
vgnull/+, vg(M+Q):GAL4>
UAS:FM-Tgi
B
2.5×10^5
2.0×10^5
1.5×10^5
1.0×10^5
5.0×10^4
0
Volume (μm^3)
****
****
w1118 Total Disc
w1118 Ventral Segment
vgnull/+, vg(M+Q):GAL4 > UAS:FM-Tgi Total Disc
vgnull/+, vg(M+Q):GAL4 > UAS:FM-Tgi Ventral Segment
Genotype

Figure 3.4: Cupping of the wing is the result of cell loss in the ventral compartment. A) Comparison of third instar larval wing discs from w^{1118} (upper panels) and $vg^{null/+}$, *vg(M+Q)*:GAL4>UAS:FM-Tgi larvae. DAPI is shown in blue, anti-Tgi in green, and anti-Wg in red. Scale bar indicates 30 μm. B) Quantification of the total disc volume and ventral segment volumes for both genotypes. N = 4 for w^{1118} discs with n = 4 for each replicate, and N = 3 for $vg^{null/+}$, *vg(M+Q)*:GAL4>UAS:FM-Tgi discs with n = 4 for each replicate.

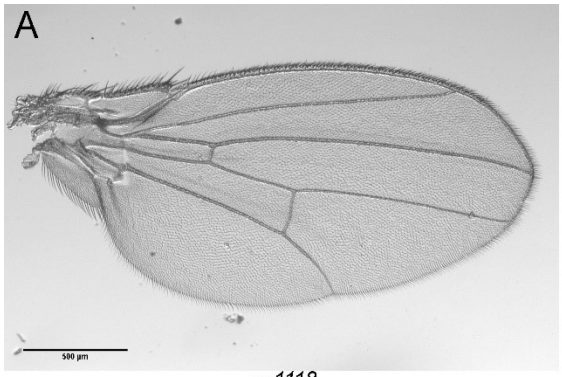

w^{1118}

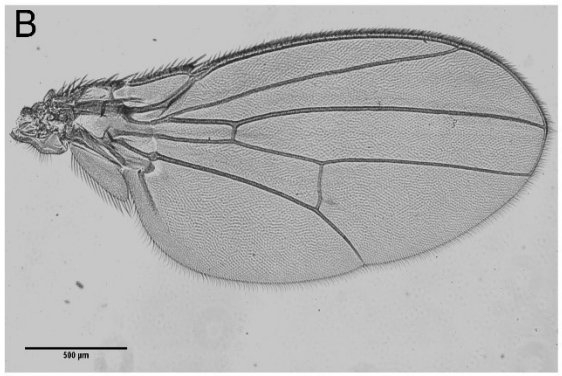

Tgi:GAL4>UAS:FM-Tgi

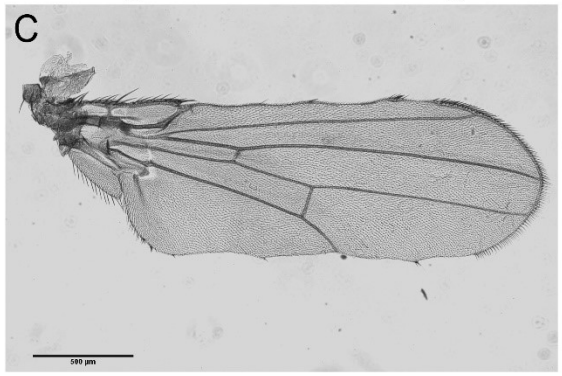

Tgi:GAL4>UAS:HA-Vg

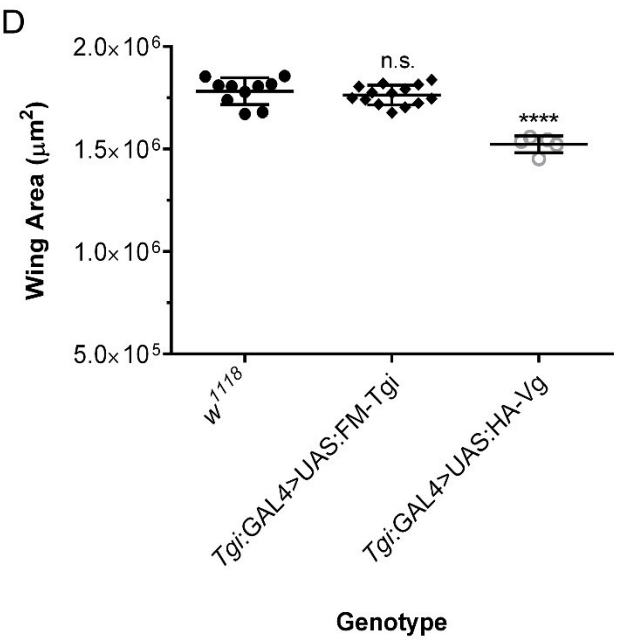

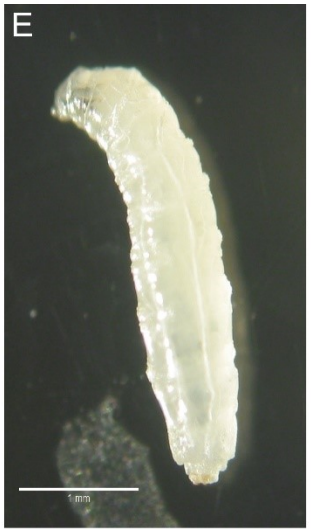

w^{1118}

Tgi:GAL4>UAS:FM-Sd

Figure 3.5: Ectopic expression of Vg or Sd in the *Tgi*:GAL4 domain results in **** A) A w^{1118} wing showing normal size and structure. N = 10 independent biological replicates with n ≥ 4 for each replicate. B) Overexpression of Tgi using the *Tgi:*GAL4 driver results in no significant change in wing size or structure. N = 14 independent biological replicates with n ≥ 4 for each replicate. C) Overexpression of Vg using the *Tgi*:GAL4 driver results in wings that are scalloped along the anterior and posterior margins. N = 5 independent biological replicates with n ≥ 6 for each replicate. D) The wing surface area of *Tgi:*GAL4>UAS:FM-Tgi is not significantly different than wildtype, but wings from the *Tgi:*GAL4>UAS:HA-Vg genotype are significantly smaller. E) A w^{1118} third instar larva showing normal size. F) Third instar larva resulting from overexpression of Sd via *Tgi:*GAL4 are very rare and smaller than wild type. Scale bar for wings indicates 500 μm and scale bar for larvae indicates 1 mm. **** indicates $p<0.001$.

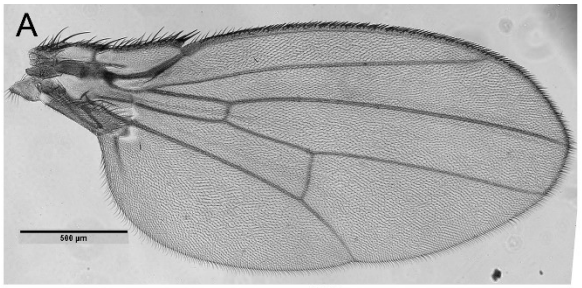

w^{1118}

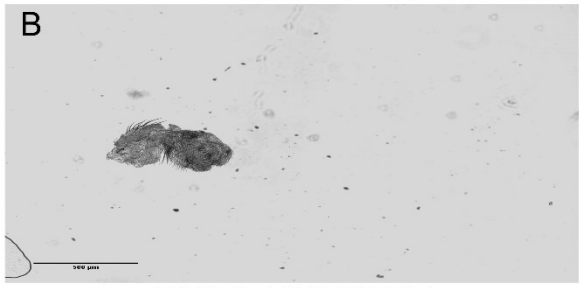

sd:GAL4>UAS:FM-Tgi

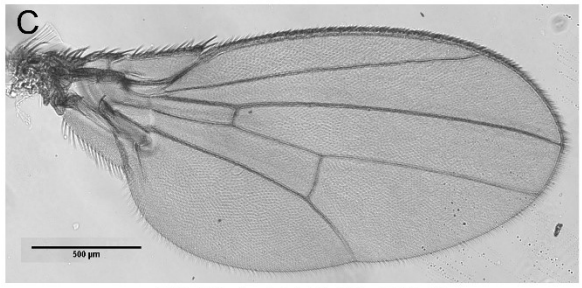

sd:GAL4>UAS:*Tgi* RNAi

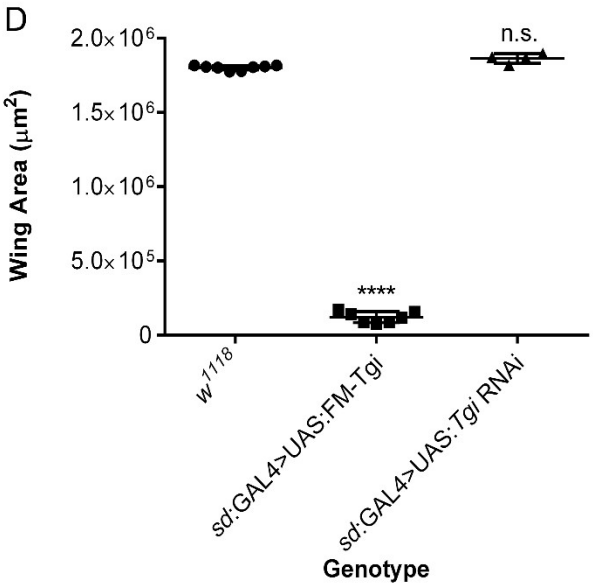

Figure 3.6: Altering Tgi expression in the Sd domain results in undifferentiated and necrotic tissue. Scale bars indicate 500 μm. A) A w^{1118} wing showing normal size and structure. N = 8 independent biological replicates with n ≥ 4 for each replicate. B) Wings from *sd*:GAL4>UAS:FM-Tgi female adults are necrotic, broadly undifferentiated, and fragile. N = 7 independent biological replicates with n ≥ 3 for each replicate. C) Expression of a dsRNA targeting *Tgi* (UAS:*Tgi* TRiP) via *sd*:GAL4 shows no change in wing differentiation or structure. N = 4 independent biological replicates with n ≥ 4 for each replicate. D) Quantification of wing area relative to controls shows a significantly smaller size for *sd*:GAL4>UAS:FM-Tgi wings, but no difference for *sd*:GAL4>UAS:*Tgi* RNAi wings.

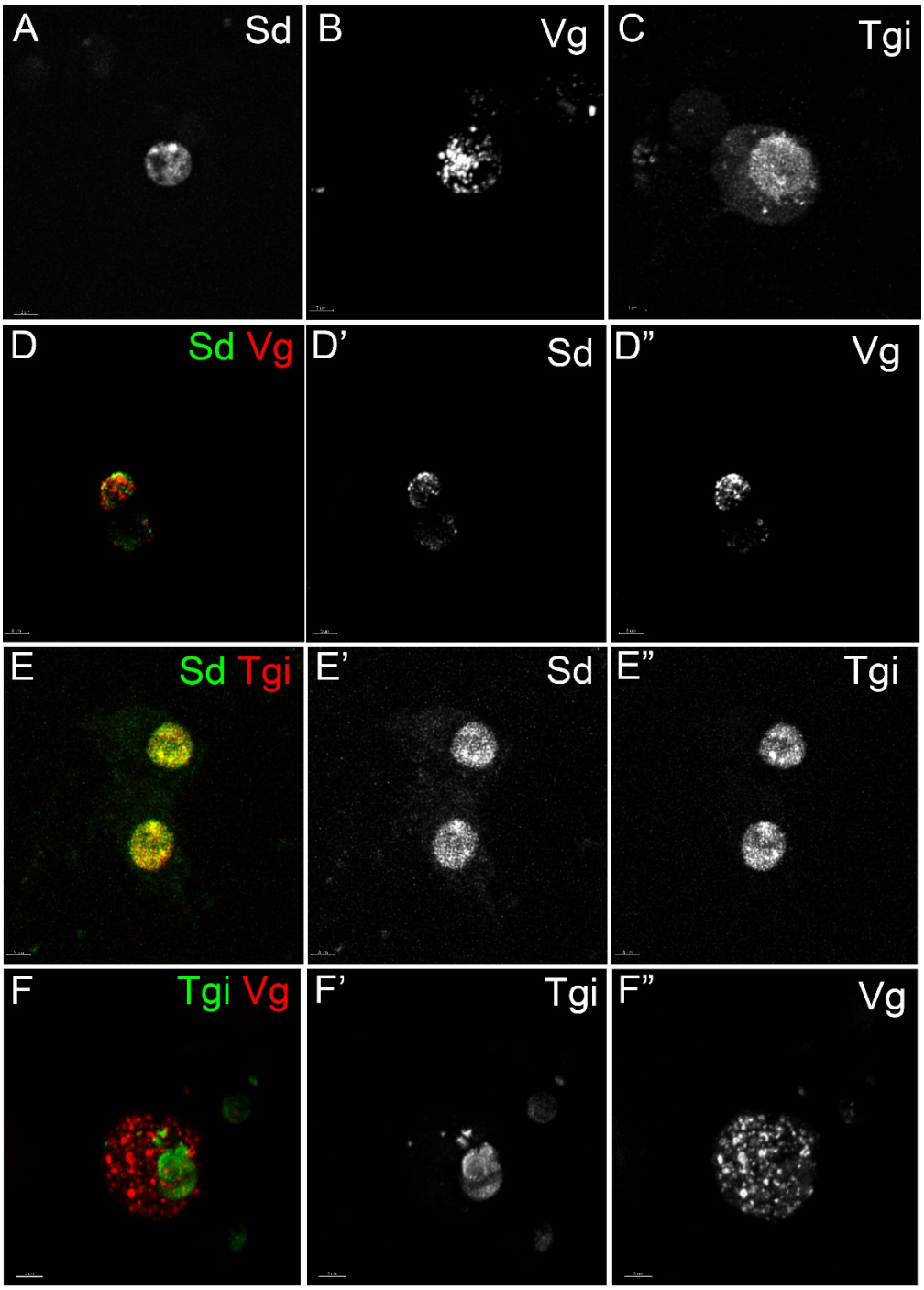
A
Sd
B
Vg
C
Tgi
D
Sd Vg
D'
Sd
D"
Vg
E
Sd Tgi
E'
Sd
E"
Tgi
F
Tgi Vg
F'
Tgi
F"
Vg

Figure 3.7: Live imaging of Kc167 cells shows subcellular separation of Vg and Tgi domains. Scale bar is 3 μm. A-C) Kc167 cells individually transfected with GFP-Sd, RFP-Vg and GFP-Tgi. Not shown is RFP-Tgi, which is identical to GFP-Tgi. D-D") Co-transfection of GFP-Sd and RFP-Vg shows a combined nuclear localization of both proteins. E-E") Co-transfection of GFP-Sd and RFP-Tgi indicates RFP-Tgi is nuclear and GFP-Sd is largely nuclear with small amounts of cytoplasmic protein. F-F") Co-transfection of GFP-Tgi and RFP-Vg shows that GFP-Tgi is localized to the nucleus while RFP-Vg is localized in punctate bodies in the cytoplasm.

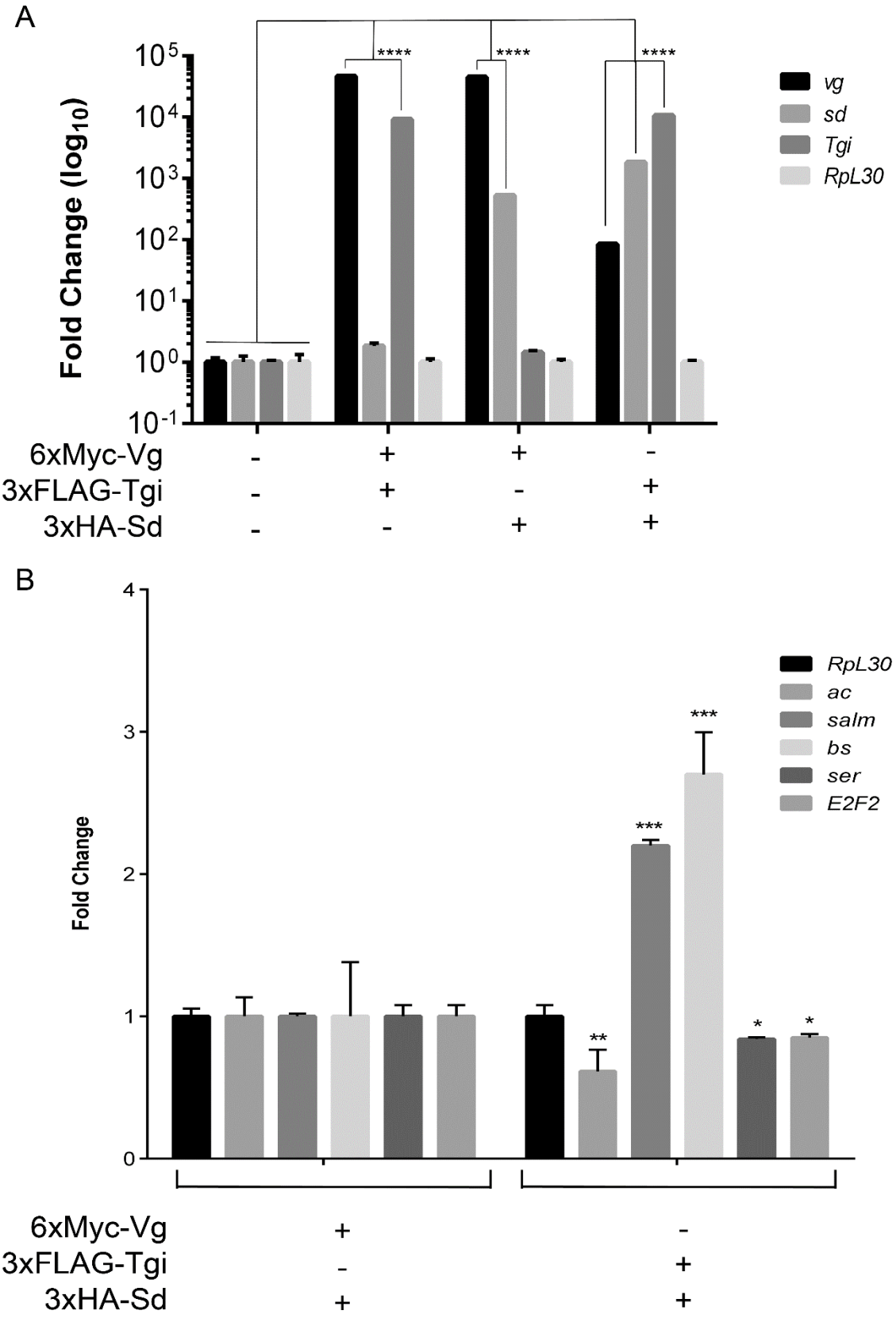
A
Fold Change (log10)
10^5
10^4
10^3
10^2
10^1
10^0
10^-1
****
****
****
vg
sd
Tgi
RpL30
6xMyc-Vg - + + -
3xFLAG-Tgi - + - +
3xHA-Sd - - + +
B
Fold Change
4
3
2
1
0
RpL30
ac
salm
bs
ser
E2F2
***
***
**
*
*
6xMyc-Vg + -
3xFLAG-Tgi - +
3xHA-Sd + +

Figure 3.8: Tgi induces expression of its own competitor by upregulating *vg* mRNA. A) qPCR analysis of Kc167 cells co-transfected with the indicated plasmids show that *Tgi* mRNA is not upregulated in response to increased expression of Vg and Sd, and *sd* expression is not induced by increased expression of Vg and Tgi. However, increased expression of Tgi and Sd causes an 84-fold upregulation of *vg* mRNA. B) qPCR of Sd target genes shows differential regulation in Kc167 cells overexpressing 6xMyc-Vg and 3xHA-Sd (left) compared to cells overexpressing 3xFLAG-Tgi and 3xHA-Sd (right). N = 3 independent biological replicates for both analyses. ** indicates $p<0.05$, ** indicates $p<0.01$, and **** indicates $p<0.001$.

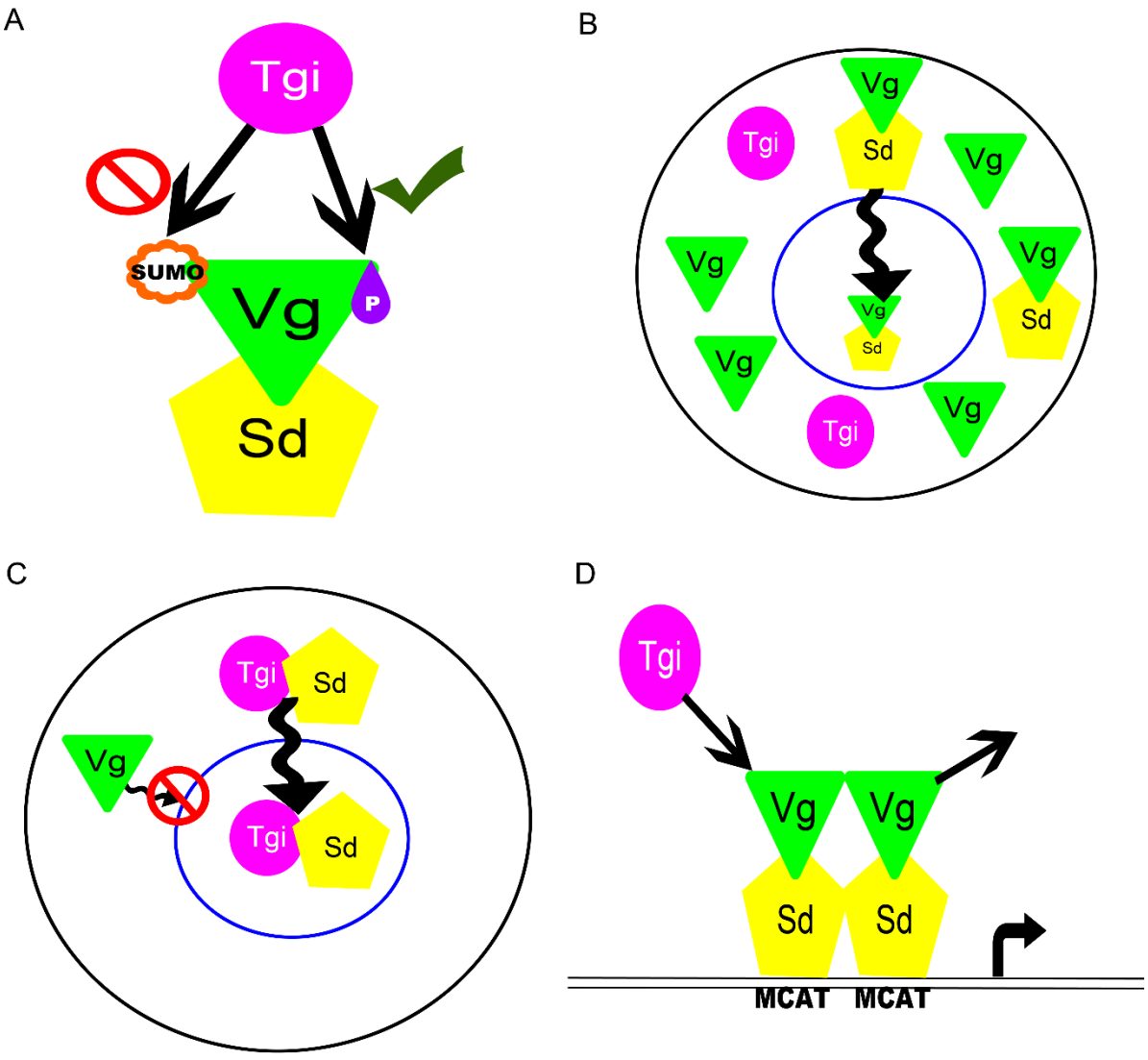
A
Tgi
SUMO
Vg
P
Sd
B
Vg
Tgi
Sd
Vg
Vg
Vg
Sd
Vg
Sd
Vg
Tgi
Vg
C
Tgi
Sd
Vg
Tgi
Sd
D
Tgi
Vg
Vg
Sd
Sd
MCAT
MCAT

Figure 3.9: Potential models for Vestigial-like family competition for Sd binding. A) Vg/Sd binding may be stabilized or destabilized by post-translational modifications, leading to a change in complex affinity and the ability of one binding partner to bump out the other. B) Relative expression levels of the Vestigial-like proteins change the Sd binding partner by increasing the frequency of stochastic interactions between them. C) Gene regulation is mediated by Sd-dependent transport of Vg or Tgi into the nucleus. D) Sd acts as a potentiator of regulation, and Vestigial-like proteins are bound or released from complexes on the DNA.

Chapter 4: General Discussion and Conclusions

4.1 Phosphorylation of Vestigial is Necessary for Proper Tissue Differentiation

In Chapter 2, evidence was provided for the regulation of Vg activity during development by phosphorylation at Serine-215 (Ser215). Prior to this, the only known post-translational modification of Vg was the addition of a SUMO moiety at an unidentified position (Takanaka and Courey, 2005). The functional relevance of sumoylation to Vg function remains unclear. There is a significant enrichment of sumoylation modifiers attached to transcription factors relative to the overall level of cellular protein modification (Cubeñas-Potts and Matunis, 2013). It is interesting to note that all forms of Vg appear to be sumoylated, which indicates that it may be a functional requirement and not a temporary modification. Sumoylation may impact the ability of Vg to interact with Sd, whether in initially forming a co-complex or in stabilizing one once it has already associated. Fine-tuning the interaction between these proteins, and how that interaction impacts the ability of Sd to interact with its many other partners may be a useful control mechanism for regulating transcriptional output.

Vg was demonstrated to undergo post-translational modification via Western blot, as shown by a pattern of multiple bands of different molecular weight. At least some of the post-translationally modified forms of Vg result from phosphorylation on Serine 215 (Ser215), and this phosphorylation is dependent on Sd (Pimmett et al., 2017). Ser-215 phosphorylation of Vg has specific physiological consequences in multiple tissues. In the adult wing, non-

phosphorylatable Vg (Vg^{S215A}) expression in Vg-specific regions of the larval wing disc result in poor differentiation of the anterior margin sensory bristles and clipping of the lateral margin; this is reinforced by diminished expression of Vg-responsive pro-neural genes in the third instar larval wing disc, as well as reduced wing disc size. Conversely, Expression of a pseudo-phosphorylated Vg isoform (Vg^{S215E}) caused duplication of posterior margin bristles (Pimmett et al., 2017). The requirement for phosphorylation was conserved in the somatic musculature as well, where non-phosphorylatable Vg caused poor muscle attachment and occasional absence of specific dorsal muscles (Pimmett et al., 2017). Finally, Vg was demonstrated to be a target of p38 MAPK for Ser-215 phosphorylation as inhibition of p38 MAPK caused reduced Vg phosphorylation, and p38b was able to co-immunoprecipitate with Sd (Pimmett et al., 2017).

Transcriptional regulators are frequently nodal points at which multiple signaling pathways are integrated to direct cellular function on multiple levels such as migration, metabolism, fate and communication outward with neighbouring cells. Tightly controlling their function is integral for cells to appropriately respond to signals by directing gene expression. Post-translational modification of transcriptional regulators is a way to restrict protein activity without the lag time associated with *de novo* protein translation. Post-translational modifications of transcriptional regulators in general have multiple potential consequences: a modification may alter subcellular localization, stability, the ability to form complexes and associate with other proteins, and/or the ability to associate with the DNA (Filtz et al., 2014). The rapid tunability of transcriptional coregulators may be particularly important during

development, where organisms are undergoing rapid changes in cell identity, adhesion and migration, and proliferation/survival.

The only currently established interactors of Vg are Sd, Mef2 and Yki (Deng et al., 2009; Li et al., 2015a; Simmonds et al., 1998), although that certainly does not preclude any other as-yet unidentified interactors. The identity of other physically interacting proteins is a large hole in the current knowledge about Vg. One of the challenges faced by current high-throughput mass spectrometry proteome screens is that proteins with low abundance and weaker interaction partners are missed due to the inability of the mass spectrometry analysis algorithms to identify the peptides at a sufficiently high level, the absence of the protein of interest in the input material, or the stringency of the protein purification protocol disrupting weaker interactions. Both a general mass spectrometry interaction screen and a phospho-protein specific screen have been performed on the *Drosophila* proteome (Bo Zhai et al., 2008; Giot et al., 2003; Murali et al., 2011). The DroID screen (Murali et al., 2011) used a two-hybrid based approach and was able to confirm the Vg/Sd interaction, a good positive control, as well as 10 other potential interactors. This list included proteins like Mad, which seems to be likely based on the combined requirement for *vg* enhancer activation (Kim et al., 1997). It also identified another DNA-binding protein, deformed wings (Dwg), as a potential interactor. *dwg* is a zinc finger C2H2-type transcription factor that is associated with insulator elements and the boundaries of topologically associated domains (Zolotarev et al., 2016). However, none of the novel DroID interactions have been validated outside of large screens, which is a significant gap in the knowledge base for an otherwise well-studied protein. Further, there has been no investigation into different binding partners of Vg across

multiple contexts. Are the binding partners in the wing disc the same as those in the muscle? Is there a partial overlap, or is the complex entirely novel? And importantly, how does that affect gene targeting in the wing compared to the muscle?

Another interesting question is how Vg post-translational modification regulates transcription of its target genes. The full spectrum of Vg post-translational modification has yet to be explored. Two-dimensional gel analysis of Vg indicates that there are at least three forms of Vg, all of which are sumoylated and at least one of which is also the result of phosphorylation. However, that still leaves at least one form entirely unexplained. Secondary to this is the fact that the sumoylation conjugation point is unknown. A SUMO modifier is linked to its target protein via a lysine residue, similar to that of the closely related ubiquitin moiety (Lomelí and Vázquez, 2011). The target residue generally is found in a ψKxE motif, where ψ is a large hydrophobic residue and x is any amino acid. Vg had 5 lysine residues (Lys-180, Lys-227, Lys-315, Lys-318, and Lys-448), but none of them are found within a canonical sumoylation target motif. Mutagenesis of Lys-180 (Takanaka and Courey, 2005) and Lys-257 (Hua Deng, unpublished observations) does not affect sumoylation. How is sumoylation affecting Vg function? Is it reducing the ability of Vg and Sd to form complexes, blocking nuclear translocation, or stopping recruitment of the transcriptional machinery? This is an area where targeted proteomic analysis would be ideal to locate the position of the sumoylation linkage. Analysis in Chapter 2 showed that there were no un-sumoylated forms of Vg identifiable by Western blot, but it is possible that a more sensitive detection method would be able to isolate a small pool of un-sumoylated Vg.

It is unclear if there is a signal that induces Vg phosphorylation, or what that signal may be. Vg does not appear to be automatically phosphorylated in the wing disc upon completion of protein folding, as expression of a pseudo-phosphorylated protein results in incorrect specification of the posterior wing margin, so some mechanism of induction must be required. Studying this *in vitro* or *in vivo* will require development of a phospho-specific Vg antibody to detect this change; as yet, production of this antibody has proven extremely difficult, as is even getting a high quality antibody to Vg with no mind to modifications (Williams et al., 1991). While phosphorylation was shown to be Sd-dependent, it is not likely that the signal is expression of the Sd protein itself as both proteins have temporally overlapping patterns of expression that are not sequential. One possibility may be post-translational modification of Sd. Sd is known to be palmitoylated in *Drosophila* (Chan et al., 2016; Magico and Bell, 2011), and in both mice and humans TEAD4 is targeted by the p38 MAPK pathway to regulate shuttling between the cytoplasm and nucleus (Lin et al., 2017a). An alternative theory is that p38 MAPK function is induced by the activity of Dpp, a TGF-β family secreted ligand in the developing wing. *vg* is a target of Dpp via Mothers against dpp (Mad) (Kim et al., 1997), and Vg is required for overgrowth mediated by the Dpp receptor *tkv* (Martín-Castellanos and Edgar, 2002). Further, p38 MAPK signaling via p38b is a known modulator of Dpp signaling downstream of Tkv, and expression in the wing disc of a constitutively active *tkv* mutant in a hemizygous p38 genetic background causes wing phenotypes similar to the non-phosphorylatable Vg mutant (Adachi-Yamada et al., 1999). In the same vein, it is unclear whether there is a phosphatase able to reverse Vg phosphorylation, and whether de-phosphorylation of Vg would also be dependent on Sd. There is a body of evidence for interplay between phosphorylation and ubiquitination in

targeting proteins for degradation (Nguyen et al., 2013). Vg phosphorylation may not stabilize the Vg/Sd complex, but instead destabilize it for proteasomal degradation. A similar mechanism is well understood for the cyclin/cyclin-dependent kinase interplay at cell cycle checkpoints (Santo et al., 2015). If Vg is destabilized, Tgi may be able to interfere with a weaker Vg/Sd interaction or Vg may just simply be absent from the competition altogether. This seems unlikely, however, as both pseudo-phosphorylated and phosphorylated Vg are able to rescue the homozygous vg^{null} mutant phenotype; if phosphorylated or dephosphorylated Vg was targeted for degradation, one of these classes of mutant would most likely have a phenotype unable to so thoroughly recapitulate the expression of Vg.

Does Vg phosphorylation or sumoylation affect its ability to form larger complexes with transcriptional regulators beyond Sd? It does not impede the ability of the Vg-Sd complex to recruit RNA polymerase to the transcriptional start site, as rescue of the homozygous vg^{null} phenotype, which would have no wings, with a pseudo-phosphorylated or non-phosphorylatable mutant still results in identifiable adult wings with relatively minor specification defects. How does phosphorylation cause discrimination between posterior and anterior margin genes in the wing disc? It is well established that binding of Vg and Sd causes the target motif for Sd-DNA interaction to switch from a single MCAT element to paired MCAT elements (Halder and Carroll, 2001). Why Vg and Sd forms a heterotetramer when bound to DNA is unclear, but it could potentially be mediated by Vg phosphorylation. If phosphorylated and unphosphorylated forms of Vg cause target switching from single to paired MCAT elements, then genes required for implementation of posterior versus anterior margin fate could be identified based on the number and positioning of MCAT elements

within *cis*-regulatory elements. To test this, re-imagining of the original electrophoretic mobility shift assay experiments showing that Vg and Sd bind in heterotetramers to paired MCAT motifs (Halder and Carroll, 2001) could be employed, using purified Vg mutant protein instead of non-mutant Vg. If phosphorylation affected targeting of specific paired MCAT motifs, the shift in bound protein would be apparent. An alternative approach is to perform ChIP-seq on tissue overexpressing a tagged Vg phosphorylation mutant, followed by examining the specific sequences enriched in the ChIP. While there may be some confounding effects from ectopic Vg expression, unless the vg^{null} rescue paradigm is employed, this methodology has the benefit of enabling identification of potential co-regulatory factors. Vg and Sd are known to co-regulate target enhancers with *cubitus interruptus* (Ci), *suppressor of Hairless* (Su(H)), and Mad (Halder et al., 1998; Hepker et al., 1999; Kim et al., 1997). Other co-regulatory transcription factors are certainly possible, and their ability to associate with a Vg/Sd complex may depend on Sd phosphorylation as well.

p38 MAPK activity is a known regulator of the Mef2 muscle identity gene family in mice and humans (Han and Molkentin, 2000; Yang et al., 1999; Zhao et al., 1999). It is interesting to note that in *Drosophila*, Vg phosphorylation is necessary for terminal differentiation of somatic muscle but an unphosphorylated isoform appears to be dispensable. This contrasts to the wing disc, where both phosphorylated and unphosphorylated forms of the protein are required for fate specification (Pimmett et al., 2017). This may also be a form of target gene switching, as genes required for terminal differentiation of musculature are not necessarily the same as those required to define wing fate. Additionally, the heterotetrameric complex of Vg and Sd required for activation of wing gene transcription has never been demonstrated for

muscle-specific genes, nor for any neural-specific genes in neuronal lineages expressing Vg and Sd (Guss et al., 2008; Guss et al., 2013; Halder and Carroll, 2001). It would be noteworthy to see whether the specific motif grammar of wing *cis*-regulatory elements must be maintained in other lineages co-expressing Vg and Sd, and what impact phosphorylation of Vg has on target gene activation or repression. Examining this by tissue-specific ChIP-seq paired with RNA-seq or qPCR to look at both binding targets and resulting gene expression changes is a straightforward methodology. This could even be accomplished from difficult to isolate tissue such as the embryonic musculature using one several protocols that isolate specific cells or nuclei via FACS using fluorescent labelling in live cells or with fluorophore-conjugated antibodies in fixed cells (Bonn et al., 2012; Deal and Henikoff, 2010).

4.2 Tondu domain-containing Growth Inhibitor is an inhibitor of Vestigial in Drosophila wing development

There is very little information available with regards to its expression and function of Tgi during *Drosophila* development It clearly has a biologically relevant role, as loss of Tgi expression is lethal in Drosophila (Guo et al., 2013; Koontz et al., 2013), and its conservation across a broad range of metazoans, particularly with regard to the TONDU domains, argues the same. Here we have shown that Tgi is capable of interacting *in vitro* with Sd, as Vg also does, but the Vg/Sd and Tgi/Sd complexes are mutually exclusive. This leads to a hypothesis that Vg and Tgi are functioning in a competitively exclusionary manner for Sd binding. *In vivo*, this hypothesis appears to be supported, as overexpression of Tgi in the Vg domain of the third instar wing disc shows a Vg dose-dependent decrease in wing size, along with

cupping of the wing structure. Analysis of the third instar wing disc shows that this is likely a result of both a smaller wing disc in general, as well as a relative decrease in the proportion of ventral wing tissue that causes the cupped phenotype. Tgi overexpression in the wing disc using *sd*:GAL4 caused a largely pupal lethal phenotype with exclusively female escapers showing entirely necrotic tissue with no differentiation in place of the wing; no male escapers were ever observed, and escaper females were entirely sterile. Overexpression of Sd using *Tgi*:GAL4 resulted in a larval lethal phenotype similar to that previously described for $Tgi^{-/-}$ (Guo et al., 2013; Koontz et al., 2013) with no escapers. Furthering the competitive exclusion hypothesis *in vitro*, Kc167 cells transfected with Vg and Sd or Tgi and Sd showed nuclear import of both Vestigial-like family genes and colocalization with Sd, but co-transfection of Vg and Tgi together showed that Tgi was preferentially transported into the nucleus over Vg. As neither Tgi nor Vg contain a canonical nuclear localization signal, and instead must rely on Sd for import, this evidence points towards Tgi being a preferential partner for Sd over Vg. An autoregulatory loop could potentially form to fine-tune the titration of available Sd, however. Although co-transfection of Vg and Sd does not increase Tgi mRNA expression in Kc167 cells, and co-transfection of Vg and Tgi did not upregulate Sd mRNA, a significant increase in Vg mRNA was noted when Tgi and Sd were coexpressed in Kc167 cells. This points to a fine balance between Vg and Tgi for Sd binding, one that may alter its own balance through a negative feedback loop. The role of Tgi as an activator of Vg expression is also unexpected, as both Tgi and its mammalian counterpart VGLL4 are considered tumor suppressors when Tgi/VGLL4 is bound to Sd/TEAD in the absence of Yki/YAP/TAZ (Koontz et al., 2013; Li et al., 2015a; Zhang et al., 2014).

There is a vast number of unanswered questions regarding the function of Tgi. Chapter 4, as well as other groups, have shown *Tgi* expression in several larval tissues including the wing disc, haltere disc, ovaries, and the ventral nerve cord of the brain via a newly developed Tgi antibody (Guo et al., 2013; Koontz et al., 2013). There has also been shown a functional requirement for Tgi in the adult fly heart (Yu et al., 2015). The full expression pattern of *Tgi*, including regions of overlap and non-overlap with Vg and Sd, has yet to be fully elucidated, particularly the embryonic expression pattern. Both overlapping and non-overlapping regions of cells expressing *Tgi* and *vg/sd* are interesting for different reasons. The degree to which Vg and Tgi compete for Sd binding, and the effect of this on gene regulation, has interesting implications for the function of Vg as an oncogene and Tgi as a tumor suppressor as proposed to be the case in several different cancers (Castilla et al., 2014; Zhang et al., 2014; Zhang et al., 2017b). If the balance between them could be altered pharmacologically to drive differentiation of de-differentiated tumor cells, this may be a promising chemotherapeutic target (Jiao et al., 2014; Jiao et al., 2017). On the other hand, regions where expression of Tgi does not overlap with Vg, such as the heart, may indicate that Vg and Tgi do not necessarily act as repressors or activators of the same genes and instead may have exclusive subsets of Sd target genes. Finally, any potential regions where Tgi does not overlap with Sd could show evidence for interaction with other transcriptional regulators that Vg does not share. Although Vg is known to interact with Sd directly, and at the least indirectly with Mef2 and Yki, it has no other known binding partners (Deng et al., 2009; Li et al., 2015a; Paumard-Rigal et al., 1998; Simmonds et al., 1998). Sd has a host of transcription factors and coregulators that it interacts with in different contexts (Deng et al., 2009; Paumard-Rigal et al., 1998; Sansores-Garcia et al., 2013; Simmonds et al., 1998; Wu et al.,

2008; Zhang et al., 2008; Zhang et al., 2017a), consistent with its role as an integrator of multiple signaling pathways. The only known interactors of Tgi are Sd and Yki (Guo et al., 2013; Koontz et al., 2013; Kwon et al., 2013), so cells expressing Tgi but not Sd would be strongly indicative of other DNA binding partners for Tgi, a novel finding for VGLL proteins in Drosophila.

The gene targets of a Tgi regulatory complex are also unknown. There is only one published target of Tgi in *diap1*; this is a known target of the Hippo signaling pathway (Koontz et al., 2013). It is safe to assume that this is not the only gene regulated by Tgi. What precisely the other targets are, however, is deserving of attention. Do all Tgi target genes have MCAT elements in the *cis*-regulatory sequence? A no would imply that Tgi is able to interact somehow with other DNA-binding proteins or that it affects transcription through alternative regulatory mechanisms. Is the MCAT element motif grammar maintained between Vg and Tgi target genes? As Tgi has two TONDU domains and thus is possibly coordinating Sd in a 1:2 stoichiometry, it would seem likely that the paired MCAT motif would be key to the function of a Tgi/Sd complex. To what degree do Vg and Tgi target genes overlap? A competitive exclusion relationship between Vg and Tgi would indicate that a substantial degree of overlap between the two should exist. Vg has previously been shown to repress transcription of certain target genes in the embryonic musculature (Deng et al., 2009), and to activate its own transcription in the wing disc (Halder et al., 1998; Zecca and Struhl, 2007a). The genes cross-regulated by Vg/Sd and Tgi/Sd complexes identified here have not been shown to be direct targets and may in fact be secondary effects to loss of another regulator. It is interesting, however, that targets of this complex affect both the cell cycle and

differentiation. When this is considered with the concept of differentiation therapy in mind, as well as the known pharmacological mimics of VGLL4 in mice, it is easy to imagine a scenario where the ability to adjust the balance between Vg and Tgi, or their mammalian homologues, could be used to drive the differentiation of cancer cells and prevent the hyperproliferative phenotype key to the disease. The bifunctionality of Vg as an activator or repressor of transcription is curious, and how Tgi might play into the activate versus repress decision is deserving of further study.

VGLL have been shown to interact with other non-TEAD partners in other species (Jiao et al., 2017; Lee et al., 2011), but this has never been replicated in *Drosophila*, nor has any large-scale screen for interacting partners or genetic suppressors or enhancers ever been performed using Tgi as the bait. There are several potential methods of studying this, including a mass spectrometry co-immunoprecipitation screening of Tgi interactors either from cell culture or using tissues with known *Tgi* expression. A ChIP grade Tgi antibody does not currently exist, so this would be limited by ectopic expression of a tagged transgene/construct unless an endogenous tag could be inserted into the genome either in cell lines or *in vivo* (Bottcher et al., 2014; Koles et al., 2015; Kunzelmann et al., 2016). To look at genetic interactors with Tgi, a complementation screen in wings using the commercially available deficiency kit from the Bloomington Drosophila Resource Centre or the RNAi library from the Vienna *Drosophila* Resource Centre would be feasible, albeit labour-intensive. This screen would could be handily done in the wing, which is not a strictly necessary tissue in adults, but is complicated by the fact that $Tgi^{-/-}$ flies die in larval stages. A hemizygous $Tgi^{-/+}$ background could be employed, or the previously mentioned new tissue-

specific CRISPR/Cas9 schema used to reduce *Tgi* expression (Jia et al., 2018; Lee et al., 2018; Port et al., 2014). Alternatively, this screen could also be performed to look for genes that are able to attenuate the *Tgi* overexpression phenotype in the wing. While the wings are strongly reduced in size and development, the fertility of the adults does not seem to be substantially affected. This approach would be complicated by the fact that identifying weaker modifiers of an already visually strong phenotype would be complex, and this screen would therefore quite possibly overrepresent strong enhancers and suppressors while missing less obvious ones.

An obvious parallel to the work described in Chapter 2 and Pimmett et al. (2017) is an analysis of Tgi post-translational modification. VGLL4 is known to be acetylated on Lys-225 in the mouse heart (Lin et al., 2016). Acetylation of Vgll4 reduces its interaction with TEAD1, and expression of a mutant VGLL4 caused diminished proliferation and necrosis in cardiomyocytes (Lin et al., 2016). While this was examined in the context of a competitive interaction for TEAD1 between VGLL4 and YAP, there are certainly parallels with Tgi and Sd. Lys-225 in mouse VGLL4 is not conserved in either Tgi isoform. Additionally, other large mammalian mass spectrometry screens have identified four separate sites of VGLL4 phosphorylation, including one specifically on the mitotic phospho-proteome (Dephoure et al., 2008; Zhou et al., 2013), and VGLL4 has been shown experimentally to be a target of CDK-1 phosphorylation (Zeng et al., 2017) and de-ubiquitination at the amino terminal by Ubiquitin-specific protease 11 (Zhang et al., 2016). Analysis of the Tgi amino acid sequence by post-translational modification predictors indicates that Tgi may be a target for sumoylation at three separate positions, as well as numerous phosphorylation sites and a

putative glycosaminoglycan linkage. The post-translational modification of Vg and its importance in development, along with many other known requirements with other proteins, speaks to the usefulness of exploring this avenue.

There are two different splice isoforms of Tgi, the *Tgi-RA*/Tgi-PA and *Tgi-RB*/Tgi-PB variants. These two isoforms differ in both the 5' untranslated region (UTR) as well as the amino terminal coding sequence. Splice isoforms are a conserved and useful way to increase the coding capacity of the genome by encoding different mRNAs within the same sequence. Variances in the 5' and 3' UTR can affect transcript stability and localization, and coding sequence variation can confer differences in protein-protein, protein-DNA and protein-RNA interactions, changes in post-translational modification, changes in compartment targeting or trafficking, or other functional alterations. Curiously, there is some debate as to whether or not splicing is actually a major regulator of functional variation; some groups hold that the majority of splice isoforms are evolutionarily neutral variants with no actual different function from the canonical sequence while others have shown that the majority of isoform variants retain less than 50% of their interactors in common (Tress et al., 2017; Yang et al., 2016). In *Drosophila*, alternative splicing is key to the sex determination pathway. Alternative splicing of *sex-lethal* (*sxl*) is regulated by the ratio of X chromosomes to autosomes, such that flies with a sex:autosome ratio >0.5 will make one splice isoform that defines female-specific tissue, while a ratio of ≤0.5 directs a second splice isoform containing an extra exon and stop codon that encodes a truncated male-specific Sxl protein (Hartmann et al., 2011; Moschall et al., 2017; Sun et al., 2015b). Alternative splicing is maintained as a sex determination pathway subsequent to Sxl, as there is also female-specific

splicing of *transformer* (*tra*) mRNA as well as *doublesex* (*dsx*) and *fruitless* (*fru*) (Moschall et al., 2017). The two alternative splice isoforms of *Tgi* were established by *in situ* hybridization to be expressed in the same larval tissues (Koontz et al., 2013) but there is little evidence in the embryo to show where and when *Tgi* is expressed, nor which splice isoform is employed. The small number of groups studying *Tgi* expression and function have collectively declared the Tgi-PB isoform to be the canonical form, but there's limited rationale for this choice. There are no identified functional domains or motifs in either splice isoform N-terminal region, but that does not necessarily mean that there are not different interactors that connect at this region. The 5'UTRs are also quite different even though the final two exons and 3' UTRs are shared. Some evidence exists that transcription factors themselves regulate alternative splicing (Han et al., 2017), which is a yet further complex layer of regulatory control. The ability of the Tgi-PA isoform to compete with Vg and Tgi-PB for Sd binding could be tested by co-immunoprecipitation, and its expression pattern monitored against the Tgi-PB isoform in the embryo by use of dual-labelled *in situ* hybridization probes against unique sequences in each transcript. It would be difficult to completely inhibit the expression of the Tgi-PA isoform by mutagenesis, as the isoform starts from an internal transcriptional start site in the second intron of the *Tgi-RB* isoform. This intron contains regulatory regions, shown by some preliminary luciferase assay data and the presence of the *Tgi*:GAL4 P-element insertion, so mutagenesis of the transcriptional start site may have some secondary effects. However, it may be possible to mutate the transcriptional start site for the *Tgi-RB* isoform using CRISPR/Cas9 to see if the *Tgi-RA* isoform is able to functionally substitute during development.

4.3 Conclusions

The VGLL family, despite a long history of study in *Drosophila*, is still an area of research with information yet to be discovered. Here I have shown that Vg phosphorylation on Ser-215 is a key regulatory post-translational modification with phenotypic consequences. Rescue of the vg^{null} phenotype using a non-phosphorylatable mutant Vg transgene results in anterior margin bristle loss and the inability to activate the *vgME* in larval wing discs, while the same rescue with a phosphomimetic transgene causes duplication of posterior bristles but no change to margin activation. The requirement for Vg post-translational modification is only partly recapitulated in the mesoderm-derived embryonic musculature, as non-phosphorylatable Vg causes loss of some muscles as well as poor terminal differentiation and attachment. The phosphorylation of Vg is Sd-dependent, and likely due to p38β, as Ser-215 is positioned within a p38 MAPK motif and the specific kinase is able to interact with Sd.

Second, I have shown that there is a likely competitive interaction between Vg and Tgi, a second member of the *Drosophila* Vestigial-like family of transcription co-factors. Tgi is an evolutionarily conserved protein that is able to interact with Sd similarly to Vg but is unable to form a co-complex with Vg in Kc167 cells. This presents a theory that Vg and Tgi are in competition for Sd binding. *In vivo* examination of the competition theory in wing discs showed that the effect of Tgi overexpression in the Vg domain of the wing disc is dependent on the level of Vg expression, and overexpression of Vg in the Tgi domain causes a *sd* mutant phenotype in the adult wing. Overexpression of Sd in the Tgi domain results in a phenotype very similar to a $Tgi^{-/-}$ larvae, both of which die in late second or early third instar.

Furthering the competitive hypothesis, live cell imaging of Vg, Tgi and Sd showed that while Vg/Sd and Tgi/Sd mis-expression resulted in nuclear localization of both proteins, co-expression of Tgi and Vg caused a nuclear localization of Tgi and a cytoplasmic sequestration of Vg. Tgi upregulates its own inhibitor, as co-transfection of Tgi and Sd in Kc167 cells results in an 84-fold upregulation of Vg. Known Sd target genes are also cross-regulated by Vg/Sd and Tgi/Sd co-expression, although not in a clear activating versus repressive complex fashion. Further investigation into the role of Tgi during development, both as a partner of Sd and as an antagonist of Vg, could provide interesting new directions for modulating Hippo pathway signaling.

As a unifying model for these observations, it is possible that Tgi and Sd are interacting in the wing disc (**Figure 4.1**), as Sd appears to preferentially ensure Tgi remains in the nucleus *in vitro*. Tgi acts in concert with Sd to repress some Sd target genes while increasing the expression of Vg. However, increasing the amount of available Vg in the cell titrates Sd away from Tgi binding (**Figure 4.2**), which inverts the regulation of Sd target genes. The affinity of Vg for Sd binding may be mediated by the phosphorylation of Vg such that changes in the post-translational modification of Vg either destabilize Vg itself or the ability of the Vg/Sd complex to form and regulate target genes appropriately.

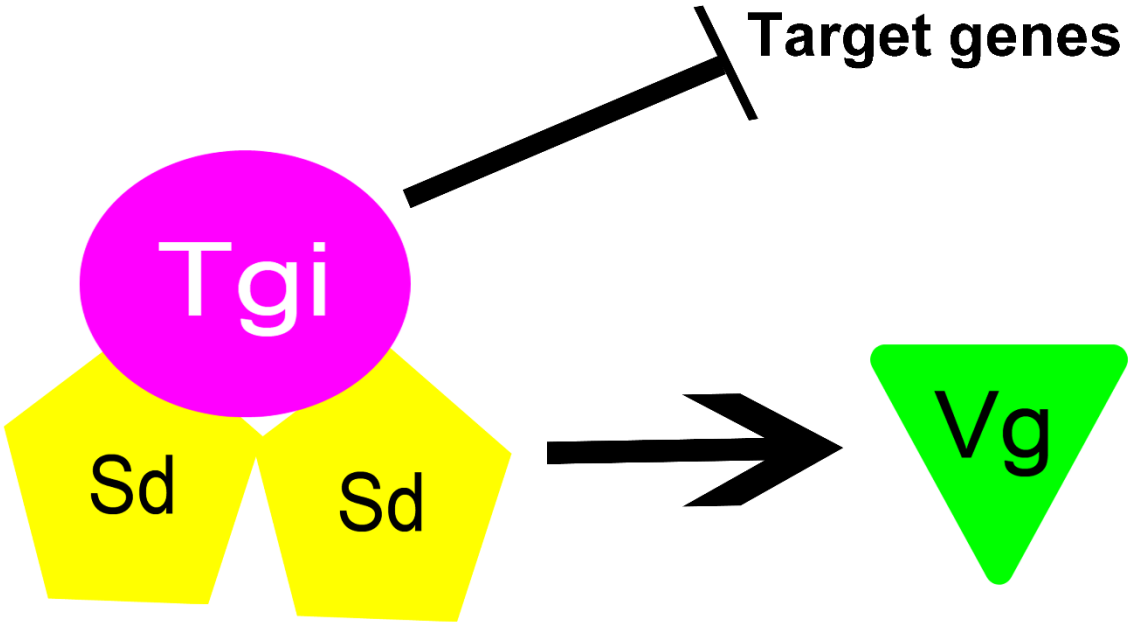
Target genes
Tgi
Sd
Sd
Vg

Figure 4.1: Sd and Tgi act to repress transcription of a set of Sd target genes while activating expression of Vg.

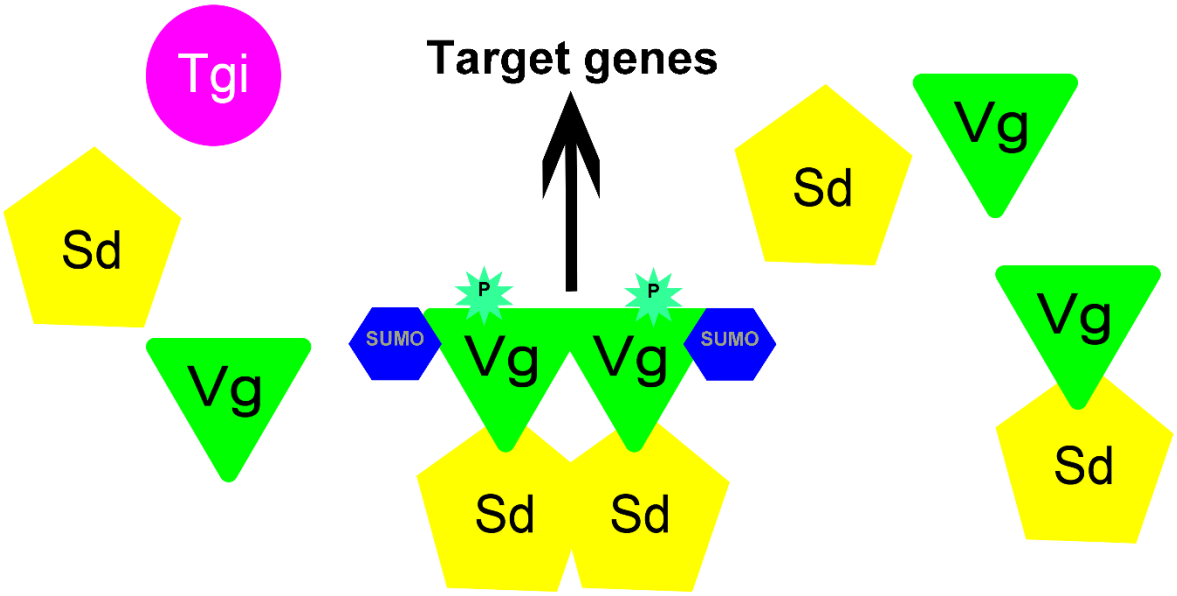
Tgi
Target genes
Sd
Vg
Sd
Vg
P
P
SUMO
Vg
Vg
SUMO
Sd
Sd
Vg
Sd
Vg

Figure 4.2: The Vg/Sd interaction is mediated by the post-translational modification of Vg. Increased Vg expression titrates available Sd away from binding to Tgi. This interaction is mediated by phosphorylation of Vg, which may alter the stability of Vg itself or the ability of Vg and Sd to form stable interacting complexes.

Chapter 5: Materials and Methods

Cell culture and transfection

Drosophila Schneider-2 (S2) cells were grown at 25°C in SFX media (Invitrogen) supplemented with 100U/mL penicillin and 100µg/mL streptomycin (Invitrogen). Kc167 cells were obtained from the *Drosophila* Genomics Resource Centre and grown at 25°C in M3 medium (Invitrogen) supplemented with Bacto-Peptone and yeast extract (Difco) and 5% fetal calf serum (Invitrogen). Transfections of S2 cells were carried out using didecyldimethylammonium bromide (Han, 1996). Kc167 cells were transfected using Effectene transfection reagent (Qiagen). SB203580 (Cuenda et al., 1995) was solubilized in DMSO and used as previously described (Han et al., 1998).

Drosophila strains

All crosses were performed at 25°C. The UAS:3xHA-Vg, UAS:3xHA-Vg^{S215A}, UAS:3xHA-Vg^{S215E}, and UAS:3xFLAG-6xMyc-Sd strains were made in the Simmonds laboratory using P-element mediated insertion. The UAS:3xFLAG-6xMyc-Tgi strain was made by BestGene Inc. using P-element mediated insertion. The vg^{null} derivative strains, including $vg^{null/+}$, UAS:3xHA-Vg and related mutants, $vg^{null/+}$, *vg(M+Q)*:GAL4 and $vg^{null/+}$, *Mef2*:GAL4 strains, were developed in the Simmonds laboratory. The UAS:*Tgi* RNAi line was obtained from the Vienna *Drosophila* Resource Centre. All other lines were obtained from the Bloomington *Drosophila* Stock Centre.

Plasmids

Vectors made for use in S2 and Kc167 cells were made using Gateway Technology (Invitrogen) to clone appropriate coding sequences into pENTR/D-Topo, followed by LR cloning (Invitrogen) into the *Drosophila* Gateway destination vector collection (Terrence Murphy, Carnegie Institute of Washington). Plasmids used for expression of epitope-tagged or fluorescently tagged proteins used the *Drosophila Actin5c* (*Act5c*) promoter with the exception of GFP-Sd (Chapter 2), which was expressed using the *Drosophila Heat-shock-protein 70* (*Hsp70*) *87A7* promoter (Huynh and Zieler, 1999) Site directed mutagenesis was used to make point mutations in the *vg* coding sequence based on the QuickChange Site-Directed Mutagenesis Kit (Stratagene). The pNL3.1-*vgQE* reporter plasmid was constructed by PCR amplification of the *vgQE* enhancer (Guss et al., 2001) and inserted via Gibson cloning (New England Biolabs). The pGL4.54 vector (Promega) was a gift from Dr. Francesca Di Cara.

Immunoprecipitation and Immunoblotting

S2 and Kc167 cells were transfected in T25 flasks with the relevant constructs, using either the *Act5c* or *Hsp70* promoter as indicated in the above section. For the *Hsp70* promoter, cells were subject to two rounds of heat shock consisting of 30 minutes at 37°C followed by a 30 minute recovery at 25°C, and a final round at 37°C for 30 minutes followed by recovery for ≥6 hours. Immunoprecipitations were performed using Radio-IP (RIPA) buffer (50 mM Tris pH 8.0, 150 mM sodium chloride, 1.0% NP-40, 0.5% sodium deoxycholate, 0.1% SDS)

supplemented with Complete protease inhibitor (Roche) and PhosStop (Roche). Co-immunoprecipitations were performed using modified mild lysis buffer (20 mM HEPES pH7.5, 100 mM potassium chloride, 0.05% Triton X-100, 2.5 mM EDTA) (Ceriani, 2007) supplemented with Complete protease inhibitor (Roche) and PhosStop (Roche). Antibodies for immunoprecipitation include mouse anti-FLAG M2 (Sigma), rat anti-HA (Roche), and mouse anti-myc 9E10 (a gift from Dr. Paul LaPointe). Protein G-sepharose beads (Biovision) or MycTrap beads (Chromotek) were used for capture. Vg resolution for phosphorylation state was performed on a low-bis-acrylamide (118:1) polyacrylamide gel. All others were performed on standard 10-12% bis-acrylamide gels. After transfer to nitrocellulose membrane, blots were blocked using 50% LI-COR blocking buffer/50% PBS for minimum of 1h at room temperature. Primary antibodies for immunoblotting include mouse anti-FLAG M2 (Sigma, 1:1000), rat anti-HA (Roche, 1:500), rabbit anti-Vg (1:400, Williams et al., 1991), rabbit anti-myc (Abcam, 1:2000), mouse anti-myc 9E10 (Dr. P. LaPointe), rabbit anti-SUMO Smt3 (Abcam, 1:1000), and mouse anti-GFP (Sigma, 1:1000). Secondary antibodies were obtained from Invitrogen or Jackson ImmunoResearch and include goat anti-mouse AF680 and AF790 (Abcam), goat anti-rabbit AF680 and 790 (Abcam), donkey anti-mouse CF680, donkey anti-rabbit CF790, and donkey anti-rat CF680 and CF790 (all 1:10000, Sigma). Blots were resolved using the Odyssey Infrared Imaging System (LI-COR).

2-Dimensional gel electrophoresis

S2 cells were transfected and heat shocked as described above, and cells were flash frozen in liquid nitrogen for storage at -80°C. The cell pellet was resuspended in mild lysis buffer (20

mM HEPES pH7.0, 50 mM sodium chloride, 1 mM EDTA, 1 mM EGTA, 1.0% Triton X-100) with Complete protease inhibitor (Roche) and PhosStop (Roche). Cells were lysed via Dounce homogenization and sheared with a 22G needle. Immunoprecipitation was performed using MycTrap beads (Chromotek) at 4°C overnight followed by washing and sample division into two. One of the two samples was treated with λ-phosphatase (New England Biolabs) for 45 minutes at 37°C. Samples were resuspended in a rehydration buffer with DTT followed by overnight isoelectric focusing on a Pharmacia IPGphor using an Immobiline DryStrip pH 4-7 (GE Healthcare). Second dimension resolution was performed on a 10% polyacrylamide gel. Immunoblotting was performed with mouse anti-myc 9E10 (Dr. P LaPointe) and rabbit anti-Vg (Williams et al., 1991, Simmonds lab), followed with donkey anti-mouse AF790 and donkey anti-rabbit AF680 (1:5000, Abcam). Blots were resolved using the Odyssey Infrared Imaging System (LI-COR), and analyzed using the Odyssey software package (LI-COR), Excel (Microsoft) and Prism (Graphpad).

qPCR

qPCR analysis of wing discs was performed by isolating 25 pairs of wing discs from third instar larvae of the indicated genotype. RNA was isolated by mechanical disruption followed by TRIzol purification of RNA (Life Technologies). RNA was reverse transcribed using the iScript Select cDNA synthesis kit with an oligo$(dT)_{20}$ primer (BioRad) on an Mastercycler (Eppendorf AG). Relative quantification of transcript abundance was performed using an Mastercycler Realplex2 (Eppendorf AG) and iQ SYBR Green supermix (BioRad) following manufacturer's protocol. Primers were designed to target the transgene via the epitope tag.

All genotypes were quantified in biological triplicate replicates and compared to *Rp49* amplification using Excel (Microsoft) and Prism (Graphpad). Statistical significance was tested using Student's t-test.

qPCR analysis of Kc167 cells was performed by pelleting of a T-25 transfected as described above, followed by TRIzol purification of RNA (Life Technologies). RNA was reverse transcribed using the iScript Select cDNA synthesis kit with an oligo$(dT)_{20}$ primer (BioRad) on an Eppendorf Mastercycler (Eppendorf AG). Relative quantification of transcript abundance was performed using an Eppendorf Mastercycler realplex2 (Eppendorf AG) and iQ SYBR Green supermix (BioRad) following manufacturer's protocol. Primers were either individually designed or derived from FlyPrimerBank (Hu et al., 2013). Quantification was performed in biological triplicate replicates and compared to *Rp30* amplification using Excel (Microsoft) and Prism (Graphpad). Statistical significance was tested using Student's t-test.

Luciferase Assay

S2 or Kc167 cells were transfected as described above using the relevant constructs. Activation of the *vgQE* enhancer was monitored using the Nano-Glo Dual Luciferase Assay kit (Promega) in 96 well plate format. Luminescence was measured on a BioTek Synergy2 plate reader. Analysis was performed using Excel (Microsoft) and Prism (Graphpad), and significance was tested using a two-tailed analysis of variance (ANOVA).

Antibody Generation

The Tgi-RB coding sequence was cloned into pDEST17 using the Gateway cloning system (Invitrogen). The plasmid was transformed into BL21 DE3 cells (New England Biolabs) to generate full length 6xHIS-Tgi. Purified protein was isolated from crude lysate using the ÄKTA liquid chromatography system and HisTrap FF column (GE Healthcare). Purified protein was sent to Pocono Rabbit Farms & Laboratories for injection into two guinea pigs. Serum from guinea pigs was then affinity purified against a column with full length Tgi-PB protein.

Fluorescence Microscopy

Wing imaginal discs were dissected, fixed with 4% paraformaldehyde in phosphate-buffered saline and stained as described previously (Hughes and Krause, 1999). Embryos were collected in 2 hour intervals using apple juice agar plates, fixed using 4% paraformaldehyde, and stained as previously described (Hughes and Krause, 1999). The following primary antibodies were used at the indicated concentrations: rat anti-HA (1:500, Roche), mouse anti-Cut (1:20, deposited by Gerald M Rubin and obtained from the Developmental Studies Hybridoma Bank), rat anti-myosin (1:1000, Abcam), mouse anti-Wg 4D4 (1:200, Developmental Studies Hybridoma Bank), guinea pig anti-Tgi (1:250). Species specific fluorophore-conjugated secondary antibodies were used to amplify primary antibody signal for imaging (1:5000, Abcam, Jackson ImmunoResearch), along with 4', 6'-diamidino-2-phenylindole (1:5000, Thermo Fisher). Imaging was performed on a Zeiss LSM 700 using a

Plan-Apochromat 20x lens (NA=0.8, Zeiss). Analysis was performed using Huygens Professional (SVI), Imaris (Bitplane), and Prism (Graphpad), and statistical significance was analyzed using Student's t-test.

Live cell imaging was performed by transfecting Kc167 cells as described above in LabTek-II chambered coverslip dishes (Sigma). Image acquisition was performed using a spinning disc confocal system (Ultraview ERS; PE Biosciences) and Axioimager M2 (Zeiss) with a 63x Plan-Apochromat oil lens (NA=1.4, Zeiss), and Volocity acquisition software (PE Biosciences). Analysis was performed using Huygens Professional (SVI) and Imaris (Bitplane).

Adult Wing Analysis

Female adult flies from the labelled genotypes were collected and stored for a minimum of 24 hours in 70% ethanol to soften the cuticle. Wings were removed and mounted using Aquamount (Invitrogen) prior to imaging on an Axioplan 2 (Zeiss) using a Fluar 5x lens (NA=0.17, Zeiss). Analysis was performed using ImageJ and Prism (Graphpad), and statistical significance was examined using a two-tailed analysis of variance (ANOVA).

Table 1: List of Drosophila Gene Abbreviations

Abbreviation	Gene
ac	*achaete*
ap	*apterous*
Atf-2	*Activating transcription factor-2*
bs	*blistered*
ct	*cut*
ci	*cubitus interruptus*
CycE	*Cyclin E*
Dcr-2	*Dicer-2*
dE2F2	*E2F transcription factor 2*
Diap1	*Death-associated inhibitor of apoptosis-1*
dl	*dorsal*
dpp	*decapentaplegic*
dsx	*doublesex*
ed	*echinoid*
en	*engrailed*
fru	*fruitless*
gbb	*glass-bottom boat*
hh	*hedgehog*
hth	*homothorax*
kni	*knirps*
Mad	*Mothers against decapentaplegic*
mats	*mob as tumor suppressor*
Mef2	*Myocyte enhancer factor-2*
mpk2	*mpk2/p38α MAP kinase*
N	*Notch*
p38β	*p38β*
RpL30	*Ribosomal protein L30*
salm	*spalt major*
sav	*salvador*
sd	*scalloped*
sens	*senseless*
ser	*serrate*
Su(H)	*Suppressor of Hairless*
sxl	*sex-lethal*
Tgi	*Tondu domain-containing Growth Inhibitor*
tkv	*thickvein*
tra	*transformer*

tsh	*teashirt*
Ubc9	*lesswright/Ubc9*
vg	*vestigial*
wg	*wingless*
wts	*warts*
yki	*yorkie*

Bibliography

Adachi-Yamada, T., Nakamura, M., Irie, K., Tomoyasu, Y., Sano, Y., Mori, E., Goto, S., Ueno, N., Nishida, Y. and Matsumoto, K. (1999). p38 mitogen-activated protein kinase can be involved in transforming growth factor beta superfamily signal transduction in Drosophila wing morphogenesis. *Mol. Cell. Biol.* **19**, 2322–2329.

Adams, M. D., Celniker, S. E., Holt, R. A., Evans, C. A., Gocayne, J. D., Amanatides, P. G., Scherer, S. E., Li, P. W., Hoskins, R. A., Galle, R. F., et al. (2000). The genome sequence of Drosophila melanogaster. *Science (80-.).* **287**, 2185–2195.

Ahmad, S. M. (2017). Conserved signaling mechanisms in Drosophila heart development. *Dev. Dyn.* **246**, 641–656.

Aiello, N. M. and Stanger, B. Z. (2016). Echoes of the embryo: using the developmental biology toolkit to study cancer. *Dis. Model. Mech.* **9**, 105–114.

Akiyama, T. and Gibson, M. C. (2015). Decapentaplegic and growth control in the developing Drosophila wing. *Nature* **527**, 375–378.

Alaggio, R., Zhang, L., Sung, Y., Huang, S., Chen, C., Bisogno, G., Zin, A., Agaram, N. P., LaQuaglia, M. P., Wexler, L. H., et al. (2016). A Molecular Study of Pediatric Spindle and Sclerosing Rhabdomyosarcoma: Identification of Novel and Recurrent VGLL2-related Fusions in Infantile Cases. *Am. J. Surg. Pathol.* **40**, 224–35.

Anand, A., Fernandes, J., Arunan, M. C., Bhosekar, S., Chopra, A., Dedhia, N., Sequiera, K., Hasan, G., Palazzolo, M. J., Raghavan, K. V., et al. (1990). Drosophila "enhancer-trap" transposants: Gene expression in chemosensory and motor pathways

and identification of mutants affected in smell and taste ability. *J. Genet.* **69**, 151–168.

Anbanandam, A., Albarado, D. C., Nguyen, C. T., Halder, G., Gao, X. and Veeraraghavan, S. (2006). Insights into transcription enhancer factor 1 (TEF-1) activity from the solution structure of the TEA domain. *Proc. Natl. Acad. Sci.* **103**, 17225–30.

Antonescu, C. R., Zhang, L., Nielsen, G. P., Rosenberg, A. E., Cin, P. D. and Fletcher, C. D. M. (2011). Consistent t(1;10) with rearrangements of TGFBR3 and MGEA5 in both myxoinflammatory fibroblastic sarcoma and hemosiderotic fibrolipomatous tumor. *Genes Chromosom. Cancer* **50**, 757–764.

Arbeitman, M. N., Furlong, E. E. M., Imam, F., Johnson, E., Null, B. H., Baker, B. S., Krasnow, M. A., Scott, M. P., Davis, R. W. and White, K. P. (2002). Gene expression during the life cycle of Drosophila melanogaster. *Science (80-.).* **297**, 2270–5.

Ashton-Beaucage, D. and Therrien, M. (2017). How Genetics Has Helped Piece Together the MAPK Signaling Pathway.pp. 1–21.

Bai, J. M., Chiu, W. H., Wang, J. C., Tzeng, T. H., Perrimon, N. and Hsu, J. C. (2001). The cell adhesion molecule Echinoid defines a new pathway that antagonizes the Drosophila EGF receptor signaling pathway. *Development* **128**, 591–601.

Baker, N. E. (2017). Mechanisms of cell competition emerging from Drosophila studies. *Curr. Opin. Cell Biol.* **48**, 40–46.

Bangi, E. and Wharton, K. (2006). Dpp and Gbb exhibit different effective ranges in the establishment of the BMP activity gradient critical for Drosophila wing patterning. *Dev. Biol.* **295**, 178–193.

Barrionuevo, M. G., Aybar, M. J. and Tríbulo, C. (2014). Two different vestigial like 4 genes are differentially expressed during Xenopus laevis development. *Int. J. Dev. Biol.* **58**, 369–377.

Basler, K. and Struhl, G. (1994). Compartment boundaries and the control of Drosophila limb pattern by hedgehog protein. *Nature* **368**, 208–14.

Bataillé, L., Delon, I., Da Ponte, J. P., Brown, N. H. and Jagla, K. (2010). Downstream of identity genes: Muscle-type-specific regulation of the fusion process. *Dev. Cell* **19**, 317–328.

Bate, M. and Arias, A. M. (1991). The embryonic origin of imaginal discs in Drosophila. *Development* **112**, 755–761.

Baylies, M. K., Bate, M. and Gomez, M. R. (1998). Myogenesis: A view from Drosophila. *Cell* **93**, 921–927.

Beira, J. V and Paro, R. (2016). The legacy of Drosophila imaginal discs. *Chromosoma* **125**, 573–592.

Belozerov, V. E., Ratkovic, S., McNeill, H., Hilliker, A. J. and McDermott, J. C. (2014). In Vivo Interaction Proteomics Reveal a Novel p38 Mitogen-Activated Protein Kinase/Rack1 Pathway Regulating Proteostasis in Drosophila Muscle. *Mol. Cell. Biol.* **34**, 474–84.

Bernard, F., Lalouette, A., Gullaud, M., Jeantet, A. Y., Cossard, R., Zider, A., Ferveur, J. F. and Silber, J. (2003). Control of apterous by vestigial drives indirect flight muscle development in Drosophila. *Dev. Biol.* **260**, 391–403.

Bernard, F., Kasherov, P., Grenetier, S., Dutriaux, A., Zider, A., Silber, J. and Lalouette, A. (2009). Integration of differentiation signals during indirect flight muscle

formation by a novel enhancer of Drosophila vestigial gene. *Dev. Biol.* **332**, 258–272.

Bevington, S. L., Cauchy, P. and Cockerill, P. N. (2017). Chromatin priming elements establish immunological memory in T cells without activating transcription: T cell memory is maintained by DNA elements which stably prime inducible genes without activating steady state transcription. *BioEssays* **39**, 1–12.

Blochlinger, K., Jan, L. Y. and Jan, Y. N. (1991). Transformation of sensory organ identity by ectopic expression of Cut in Drosophila. *Genes Dev.* **5**, 1124–1135.

Bo Zhai, J. V., Beausoleil, S. A., Mintseris, J. and Gygi, S. P. (2008). Phosphoproteome analysis of drosophila melanogaster embryos. *J. Proteome Res.* **7**, 1675–1682.

Bonn, S., Zinzen, R. P., Perez-Gonzalez, A., Riddell, A., Gavin, A.-C. and Furlong, E. E. M. (2012). Cell type-specific chromatin immunoprecipitation from multicellular complex samples using BiTS-ChIP. *Nat. Protoc.* **7**, 978–94.

Boone, E., Colombani, J., Andersen, D. S. and Léopold, P. (2016). The Hippo signalling pathway coordinates organ growth and limits developmental variability by controlling dilp8 expression. *Nat. Commun.* **7**, 13505.

Bosch, P. S., Ziukaite, R., Alexandre, C., Basler, K. and Vincent, J.-P. (2017). Dpp controls growth and patterning in Drosophila wing precursors through distinct modes of action. *Elife* **6**, 1–16.

Bottcher, R., Hollmann, M., Merk, K., Nitschko, V., Obermaier, C., Philippou-Massier, J., Wieland, I., Gaul, U. and Forstemann, K. (2014). Efficient chromosomal gene modification with CRISPR/cas9 and PCR-based homologous recombination donors in cultured Drosophila cells. *Nucleic Acids Res.* **42**, e89–e89.

Brown, N. H., Gregory, S. L., Rickoll, W. L., Fessler, L. I., Prout, M., White, R. A. H.

and Fristrom, J. W. (2002). Talin is essential for integrin function in Drosophila. *Dev. Cell* **3**, 569–579.

Bürglin, T. R. (1991). The TEA domain: A novel, highly conserved DNA-binding motif. *Cell* **66**, 11–12.

Campbell, S. D., Duttaroy, A., Katzen, A. L. and Chovnick, A. (1991). Cloning and characterization of the scalloped region of Drosophila melanogaster. *Genetics* **127**, 367–80.

Campbell, S., Inamdar, M., Rodrigues, V., Raghavan, V., Palazzolo, M. and Chovnick, A. (1992). The scalloped gene encodes a novel, evolutionarily conserved transcription factor required for sensory organ differentiation in Drosophila. *Genes Dev.* **6**, 367–379.

Castilla, M. A., Lopez-Garcia, M. A., Atienza, M. R., Rosa-Rosa, J. M., Diaz-Martin, J., Pecero, M. L., Vieites, B., Romero-Perez, L., Benitez, J., Calcabrini, A., et al. (2014). VGLL1 expression is associated with a triple-negative basal-like phenotype in breast cancer. *Endocr. Relat. Cancer* **21**, 587–599.

Ceriani, M. F. (2007). Coimmunoprecipitation on Drosophila cells in culture. *Methods Mol. Biol.* **362**, 423–7.

Chan, P., Han, X., Zheng, B., Deran, M., Yu, J., Jarugumilli, G. K., Deng, H., Pan, D., Luo, X. and Wu, X. (2016). Autopalmitoylation of TEAD proteins regulates transcriptional output of the Hippo pathway. *Nat. Chem. Biol.* **12**, 282–289.

Chen, Z., Friedrich, G. A. and Soriano, P. (1994). Transcriptional enhancer factor 1 disruption by a retroviral gene trap leads to heart defects and embryonic lethality in mice. *Genes Dev.* **8**, 2293–2301.

Chen, H. H., Mullett, S. J. and Stewart, A. F. R. (2004a). Vgl-4, a novel member of the

vestigial-like family of transcription co-factors, regulates alpha1-adrenergic activation of gene expression in cardiac myocytes. *J. Biol. Chem.* **279**, 30800–30806.

Chen, H. H., Maeda, T., Mullett, S. J. and Stewart, A. F. R. (2004b). Transcription co-factor Vgl-2 is required for skeletal muscle differentiation. *Genesis* **39**, 273–279.

Chen, J., Xie, C., Tian, L., Hong, L., Wu, X. and Han, J. (2010). Participation of the p38 pathway in Drosophila host defense against pathogenic bacteria and fungi. *Proc. Natl. Acad. Sci.* **107**, 20774–9.

Cherbas, L., Willingham, A., Zhang, D., Yang, L., Zou, Y., Eads, B. D., Carlson, J. W., Landolin, J. M., Kapranov, P., Dumais, J., et al. (2011). The transcriptional diversity of 25 Drosophila cell lines. *Genome Res.* **21**, 301–314.

Cho, E. and Irvine, K. D. (2004). Action of fat, four-jointed, dachsous and dachs in distal-to-proximal wing signaling. *Development* **131**, 4489–4500.

Ciepla, P., Magee, A. I. and Tate, E. W. (2015). Cholesterylation: a tail of hedgehog: Figure 1. *Biochem. Soc. Trans.* **43**, 262–267.

Clevers, H. (2011). The cancer stem cell: premises, promises and challenges. *Nat. Med.* **17**, 313–319.

Cody, N. A. L., Shen, Z., Ripeau, J. S., Provencher, D. M., Mes-Masson, A. M., Chevrette, M. and Tonin, P. N. (2009). Characterization of the 3p12.3-pcen region associated with tumor suppression in a novel ovarian cancer cell line model genetically modified by chromosome 3 fragment transfer. *Mol. Carcinog.* **48**, 1077–1092.

Cohen, B., Simcox, A. A. and Cohen, S. M. (1993). Allocation of the imaginal primordia in the Drosophila embryo. *Development* **117**, 597–608.

Couso, J. P., Knust, E. and Martinez Arias, A. (1995). Serrate and wingless cooperate to

induce vestigial gene expression and wing formation in Drosophila. *Curr. Biol.* **5**, 1437–1448.

Cubeñas-Potts, C. and Matunis, M. J. (2013). SUMO: A Multifaceted Modifier of Chromatin Structure and Function. *Dev. Cell* **24**, 1–12.

Cuenda, A., Rouse, J., Doza, Y. N., Meier, R., Cohen, P., Gallagher, T. F., Young, P. R. and Lee, J. C. (1995). SB-203580 is a specific inhibitor of a MAP kinase homolog which is activated by cellular stresses and interleukin-1. *FEBS Lett.* **364**, 229–233.

Danielsen, E. T., Moeller, M. E. and Rewitz, K. F. (2013). Nutrient Signaling and Developmental Timing of Maturation. In *Current Topics in Developmental Biology*, pp. 37–67. Elsevier Inc.

Davidson, I., Xiao, J. H., Rosales, R., Staub, A. and Chambon, P. (1988). The HeLa cell protein TEF-1 binds specifically and cooperatively to two SV40 enhancer motifs of unrelated sequence. *Cell* **54**, 931–942.

Davies, S. P., Reddy, H., Caivano, M. and Cohen, P. (2000). Specificity and mechanism of action of some commonly used protein kinase inhibitors. *Biochem. J.* **351**, 95–105.

Davis, R. (1993). The mitogen-activated protein kinase signal transduction pathway. *J. Biol. Chem.* **268**, 14553–14556.

De Craene, B. and Berx, G. (2013). Regulatory networks defining EMT during cancer initiation and progression. *Nat. Rev. Cancer* **13**, 97–110.

Deal, R. B. and Henikoff, S. (2010). A simple method for gene expression and chromatin profiling of individual cell types within a tissue. *Dev. Cell* **18**, 1030–1040.

Delanoue, R., Legent, K., Godefroy, N., Flagiello, D., Dutriaux, A., Vaudin, P., Becker, J. L. and Silber, J. (2004). The Drosophila wing differentiation factor vestigial-

scalloped is required for cell proliferation and cell survival at the dorso-ventral boundary of the wing imaginal disc. *Cell Death Differ.* **11**, 110–122.

Deng, H., Hughes, S. C., Bell, J. B. and Simmonds, A. J. (2009). Alternative requirements for Vestigial, Scalloped, and Dmef2 during muscle differentiation in Drosophila melanogaster. *Mol. Biol. Cell* **20**, 256–69.

Deng, H., Bell, J. B. and Simmonds, A. J. (2010). Vestigial is required during late-stage muscle differentiation in Drosophila melanogaster embryos. *Mol. Biol. Cell* **21**, 3304–16.

Dephoure, N., Zhou, C., Villen, J., Beausoleil, S. A., Bakalarski, C. E., Elledge, S. J. and Gygi, S. P. (2008). A quantitative atlas of mitotic phosphorylation. *Proc. Natl. Acad. Sci.* **105**, 10762–10767.

Deshpande, N., Chopra, A., Rangarajan, A., Shashidhara, L. S., Rodrigues, V. and Krishna, S. (1997). The human transcription enhancer factor-1, TEF-1, can substitute for Drosophila scalloped during wingblade development. *J. Biol. Chem.* **272**, 10664–10668.

Diaz-Benjumea, F. J. and Cohen, S. M. (1993). Interaction between dorsal and ventral cells in the imaginal disc directs wing development in Drosophila. *Cell* **75**, 741–52.

Díaz-Benjumea, J., Gaitán, M. A. F. G. and García-Bellido, A. (1989). Developmental genetics of the wing vein pattern of Drosophila. *Genome* **31**, 612–619.

Dobi, K. C., Schulman, V. K. and Baylies, M. K. (2015). Specification of the somatic musculature in Drosophila. *Wiley Interdiscip. Rev. Dev. Biol.* **4**, 357–375.

Dominguez-Gimenez, P., Brown, N. H. and Martin-Bermudo, M. D. (2007). Integrin-ECM interactions regulate the changes in cell shape driving the morphogenesis of the

Drosophila wing epithelium. *J. Cell Sci.* **120**, 1061–1071.

Eivers, E., Fuentealba, L. C., Sander, V., Clemens, J. C., Hartnett, L. and De Robertis, E. M. (2009). Mad is required for wingless signaling in wing development and segment patterning in Drosophila. *PLoS One* **4**, e6543.

Farrance, I. K. G., Mar, J. H. and Ordahl, C. P. (1992). M-CAT binding factor is related to the SV40 enhancer binding factor, TEF-1. *J. Biol. Chem.* **267**, 17234–17240.

Faucheux, C., Naye, F., Treguer, K., Fedou, S., Thiebaud, P. and Theze, N. (2010). Vestigial like gene family expression in Xenopus: Common and divergent features with other vertebrates. *Int. J. Dev. Biol.* **54**, 1375–1382.

Ffrench, B., Gasch, C., Hokamp, K., Spillane, C., Blackshields, G., Mahgoub, T. M., Bates, M., Kehoe, L., Mooney, A., Doyle, R., et al. (2017). CD10−/ALDH− cells are the sole cisplatin-resistant component of a novel ovarian cancer stem cell hierarchy. *Cell Death Dis.* **8**, e3128.

Filtz, T. M., Vogel, W. K. and Leid, M. (2014). Regulation of transcription factor activity by interconnected post-translational modifications. *Trends Pharmacol. Sci.* **35**, 76–85.

Fry, A. M., Bayliss, R. and Roig, J. (2017). Mitotic Regulation by NEK Kinase Networks. *Front. Cell Dev. Biol.* **5**, 1–13.

Gambaro, K., Quinn, M. C. J., Wojnarowicz, P. M., Arcand, S. L., de Ladurantaye, M., Barrès, V., Ripeau, J. S., Killary, A. M., Davis, E. C., Lavoie, J., et al. (2013). VGLL3 expression is associated with a tumor suppressor phenotype in epithelial ovarian cancer. *Mol. Oncol.* **7**, 513–530.

Garcia-Bellido, A., Ripoll, P. and Morata, G. (1973). Developmental compartmentalisation of the wing disk of Drosophila. *Nat. New Biol.* **245**, 251–3.

Garg, A., Srivastava, A., Davis, M. M., O'Keefe, S. L., Chow, L. and Bell, J. B. (2007). Antagonizing scalloped with a novel vestigial construct reveals an important role for scalloped in Drosophila melanogaster leg, eye and optic lobe development. *Genetics* **175**, 659–669.

Gascuel, O. (1997). BIONJ: an improved version of the NJ algorithm based on a simple model of sequence data. *Mol. Biol. Evol.* **14**, 685–695.

Giot, L., Bader, J. S., Brouwer, C., Chaudhuri, A., Kuang, B., Li, Y., Hao, Y. L., Ooi, C. E., Godwin, B., Vitols, E., et al. (2003). A Protein Interaction Map of Drosophila melanogaster. *Mol. Med.* **302**, 1727–36.

Giraldez, A. J. and Cohen, S. M. (2003). Wingless and Notch signaling provide cell survival cues and control cell proliferation during wing development. *Development* **130**, 6533–43.

Gohl, D. M., Silies, M. A., Gao, X. J., Bhalerao, S., Luongo, F. J., Lin, C.-C., Potter, C. J. and Clandinin, T. R. (2011). A versatile in vivo system for directed dissection of gene expression patterns. *Nat. Methods* **8**, 231–7.

Gómez-Skarmeta, J. L., Rodríguez, I., Martínez, C., Culí, J., Ferrés-Marcó, D., Beamonte, D. and Modolell, J. (1995). Cis-regulation of achaete and scute: Shared enhancer-like elements drive their coexpression in proneural clusters of the imaginai discs. *Genes Dev.* **9**, 1869–1882.

Goulev, Y., Fauny, J. D., Gonzalez-Marti, B., Flagiello, D., Silber, J. and Zider, A. (2008). SCALLOPED Interacts with YORKIE, the Nuclear Effector of the Hippo Tumor-Suppressor Pathway in Drosophila. *Curr. Biol.* **18**, 435–441.

Green, M. M. (1945). A study in gene action using different dosages and alleles of vestigial

in Drosophila melanogaster. *Genetics* **31**, 1–20.

Gruneberg, H. (1929). Ein Beitrag zur Kenntnis der Rontgenmutationen des X-Chromosoms von Drosophila melanogaster. *Biol. Zent. Bl.* **49**, 680–694.

Günther, S., Mielcarek, M., Krüger, M. and Braun, T. (2004). VITO-1 is an essential co-factor of TEF1-dependent muscle-specific gene regulation. *Nucleic Acids Res.* **32**, 791–802.

Guo, T., Lu, Y., Li, P., Yin, M.-X., Lv, D., Zhang, W., Wang, H., Zhou, Z., Ji, H., Zhao, Y., et al. (2013). A novel partner of Scalloped regulates Hippo signaling via antagonizing Scalloped-Yorkie activity. *Cell Res.* **23**, 1201–14.

Gupta, M. P., Kogut, P. and Gupta, M. (2000). Protein kinase-A dependent phosphorylation of transcription enhancer factor-1 represses its DNA-binding activity but enhances its gene activation ability. *Nucleic Acids Res.* **28**, 3168–77.

Gupta, M., Kogut, P., Davis, F. J., Belaguli, N. S., Schwartz, R. J. and Gupta, M. P. (2001). Physical Interaction between the MADS Box of Serum Response Factor and the TEA/ATTS DNA-binding Domain of Transcription Enhancer Factor-1. *J. Biol. Chem.* **276**, 10413–10422.

Guss, K. A., Nelson, C. E., Hudson, A., Kraus, M. E., Carroll, S. B., Guss, K. A., Nelson, C. E., Hudson, A., Kraus, M. E. and Carrollt, S. B. (2001). Control of a Genetic Regulatory Network by a Selector Gene. *Science (80-.).* **292**, 1164–1167.

Guss, K. A., Mistry, H. and Skeath, J. B. (2008). Vestigial expression in the Drosophila embryonic central nervous system. *Dev. Dyn.* **237**, 2483–2489.

Guss, K. A., Benson, M., Gubitosi, N., Brondell, K., Broadie, K. and Skeath, J. B. (2013). Expression and function of scalloped during Drosophila development. *Dev. Dyn.*

242, 874–885.

Halder, G. and Carroll, S. B. (2001). Binding of the Vestigial co-factor switches the DNA-target selectivity of the Scalloped selector protein. *Development* **128**, 3295–3305.

Halder, G., Polaczyk, P., Kraus, M. E., Hudson, A., Kim, J., Laughon, A. and Carroll, S. B. (1998). The Vestigial and Scalloped proteins act together to directly regulate wing-specific gene expression in Drosophila. *Genes Dev.* **12**, 3900–3909.

Hales, K. G., Korey, C. A., Larracuente, A. M. and Roberts, D. M. (2015). Genetics on the fly: A primer on the drosophila model system. *Genetics* **201**, 815–842.

Halperin, D. S., Pan, C., Lusis, A. J. and Tontonoz, P. (2013). Vestigial-like 3 is an inhibitor of adipocyte differentiation. *J. Lipid Res.* **54**, 473–481.

Hamaratoglu, F., de Lachapelle, A. M., Pyrowolakis, G., Bergmann, S. and Affolter, M. (2011). Dpp signaling activity requires pentagone to scale with tissue size in the growing drosophila wing imaginal disc. *PLoS Biol.* **9**,.

Han, K. (1996). An efficient DDAB-mediated transfection of Drosophila S2 cells. *Nucleic Acids Res.* **24**, 4362–4363.

Han, J. and Molkentin, J. D. (2000). Regulation of MEF2 by p38 MAPK and its implication in cardiomyocyte biology. *Trends Cardiovasc. Med.* **10**, 19–22.

Han, Z. S., Enslen, H., Hu, X., Meng, X., Wu, I.-H. H., Barrett, T., Davis, R. J. and Ip, Y. T. (1998). A conserved p38 mitogen-activated protein kinase pathway regulates Drosophila immunity gene expression. *Mol. Cell. Biol.* **18**, 3527–3539.

Han, H., Braunschweig, U., Gonatopoulos-Pournatzis, T., Weatheritt, R. J., Hirsch, C. L., Ha, K. C. H., Radovani, E., Nabeel-Shah, S., Sterne-Weiler, T., Wang, J., et al. (2017). Multilayered Control of Alternative Splicing Regulatory Networks by

Transcription Factors. *Mol. Cell* **65**, 539–553.e7.

Hariharan, I. K. (2015). Organ Size Control: Lessons from Drosophila. *Dev. Cell* **34**, 255–265.

Hartmann, B., Castelo, R., Minana, B., Peden, E., Blanchette, M., Rio, D. C., Singh, R. and Valcarcel, J. (2011). Distinct regulatory programs establish widespread sex-specific alternative splicing in Drosophila melanogaster. *RNA* **17**, 453–468.

Hay, B. A., Wassarman, D. A. and Rubin, G. M. (1995). Drosophila homologs of baculovirus inhibitor of apoptosis proteins function to block cell death. *Cell* **83**, 1253–1262.

Heallen, T., Zhang, M., Wang, J., Bonilla-Claudio, M., Klysik, E., Johnson, R. L. and Martin, J. F. (2011). Hippo Pathway Inhibits Wnt Signaling to Restrain Cardiomyocyte Proliferation and Heart Size. *Science (80-.).* **332**, 458–461.

Heinz, S., Romanoski, C. E., Benner, C. and Glass, C. K. (2015). The selection and function of cell type-specific enhancers. *Nat. Rev. Mol. Cell Biol.* **16**, 144–54.

Hélias-Rodzewicz, Z., Pérot, G., Chibon, F., Ferreira, C., Lagarde, P., Terrier, P., Coindre, J. M. and Aurias, A. (2009). YAP1 and VGLL3, encoding two co-factors of TEAD transcription factors, are amplified and overexpressed in a subset of soft tissue sarcomas. *Genes Chromosom. Cancer* **49**, 1161–1171.

Hepker, J., Blackman, R. K. and Holmgren, R. (1999). Cubitus interruptus is necessary but not sufficient for direct activation of a wing-specific decapentaplegic enhancer. *Development* **126**, 3669–3677.

Honda, M., Hidaka, K., Fukada, S., Sugawa, R., Shirai, M., Ikawa, M. and Morisaki, T. (2017). Vestigial-like 2 contributes to normal muscle fiber type distribution in mice. *Sci.*

Rep. **7**, 7168.

Hu, H., Hilton, M. J., Tu, X., Yu, K., Ornitz, D. M. and Long, F. (2004). Sequential roles of Hedgehog and Wnt signaling in osteoblast development. *Development* **132**, 49–60.

Hu, Y., Sopko, R., Foos, M., Kelley, C., Flockhart, I., Ammeux, N., Wang, X., Perkins, L., Perrimon, N. and Mohr, S. E. (2013). FlyPrimerBank: an online database for Drosophila melanogaster gene expression analysis and knockdown evaluation of RNAi reagents. *G3 Genes|Genomes|Genetics* **3**, 1607–16.

Huang, J., Wu, S., Barrera, J., Matthews, K. and Pan, D. (2005). The Hippo signaling pathway coordinately regulates cell proliferation and apoptosis by inactivating Yorkie, the Drosophila homolog of YAP. *Cell* **122**, 421–434.

Huang, D., Li, X., Sun, L., Huang, P., Ying, H., Wang, H., Wu, J. and Song, H. (2016). Regulation of Hippo signalling by p38 signalling. *J. Mol. Cell Biol.* **8**, 328–337.

Huang, J., Reilein, A. and Kalderon, D. (2017). Yorkie and Hedgehog independently restrict BMP production in escort cells to permit germline differentiation in the *Drosophila* ovary. *Development* **144**, 2584–2594.

Hughes, S. C. and Krause, H. M. (1999). Single and double FISH protocols for Drosophila. *Methods Mol. Biol.* **122**, 93–101.

Huynh, C. Q. and Zieler, H. (1999). Construction of modular and versatile plasmid vectors for the high-level expression of single or multiple genes in insects and insect cell lines. *J. Mol. Biol.* **288**, 13–20.

Hwang, J.-J., Chambon, P. and Davidson, I. (1993). Characterization of the transcription activation function and the DNA binding domain of transcriptional enhancer factor-1. *EMBO J.* **12**, 2337–48.

Ingham, P. W., Nakano, Y. and Seger, C. (2011). Mechanisms and functions of Hedgehog signalling across the metazoa. *Nat. Rev. Genet.* **12**, 393–406.

Irvine, K. D. and Harvey, K. F. (2015). Control of Organ Growth by Patterning and Hippo Signaling in Drosophila. *Cold Spring Harb. Perspect. Biol.* **7**, 1–16.

Ishidate, T., Elewa, A., Kim, S., Mello, C. C. and Shirayama, M. (2014). Divide and differentiate: CDK/Cyclins and the art of development. *Cell Cycle* **13**, 1384–1391.

James, A. A. and Bryant, P. J. (1981). Mutations Causing Pattern Deficiencies and Duplication in the Imaginal Wing Disk of Drosophila melanogaster. *Dev. Biol.* **85**, 39–54.

Jang, J. W., Kim, M. K., Lee, Y. S., Lee, J. W., Kim, D. M., Song, S. H., Lee, J. Y., Choi, B. Y., Min, B., Chi, X. Z., et al. (2017). RAC-LATS1/2 signaling regulates YAP activity by switching between the YAP-binding partners TEAD4 and RUNX3. *Oncogene* **36**, 999–1011.

Jia, Y., Xu, R.-G., Ren, X., Ewen-Campen, B., Rajakumar, R., Zirin, J., Yang-Zhou, D., Zhu, R., Wang, F., Mao, D., et al. (2018). Next-generation CRISPR/Cas9 transcriptional activation in Drosophila using flySAM. *Proc. Natl. Acad. Sci.* 201800677.

Jiang, S. W., Dong, M., Trujillo, M. A., Miller, L. J. and Eberhardt, N. L. (2001). DNA Binding of TEA/ATTS Domain Factors Is Regulated by Protein Kinase C Phosphorylation in Human Choriocarcinoma Cells. *J. Biol. Chem.* **276**, 23464–23470.

Jiang, W., Yao, F., He, J., Lv, B., Fang, W., Zhu, W., He, G., Chen, J. and He, J. (2015). Downregulation of VGLL4 in the progression of esophageal squamous cell carcinoma. *Tumor Biol.* **36**, 1289–1297.

Jiao, S., Wang, H., Shi, Z., Dong, A., Zhang, W., Song, X., He, F., Wang, Y., Zhang, Z., Wang, W., et al. (2014). A Peptide Mimicking VGLL4 Function Acts as a YAP Antagonist Therapy against Gastric Cancer. *Cancer Cell* **25**, 166–180.

Jiao, S., Li, C., Hao, Q., Miao, H., Zhang, L., Li, L. and Zhou, Z. (2017). VGLL4 targets a TCF4–TEAD4 complex to coregulate Wnt and Hippo signalling in colorectal cancer. *Nat. Commun.* **8**, 14058.

Jin, H. S., Park, H. S., Shin, J. H., Kim, D. H., Jun, S. H., Lee, C. J. and Lee, T. H. (2011). A novel inhibitor of apoptosis protein (IAP)-interacting protein, Vestigial-like (Vgl)-4, counteracts apoptosis-inhibitory function of IAPs by nuclear sequestration. *Biochem. Biophys. Res. Commun.* **412**, 454–459.

Kaneko, K. J., Cullinan, E. B., Latham, K. E. and DePamphilis, M. (1997). Transcription factor mTEAD-2 is selectively expressed at the beginning of zygotic gene expression in the mouse. *Development* **124**, 1963–73.

Kansara, M., Tsang, M., Kodjabachian, L., Sims, N. A., Trivett, M. K., Ehrich, M., Dobrovic, A., Slavin, J., Choong, P. F. M., Simmons, P. J., et al. (2009). Wnt inhibitory factor 1 is epigenetically silenced in human osteosarcoma, and targeted disruption accelerates osteosarcomagenesis in mice. *J. Clin. Invest.* **119**, 837–851.

Khalsa, O., Yoon, J., Torres-Schumann, S. and Wharton, K. A. (1998). TGF-beta/BMP superfamily members, Gbb-60A and Dpp, cooperate to provide pattern information and establish cell identity in the Drosophila wing. *Development* **125**, 2723–2734.

Kim, J., Sebring, A., Esch, J. J., Kraus, M. E., Vorwerk, K., Magee, J. and Carroll, S. B. (1996). Integration of positional signals and regulation of wing formation and identity by Drosophila vestigial gene. *Nature* **382**, 133–138.

Kim, J., Johnson, K., Chen, H. J., Carroll, S. B. and Laughon, A. (1997). Drosophila Mad binds to DNA and directly mediates activation of vestigial by Decapentaplegic. *Nature* **388**, 304–308.

Klaus, A. and Birchmeier, W. (2008). Wnt signalling and its impact on development and cancer. *Nat. Rev. Cancer* **8**, 387–398.

Klein, T. and Martinez Arias, A. (1998). Different spatial and temporal interactions between Notch, wingless, and vestigial specify proximal and distal pattern elements of the wing in Drosophila. *Dev. Biol.* **194**, 196–212.

Klein, T. and Martinez Arias, A. (1999). The vestigial gene product provides a molecular context for the interpretation of signals during the development of the wing in Drosophila. *Development* **126**, 913–925.

Koles, K., Yeh, A. R. and Rodal, A. A. (2015). Tissue-specific tagging of endogenous loci in Drosophila melanogaster. *Biol. Open* **5**, 83–9.

Koontz, L. M., Liu-Chittenden, Y., Yin, F., Zheng, Y., Yu, J., Huang, B., Chen, Q., Wu, S. and Pan, D. (2013). The Hippo Effector Yorkie Controls Normal Tissue Growth by Antagonizing Scalloped-Mediated Default Repression. *Dev. Cell* **25**, 388–401.

Korenjak, M., Taylor-Harding, B., Binné, U. K., Satterlee, J. S., Stevaux, O., Aasland, R., White-Cooper, H., Dyson, N. and Brehm, A. (2004). Native E2F/RBF complexes contain Myb-interacting proteins and repress transcription of developmentally controlled E2F target genes. *Cell* **119**, 181–193.

Kreso, A., O'Brien, C. A., van Galen, P., Gan, O. I., Notta, F., Brown, A. M. K., Ng, K., Ma, J., Wienholds, E., Dunant, C., et al. (2013). Variable Clonal Repopulation Dynamics Influence Chemotherapy Response in Colorectal Cancer. *Science (80-.).* **339**,

543–548.

Kunzelmann, S., Böttcher, R., Schmidts, I. and Förstemann, K. (2016). A Comprehensive Toolbox for Genome Editing in Cultured Drosophila melanogaster Cells. *G3 Genes|Genomes|Genetics* **6**, 1777–85.

Kuraku, S., Zmasek, C. M., Nishimura, O. and Katoh, K. (2013). aLeaves facilitates on-demand exploration of metazoan gene family trees on MAFFT sequence alignment server with enhanced interactivity. *Nucleic Acids Res.* **41**, W22–W28.

Kurtova, A. V, Xiao, J., Mo, Q., Pazhanisamy, S., Krasnow, R., Lerner, S. P., Chen, F., Roh, T. T., Lay, E., Ho, P. L., et al. (2015). Blocking PGE2-induced tumour repopulation abrogates bladder cancer chemoresistance. *Nature* **517**, 209–13.

Kwon, Y., Vinayagam, A., Sun, X., Dephoure, N., Gygi, S. P., Hong, P. and Perrimon, N. (2013). The Hippo signaling pathway interactome. *Science (80-.).* **342**, 737–740.

Lamar, J. M., Stern, P., Liu, H., Schindler, J. W., Jiang, Z.-G. and Hynes, R. O. (2012). The Hippo pathway target, YAP, promotes metastasis through its TEAD-interaction domain. *Proc. Natl. Acad. Sci.* **109**, E2441-50.

Landgraf, M., Sánchez-Soriano, N., Technau, G. M., Urban, J. and Prokop, A. (2003). Charting the Drosophila neuropile: a strategy for the standardised characterisation of genetically amenable neurites. *Dev. Biol.* **260**, 207–225.

Larkin, S. B. and Ordahl, C. P. (1999). Multiple layers of control in transcriptional regulation by MCAT elements and the TEF-1 protein family. In *Heart Development* (ed. Harvey, R. P.) and Rosenthal, N.), pp. 307–329. Academic Press.

Larkin, S. B., Farrance, I. K. G. and Ordahl, C. P. (1996). Flanking sequences modulate the cell specificity of M-CAT elements. *Mol. Cell. Biol.* **16**, 3742–55.

Lee, B. and Muller, M. T. (2009). SUMOylation enhances DNA methyltransferase 1 activity. *Biochem. J.* **421**, 449–461.

Lee, K.-P., Lee, J., Kim, T.-S., Kim, T.-H., Park, H., Byun, J., Kim, M., Jeong, W.-I., Calvisi, D. F., Kim, J.-M., et al. (2010). The Hippo-Salvador pathway restrains hepatic oval cell proliferation, liver size, and liver tumorigenesis. *Proc. Natl. Acad. Sci.* **107**, 8248–8253.

Lee, O.-H., Kim, H., He, Q., Baek, H. J., Yang, D., Chen, L.-Y., Liang, J., Chae, H. K., Safari, A., Liu, D., et al. (2011). Genome-wide YFP fluorescence complementation screen identifies new regulators for telomere signaling in human cells. *Mol. Cell. Proteomics* **10**, M110.001628.

Lee, P.-T., Zirin, J., Kanca, O., Lin, W.-W., Schulze, K. L., Li-Kroeger, D., Tao, R., Devereaux, C., Hu, Y., Chung, V., et al. (2018). A gene-specific T2A-GAL4 library for Drosophila. *Elife* **7**,.

Legent, K., Dutriaux, A., Delanoue, R. and Silber, J. (2006). Cell cycle genes regulate vestigial and scalloped to ensure normal proliferation in the wing disc of Drosophila melanogaster. *Genes to Cells* **11**, 907–918.

Li, C., Kan, L., Chen, Y., Zheng, X., Li, W., Zhang, W., Cao, L. and Lin, X. (2015a). Ci antagonizes Hippo signaling in the somatic cells of the ovary to drive germline stem cell differentiation. *Cell Res.* **25**, 1152–1170.

Li, H., Wang, Z., Zhang, W., Qian, K., Liao, G., Xu, W. and Zhang, S. (2015b). VGLL4 inhibits EMT in part through suppressing Wnt/β-catenin signaling pathway in gastric cancer. *Med. Oncol.* **32**, 83.

Li, N., Yu, N., Wang, J., Xi, H., Lu, W., Xu, H., Deng, M., Zheng, G. and Liu, H.

(2015c). miR-222/VGLL4/YAP-TEAD1 regulatory loop promotes proliferation and invasion of gastric cancer cells. *Am. J. Cancer Res.* **5**, 1158–68.

Liang, Y., Tsoi, L. C., Xing, X., Beamer, M. A., Swindell, W. R., Sarkar, M. K., Berthier, C. C., Stuart, P. E., Harms, P. W., Nair, R. P., et al. (2016). VGLL3-regulated gene network as a promoter of gender biased autoimmune diseases. *Nat. Immunol.*

Lin, Z., Guo, H., Cao, Y., Zohrabian, S., Zhou, P., Ma, Q., VanDusen, N., Guo, Y., Zhang, J., Stevens, S. M., et al. (2016). Acetylation of VGLL4 Regulates Hippo-YAP Signaling and Postnatal Cardiac Growth. *Dev. Cell* **39**, 466–479.

Lin, K. C., Moroishi, T., Meng, Z., Jeong, H.-S., Plouffe, S. W., Sekido, Y., Han, J., Park, H. W. and Guan, K.-L. (2017a). Regulation of Hippo pathway transcription factor TEAD by p38 MAPK-induced cytoplasmic translocation. *Nat. Cell Biol.* **19**, 996–1002.

Lin, K. C., Park, H. W. and Guan, K.-L. (2017b). Regulation of the Hippo Pathway Transcription Factor TEAD. *Trends Biochem. Sci.* **xx**, 1–11.

Liu-Chittenden, Y., Huang, B., Shim, J. S., Chen, Q., Lee, S. J., Anders, R. A., Liu, J. O. and Pan, D. (2012). Genetic and pharmacological disruption of the TEAD-YAP complex suppresses the oncogenic activity of YAP. *Genes Dev.* **26**, 1300–1305.

Liu, X., Grammont, M. and Irvine, K. D. (2000). Roles for scalloped and vestigial in regulating cell affinity and interactions between the wing blade and the wing hinge. *Dev. Biol.* **228**, 287–303.

Liu, X., Kong, C. and Zhang, Z. (2018). miR-130b promotes bladder cancer cell proliferation, migration and invasion by targeting VGLL4. *Oncol. Rep.* **39**, 2324–2332.

Lomelí, H. and Vázquez, M. (2011). Emerging roles of the SUMO pathway in development. *Cell. Mol. Life Sci.* **68**, 4045–4064.

Ludlow, C., Choy, R. and Blochlinger, K. (1996). Functional analysis of Drosophila and mammalian cut proteins in files. *Dev. Biol.* **178**, 149–59.

MacKay, J. O., Soanes, K. H., Srivastava, A., Simmonds, A. J., Brook, W. J. and Bell, J. B. (2003). An in vivo analysis of the Vestigial gene in Drosophila melanogaster defines the domains required for VG function. *Genetics* **163**, 1365–1373.

Madhavan, M. M. and Schneiderman, H. A. (1977). Histological analysis of the dynamics of growth of imaginal discs and histoblast nests during the larval development of Drosophila melanogaster. *Wilhelm Roux's Arch. Dev. Biol.* **183**, 269–305.

Maeda, T., Chapman, D. L. and Stewart, A. F. R. (2002a). Mammalian vestigial-like 2, a co-factor of TEF-1 and MEF2 transcription factors that promotes skeletal muscle differentiation. *J. Biol. Chem.* **277**, 48889–48898.

Maeda, T., Gupta, M. P. and Stewart, A. F. R. (2002b). TEF-1 and MEF2 transcription factors interact to regulate muscle-specific promoters. *Biochem. Biophys. Res. Commun.* **294**, 791–797.

Magico, A. C. and Bell, J. B. (2011). Identification of a classical bipartite nuclear localization signal in the Drosophila TEA/ATTS protein scalloped. *PLoS One* **6**, e21431.

Mann, C. J., Osborn, D. P. and Hughes, S. M. (2007). Vestigial-like-2b (VITO-1b) and Tead-3a (Tef-5a) expression in zebrafish skeletal muscle, brain and notochord. *Gene Expr. Patterns* **7**, 827–836.

Mann, K. M., Ward, J. M., Yew, C. C. K., Kovochich, A., Dawson, D. W., Black, M. A.,

Brett, B. T., Sheetz, T. E., Dupuy, A. J., Chang, D. K., et al. (2012). Sleeping Beauty mutagenesis reveals cooperating mutations and pathways in pancreatic adenocarcinoma. *Proc. Natl. Acad. Sci.* **109**, 5934–5941.

Mar, J. H. and Ordahl, C. P. (1988). A conserved CATTCCT motif is required for skeletal muscle-specific activity of the cardiac troponin T gene promoter. *Proc. Natl. Acad. Sci.* **85**, 6404–8.

Mar, J. H., Antin, P. B., Cooper, T. A. and Ordahl, C. P. (1988). Analysis of the upstream regions governing expression of the chicken cardiac troponin T gene in embryonic cardiac and skeletal muscle cells. *J. Cell Biol.* **107**, 573–585.

Martín-Castellanos, C. and Edgar, B. A. (2002). A characterization of the effects of Dpp signaling on cell growth and proliferation in the Drosophila wing. *Development* **129**, 1003–1013.

Martin, P. F. (1982). Direct determination of the growth rate of Drosophila imaginal discs. *J. Exp. Zool.* **222**, 97–102.

Meise, M. and Janning, W. (1993). Cell lineage of larval and imaginal thoracic anlagen cells of Drosophila melanogaster, as revealed by single-cell transplantations. *Development* **1121**, 1107–1121.

Melvin, V. S., Feng, W., Hernandez-Lagunas, L., Artinger, K. B. and Williams, T. (2013). A morpholino-based screen to identify novel genes involved in craniofacial morphogenesis. *Dev. Dyn.* **242**, 817–831.

Mendoza-Viveros, L., Bouchard-Cannon, P., Hegazi, S., Cheng, A. H., Pastore, S. and Cheng, H. Y. M. (2017). Molecular modulators of the circadian clock: lessons from flies and mice. *Cell. Mol. Life Sci.* **74**, 1035–1059.

Meserve, J. H. and Duronio, R. J. (2015). Scalloped and Yorkie are required for cell cycle re-entry of quiescent cells after tissue damage. *Development* **142**, 2740–51.

Mielcarek, M., Günther, S., Krüger, M. and Braun, T. (2002). VITO-1, a novel vestigial related protein is predominantly expressed in the skeletal muscle lineage. *Mech. Dev.* **119**, S269–S274.

Mielcarek, M., Piotrowska, I., Schneider, A., Günther, S. and Braun, T. (2009). VITO-2, a new SID domain protein, is expressed in the myogenic lineage during early mouse embryonic development. *Gene Expr. Patterns* **9**, 129–137.

Milewski, R. C., Chi, N. C., Li, J., Brown, C., Lu, M. M. and Epstein, J. A. (2004). Identification of minimal enhancer elements sufficient for Pax3 expression in neural crest and implication of Tead2 as a regulator of Pax3. *Development* **131**, 829–37.

Mohideen, F., Capili, A. D., Bilimoria, P. M., Yamada, T., Bonni, A. and Lima, C. D. (2009). A molecular basis for phosphorylation-dependent SUMO conjugation by the E2 UBC9. *Nat. Struct. Mol. Biol.* **16**, 945–52.

Monribot-Villanueva, J., Zurita, M. and Vázquez, M. (2017). Developmental transcriptional regulation by SUMOylation, an evolving field. *Genesis* **55**, e23009.

Morata, G. and Lawrence, P. A. (1977). The development of wingless, a homeotic mutation of Drosophila. *Dev. Biol.* **56**, 227–240.

Morcillo, P., Rosen, C. and Dorsett, D. (1996). Genes regulating the remote wing margin enhancer in the Drosophila cut locus. *Genetics* **144**, 1143–1154.

Morgan, T. H. and Bridges, C. B. (1919). Contributions to the genetics of Drosophila melanogaster. The origin of gynandromorphs. *Publs Carnegie Instn* **278**, 1–122.

Morrison, D. K., Murakami, M. S. and Cleghon, V. (2000). Protein kinases and

phosphatases in the Drosophila genome. *J. Cell Biol.* **150**, F57-62.

Moschall, R., Gaik, M. and Medenbach, J. (2017). Promiscuity in post-transcriptional control of gene expression: Drosophila sex-lethal and its regulatory partnerships. *FEBS Lett.* **591**, 1471–1488.

Mummery-Widmer, J. L., Yamazaki, M., Stoeger, T., Novatchkova, M., Bhalerao, S., Chen, D., Dietzl, G., Dickson, B. J. and Knoblich, J. A. (2009). Genome-wide analysis of Notch signalling in Drosophila by transgenic RNAi. *Nature* **458**, 987–992.

Murakawa, Y., Yoshihara, M., Kawaji, H., Nishikawa, M., Zayed, H., Suzuki, H. and Hayashizaki, Y. (2016). Enhanced Identification of Transcriptional Enhancers Provides Mechanistic Insights into Diseases. *Trends Genet.* **32**, 76–88.

Murali, T., Pacifico, S., Yu, J., Guest, S., Roberts, G. G. and Finley, R. L. (2011). DroID 2011: a comprehensive, integrated resource for protein, transcription factor, RNA and gene interactions for Drosophila. *Nucleic Acids Res.* **39**, D736–D743.

Ng, M., Diaz-Benjumea, F. J., Vincent, J.-P. P., Wu, J. and Cohen, S. M. (1996). Specification of the wing by localized expression of wingless protein. *Nature* **381**, 316–318.

Nguyen, L. K., Kolch, W. and Kholodenko, B. N. (2013). When ubiquitination meets phosphorylation: a systems biology perspective of EGFR/MAPK signalling. *Cell Commun. Signal.* **11**, 52.

Nienhaus, U., Aegerter-Wilmsen, T. and Aegerter, C. M. (2012). In-Vivo Imaging of the Drosophila Wing Imaginal Disc over Time: Novel Insights on Growth and Boundary Formation. *PLoS One* **7**, e47594.

Noland, C. L., Gierke, S., Schnier, P. D., Murray, J., Sandoval, W. N., Sagolla, M., Dey,

A., Hannoush, R. N., Fairbrother, W. J. and Cunningham, C. N. (2016). Palmitoylation of TEAD Transcription Factors Is Required for Their Stability and Function in Hippo Pathway Signaling. *Structure* **24**, 179–186.

Oh, H. and Irvine, K. D. (2008). In vivo regulation of Yorkie phosphorylation and localization. *Development* **135**, 1081–1088.

Oliva, C. and Hassan, B. A. (2017). Receptor Tyrosine Kinases and Phosphatases in Neuronal Wiring: Insights From Drosophila. *Curr. Top. Dev. Biol.* **123**, 399–432.

Ordóñez-Morán, P., Dafflon, C., Imajo, M., Nishida, E. and Huelsken, J. (2015). HOXA5 Counteracts Stem Cell Traits by Inhibiting Wnt Signaling in Colorectal Cancer. *Cancer Cell* **28**, 815–829.

Organista, M. F., Martín, M., de Celis, J. M., Barrio, R., López-Varea, A., Esteban, N., Casado, M. and de Celis, J. F. (2015). The Spalt Transcription Factors Generate the Transcriptional Landscape of the Drosophila melanogaster Wing Pouch Central Region. *PLoS Genet.* **11**, e1005370.

Pandey, U. B. and Nichols, C. D. (2011). Human Disease Models in Drosophila melanogaster and the Role of the Fly in Therapeutic Drug Discovery. *Pharmacol. Rev.* **63**, 411–436.

Paumard-Rigal, S., Zider, A., Vaudin, P. and Silber, J. (1998). Specific interactions between vestigial and scalloped are required to promote wing tissue proliferation in Drosophila melanogaster. *Dev. Genes Evol.* **208**, 440–446.

Peng, H. W., Slattery, M. and Mann, R. S. (2009). Transcription factor choice in the Hippo signaling pathway: Homothorax and yorkie regulation of the microRNA bantam in the progenitor domain of the Drosophila eye imaginal disc. *Genes Dev.* **23**, 2307–2319.

Peng, Z., Skoog, L., Hellborg, H., Jonstam, G., Wingmo, I.-L., Hjälm-Eriksson, M., Harmenberg, U., Cedermark, G. C., Andersson, K., Ahrlund-Richter, L., et al. (2014). An expression signature at diagnosis to estimate prostate cancer patients' overall survival. *Prostate Cancer Prostatic Dis.* **17**, 81–90.

Peng, R., Lin, G. and Li, J. (2016). Potential pitfalls of CRISPR/Cas9-mediated genome editing. *FEBS J.* **283**, 1218–1231.

Pfleger, C. M. (2017). *The Hippo Pathway: A Master Regulatory Network Important in Development and Dysregulated in Disease*. 1st ed. Elsevier Inc.

Pimmett, V. L., Deng, H., Haskins, J. A., Mercier, R. J., LaPointe, P. and Simmonds, A. J. (2017). The activity of the Drosophila Vestigial protein is modified by Scalloped-dependent phosphorylation. *Dev. Biol.* **425**, 58–69.

Pobbati, A. V. and Hong, W. (2013). Emerging roles of TEAD transcription factors and its coactivators in cancers. *Cancer Biol. Ther.* **14**, 390–398.

Port, F., Chen, H.-M., Lee, T. and Bullock, S. L. (2014). Optimized CRISPR/Cas tools for efficient germline and somatic genome engineering in *Drosophila*. *Proc. Natl. Acad. Sci.* **111**, E2967-2976.

Prabakaran, S., Lippens, G., Steen, H. and Gunawardena, J. (2012). Post-translational modification: nature's escape from genetic imprisonment and the basis for dynamic information encoding. *Wiley Interdiscip. Rev. Syst. Biol. Med.* **4**, 565–83.

Qiu, H., Wang, F., Liu, C., Xu, X. and Liu, B. (2011). TEAD1-dependent expression of the FoxO3a gene in mouse skeletal muscle. *BMC Mol. Biol.* **12**, 1.

Ray, R. P. and Wharton, K. A. (2001). Context-dependent relationships between the BMPs gbb and dpp during development of the Drosophila wing imaginal disk. *Development*

128, 3913–3925.

Reiter, L. T., Potocki, L., Chien, S., Gribskov, M. and Bier, E. (2001). A systematic analysis of human disease-associated gene sequences in Drosophila melanogaster. *Genome Res.* **11**, 1114–25.

Reiter, F., Wienerroither, S. and Stark, A. (2017). Combinatorial function of transcription factors and co-factors. *Curr. Opin. Genet. Dev.* **43**, 73–81.

Ren, F., Zhang, L. and Jiang, J. (2010). Hippo signaling regulates Yorkie nuclear localization and activity through 14-3-3 dependent and independent mechanisms. *Dev. Biol.* **337**, 303–312.

Reya, T., Duncan, A. W., Ailles, L., Domen, J., Scherer, D. C., Willert, K., Hintz, L., Nusse, R. and Weissman, I. L. (2003). A role for Wnt signalling in self-renewal of haematopoietic stem cells. *Nature* **423**, 409–414.

Rosonina, E., Duncan, S. M. and Manley, J. L. (2010). SUMO functions in constitutive transcription and during activation of inducible genes in yeast. *Genes Dev.* **24**, 1242–1252.

Ruiz-Romero, M., Blanco, E., Paricio, N., Serras, F. and Corominas, M. (2015). Cabut/dTIEG associates with the transcription factor Yorkie for growth control. *EMBO Rep.* **16**, 362–9.

Salah, Z. and Aqeilan, R. I. (2011). WW domain interactions regulate the Hippo tumor suppressor pathway. *Cell Death Dis.* **2**, e172-6.

Sano, Y., Akimaru, H., Okamura, T., Nagao, T., Okada, M. and Ishii, S. (2005). Drosophila Activating Transcription Factor-2 Is Involved in Stress Response via Activation by p38, but Not c-Jun NH 2 -Terminal Kinase. *Mol. Biol. Cell* **16**, 2934–

2946.

Sansores-Garcia, L., Atkins, M., Moya, I. M., Shahmoradgoli, M., Tao, C., Mills, G. B. and Halder, G. (2013). Mask is required for the activity of the hippo pathway effector Yki/YAP. *Curr. Biol.* **23**, 229–235.

Santo, L., Siu, K. T. and Raje, N. (2015). Targeting Cyclin-Dependent Kinases and Cell Cycle Progression in Human Cancers. *Semin. Oncol.* **42**, 788–800.

Sawada, A., Kiyonari, H., Ukita, K., Nishioka, N., Imuta, Y. Y. and Sasaki, H. (2008). Redundant Roles of Tead1 and Tead2 in Notochord Development and the Regulation of Cell Proliferation and Survival. *Mol. Cell. Biol.* **28**, 3177–3189.

Schwarzer, W. and Spitz, F. (2014). The architecture of gene expression: Integrating dispersed cis-regulatory modules into coherent regulatory domains. *Curr. Opin. Genet. Dev.* **27**, 74–82.

Sell, S. (2004). Stem cell origin of cancer and differentiation therapy. *Crit. Rev. Oncol. Hematol.* **51**, 1–28.

Serpe, M., Ralston, A., Blair, S. S. and O'Connor, M. B. (2005). Matching catalytic activity to developmental function: Tolloid-related processes Sog in order to help specify the posterior crossvein in the Drosophila wing. *Development* **132**, 2645–2656.

Shen, S., Guo, X., Yan, H., Lu, Y., Ji, X., Li, L., Liang, T., Zhou, D., Feng, X.-H., Zhao, J. C., et al. (2015). A miR-130a-YAP positive feedback loop promotes organ size and tumorigenesis. *Cell Res.* **25**, 997–1012.

Shimmi, O., Matsuda, S. and Hatakeyama, M. (2014). Insights into the molecular mechanisms underlying diversified wing venation among insects. *Proc. R. Soc. B Biol. Sci.* **281**, 20140264–20140264.

Shu, Z. and Deng, W.-M. (2017). Differential Regulation of Cyclin E by Yorkie-Scalloped Signaling in Organ Development. *G3 Genes|Genomes|Genetics* g3.117.039065.

Sidor, C. M., Brain, R. and Thompson, B. J. (2013). Mask proteins are co-factors of Yorkie/YAP in the hippo pathway. *Curr. Biol.* **23**, 223–228.

Silber, J. (1980). Penetrance of the vestigial gene in drosophila melanogaster. *Genetica* **54**, 91–99.

Simmonds, A. J., Hughes, S. C., Tse, J., Cocquyt, S. and Bell, J. B. (1997). The effect of dominant vestigial alleles upon vestigial-mediated wing patterning during development of Drosophila melanogaster. *Mech. Dev.* **67**, 17–33.

Simmonds, A. J., Liu, X., Soanes, K. H., Krause, H. M., Irvine, K. D. and Bell, J. B. (1998). Molecular interactions between Vestigial and Scalloped promote wing formation in Drosophila. *Genes Dev.* **12**, 3815–3820.

Simon, E., Faucheux, C., Zider, A., Theze, N. and Thiebaud, P. (2016). From vestigial to vestigial-like: the Drosophila gene that has taken wing. *Dev. Genes Evol.* **226**, 297–315.

Sivachenko, A., Li, Y., Abruzzi, K. C. and Rosbash, M. (2013). The Transcription Factor Mef2 Links the Drosophila Core Clock to Fas2, Neuronal Morphology, and Circadian Behavior. *Neuron* **79**, 281–292.

Skeath, J. B. and Carroll, S. B. (1991). Regulation of achaete-scute gene expression and sensory organ pattern formation in the Drosophila wing. *Genes Dev.* **5**, 984–995.

Skeath, J. B. and Carroll, S. B. (1994). The achaete-scute complex: generation of cellular pattern and fate within the Drosophila nervous system. *FASEB J.* **8**, 714–721.

Slattery, M., Voutev, R., Ma, L., Nègre, N., White, K. P. and Mann, R. S. (2013). Divergent Transcriptional Regulatory Logic at the Intersection of Tissue Growth and

Developmental Patterning. *PLoS Genet.* **9**, 22–25.

Smith, M., Turki-Judeh, W. and Courey, A. J. (2012). SUMOylation in Drosophila Development. *Biomolecules* **2**, 331–349.

Somasagara, R. R., Spencer, S. M., Tripathi, K., Clark, D. W., Mani, C., Madeira da Silva, L., Scalici, J., Kothayer, H., Westwell, A. D., Rocconi, R. P., et al. (2017). RAD6 promotes DNA repair and stem cell signaling in ovarian cancer and is a promising therapeutic target to prevent and treat acquired chemoresistance. *Oncogene* **36**, 6680–6690.

Song, I.-S., Jeong, Y. J., Seo, Y. J., Byun, J. M., Kim, Y. N., Jeong, D. H., Han, J., Kim, K. T. and Jang, S.-W. (2017). Peroxiredoxin 3 maintains the survival of endometrial cancer stem cells by regulating oxidative stress. *Oncotarget* **8**, 92788–92800.

Srivastava, A. and Bell, J. B. (2003). Further developmental roles of the Vestigial/Scalloped transcription complex during wing development in Drosophila melanogaster. *Mech. Dev.* **120**, 587–596.

Srivastava, A., MacKay, J. O. and Bell, J. B. (2002). A vestigial: Scalloped TEA domain chimera rescues the wing phenotype of a scalloped mutation in Drosophila melanogaster. *Genesis* **33**, 40–47.

Srivastava, A., Simmonds, A. J., Garg, A., Fossheim, L., Campbell, S. D. and Bell, J. B. (2004). Molecular and Functional Analysis of scalloped Recessive Lethal Alleles in Drosophila melanogaster. *Genetics* **166**, 1833–1843.

St Johnston, D. (2002). The art and design of genetic screens: Drosophila melanogaster. *Nat. Rev. Genet.* **3**, 176–188.

Stewart, A. F. R., Larkin, S. B., Farrance, I. K. G., Mar, J. H., Hall, D. E. and Ordahl,

C. P. (1994). Muscle-enriched TEF-1 isoforms bind M-CAT elements from muscle-specific promoters and differentially activate transcription. *J. Biol. Chem.* **269**, 3147–3150.

Stewart, A. F. R., Suzow, J., Kubota, T., Ueyama, T. and Chen, H.-H. (1998). Transcription Factor RTEF-1 Mediates 1-Adrenergic Reactivation of the Fetal Gene Program in Cardiac Myocytes. *Circ. Res.* **83**, 43–49.

Sun, Y., Nien, C. Y., Chen, K., Liu, H. Y., Johnston, J., Zeitlinger, J. and Rushlow, C. (2015a). Zelda overcomes the high intrinsic nucleosome barrier at enhancers during Drosophila zygotic genome activation. *Genome Res.* **25**, 1703–1714.

Sun, X., Yang, H., Sturgill, D., Oliver, B., Rabinow, L. and Samson, M.-L. (2015b). Sxl-Dependent, tra/tra2-Independent Alternative Splicing of the Drosophila melanogaster X-Linked Gene found in neurons. *G3 Genes|Genomes|Genetics* **5**, 2865–2874.

Tajonar, A., Maehr, R., Hu, G., Sneddon, J. B., Rivera-Feliciano, J., Cohen, D. E., Elledge, S. J. and Melton, D. A. (2013). Brief report: VGLL4 is a novel regulator of survival in human embryonic stem cells. *Stem Cells* **31**, 2833–2841.

Takanaka, Y. and Courey, A. J. (2005). SUMO enhances Vestigial function during wing morphogenesis. *Mech. Dev.* **122**, 1130–1137.

Talamillo, A., Sánchez, J. and Barrio, R. (2008). Functional analysis of the SUMOylation pathway in Drosophila. *Biochem. Soc. Trans.* **36**, 868–73.

Tannishtha, R., Morrison, S. J., Clarke, M. F. and Weissman, I. L. (2001). Stem Cells, Cancer, and Cancer Stem Cells. *Nature* **414**, 105–111.

Teng, A. C., Belanger, M. I. and Stewart, A. F. (2008). The muscle-specific transcription co-factor Vgll2 promotes myogenic differentiation through a casein kinase II dependent

mechanism. In *FASEB Journal*, .

Thisse, B., Pflumio, S., Fürthauer, M., Loppin, B., Heyer, V., Degrave, A., Woehl, R., Lux, A., Steffan, T., Charbonnier, X. ., et al. (2001). Expression of the zebrafish genome during embryogenesis. *ZFIN Direct Data Submiss. (NIH R01 RR15402)*.

Tian, W., Yu, J., Tomchick, D. R., Pan, D. and Luo, X. (2010). Structural and functional analysis of the YAP-binding domain of human TEAD2. *Proc. Natl. Acad. Sci.* **107**, 7293–8.

Tixier, V., Bataillé, L. and Jagla, K. (2010). Diversification of muscle types: Recent insights from Drosophila. *Exp. Cell Res.* **316**, 3019–3027.

Todeschini, A. L., Georges, A. and Veitia, R. A. (2014). Transcription factors: Specific DNA binding and specific gene regulation. *Trends Genet.* **30**, 211–219.

Tootle, T. L. and Rebay, I. (2005). Post-translational modifications influence transcription factor activity: A view from the ETS superfamily. *BioEssays* **27**, 285–298.

Tress, M. L., Abascal, F. and Valencia, A. (2017). Alternative Splicing May Not Be the Key to Proteome Complexity. *Trends Biochem. Sci.* **42**, 98–110.

Van de Bor, V., Delanoue, R., Cossard, R. and Silber, J. (1999). Truncated products of the vestigial proliferation gene induce apoptosis. *Cell Death Differ.* **6**, 557–64.

Vanderploeg, J. and Jacobs, J. R. (2017). Mapping Heart Development in Flies: Src42A Acts Non-Autonomously to Promote Heart Tube Formation in Drosophila. *Vet. Sci.* **4**, 23.

Vaudin, P., Delanoue, R., Davidson, I., Silber, J. and Zider, A. (1999). TONDU (TDU), a novel human protein related to the product of vestigial (vg) gene of Drosophila melanogaster interacts with vertebrate TEF factors and substitutes for Vg function in

wing formation. *Development* **126**, 4807–4816.

Voss, T. C. and Hager, G. L. (2014). Dynamic regulation of transcriptional states by chromatin and transcription factors. *Nat. Rev. Genet.* **15**, 69–81.

Walski, T., De Schutter, K., Van Damme, E. J. M. and Smagghe, G. (2017). Diversity and functions of protein glycosylation in insects. *Insect Biochem. Mol. Biol.* **83**, 21–34.

Wang, Y., He, L., Du, Y., Zhu, P., Huang, G., Luo, J., Yan, X., Ye, B., Li, C., Xia, P., et al. (2015). The long noncoding RNA lncTCF7 promotes self-renewal of human liver cancer stem cells through activation of Wnt signaling. *Cell Stem Cell* **16**, 413–425.

Waterhouse, R. M., Zdobnov, E. M., Tegenfeldt, F., Li, J. and Kriventseva, E. V. (2011). OrthoDB: the hierarchical catalog of eukaryotic orthologs in 2011. *Nucleic Acids Res.* **39**, D283–D288.

West, J. J. and Harris, T. J. C. (2016). Cadherin Trafficking for Tissue Morphogenesis: Control and Consequences. *Traffic* **17**, 1233–1243.

Williams, J. A., Bell, J. B. and Carroll, S. B. (1991). Control of Drosophila wing and haltere development by the nuclear vestigial gene product. *Genes Dev.* **5**, 2481–2495.

Williams, J. A., Paddock, S. W. and Carroll, S. B. (1993). Pattern formation in a secondary field: a hierarchy of regulatory genes subdivides the developing Drosophila wing disc into discrete subregions. *Development* **117**, 571–584.

Williams, J. A., Paddock, S. W., Vorwerk, K. and Carroll, S. B. (1994). Organization of wing formation and induction of a wing-patterning gene at the dorsal/ventral compartment boundary. *Nature* **368**, 299–305.

Wu, J. and Cohen, S. M. (2002). Repression of Teashirt marks the initiation of wing development. *Development* **129**, 2411–8.

Wu, S., Liu, Y., Zheng, Y., Dong, J. and Pan, D. (2008). The TEAD/TEF family protein Scalloped mediates transcriptional output of the Hippo growth-regulatory pathway. *Dev. Cell* **14**, 388–398.

Wu, F.-H., Mu, L., Li, X.-L., Hu, Y.-B., Liu, H., Han, L.-T. and Gong, J.-P. (2017). Characterization and functional analysis of a slow-cycling subpopulation in colorectal cancer enriched by cell cycle inducer combined chemotherapy. *Oncotarget* **8**, 78466–78479.

Xiao, J.-H., Davidson, I., Macchi, M., Rosales, R., Vigneron, M., Staub, A. and Chambon, P. (1987). In vitro binding of several cell-specific and ubiquitous nuclear proteins to the GT-I motif of the SV40 enhancer. *Genes Dev.* **1**, 794–807.

Xiao, J. H., Davidson, I., Matthes, H., Garnier, J.-M. and Chambon, P. (1991). Cloning, expression, and transcriptional properties of the human enhancer factor TEF-1. *Cell* **65**, 551–68.

Xue, Y., Liu, Z., Cao, J., Ma, Q., Gao, X., Wang, Q., Jin, C., Zhou, Y., Wen, L. and Ren, J. (2011). GPS 2.1: Enhanced prediction of kinase-specific phosphorylation sites with an algorithm of motif length selection. *Protein Eng. Des. Sel.* **24**, 255–260.

Yagi, R., Kohn, M. J., Karavanova, I., Kaneko, K. J., Vullhorst, D., DePamphilis, M. L. and Buonanno, A. (2007). Transcription factor TEAD4 specifies the trophectoderm lineage at the beginning of mammalian development. *Development* **134**, 3827–3836.

Yang, S. H., Galanis, A. and Sharrocks, A. D. (1999). Targeting of p38 Mitogen-Activated Protein Kinases to MEF2 Transcription Factors. *Mol. Cell. Biol.* **19**, 4028.

Yang, X., Coulombe-Huntington, J., Kang, S., Sheynkman, G. M., Hao, T., Richardson, A., Sun, S., Yang, F., Shen, Y. A., Murray, R. R., et al. (2016). Widespread

Expansion of Protein Interaction Capabilities by Alternative Splicing. *Cell* **164**, 805–817.

Yu, L., Daniels, J. P., Wu, H. and Wolf, M. J. (2015). Cardiac hypertrophy induced by active Raf depends on Yorkie-mediated transcription. *Sci. Signal.* **8**, ra13.

Zecca, M. and Struhl, G. (2007a). Control of Drosophila wing growth by the vestigial quadrant enhancer. *Development* **134**, 3011–20.

Zecca, M. and Struhl, G. (2007b). Recruitment of cells into the Drosophila wing primordium by a feed-forward circuit of vestigial autoregulation. *Development* **134**, 3011–20.

Zecca, M. and Struhl, G. (2010). A feed-forward circuit linking wingless, Fat-Dachsous signaling, and the warts-hippo pathway to drosophila wing growth. *PLoS Biol.* **8**,.

Zecca, M., Basler, K. and Struhl, G. (1995). Sequential organizing activities of engrailed, hedgehog and decapentaplegic in the Drosophila wing. *Development* **121**, 2265–78.

Zeng, Y., Stauffer, S., Zhou, J., Chen, X., Chen, Y. and Dong, J. (2017). Cyclin-dependent kinase 1 (CDK1)-mediated mitotic phosphorylation of the transcriptional co-repressor Vgll4 inhibits its tumor-suppressing activity. *J. Biol. Chem.* **292**, 15028–15038.

Zhang, L., Ren, F., Zhang, Q., Chen, Y., Wang, B. and Jiang, J. (2008). The TEAD/TEF family of transcription factor Scalloped mediates Hippo signaling in organ size control. *Dev. Cell* **14**, 377–387.

Zhang, W., Gao, Y., Li, P., Shi, Z., Guo, T., Li, F., Han, X., Feng, Y., Zheng, C., Wang, Z., et al. (2014). VGLL4 functions as a new tumor suppressor in lung cancer by negatively regulating the YAP-TEAD transcriptional complex. *Cell Res.* **24**, 331–43.

Zhang, E., Shen, B., Mu, X., Qin, Y., Zhang, F., Liu, Y., Xiao, J., Zhang, P., Wang, C., Tan, M., et al. (2016). Ubiquitin-specific protease 11 (USP11) functions as a tumor suppressor through deubiquitinating and stabilizing VGLL4 protein. *Am. J. Cancer Res.* **6**, 2901–2909.

Zhang, P., Pei, C., Wang, X., Xiang, J., Sun, B.-F. F., Cheng, Y. Y. Y., Qi, X., Marchetti, M., Xu, J.-W. W., Sun, Y.-P. P., et al. (2017a). A Balance of Yki/Sd Activator and E2F1/Sd Repressor Complexes Controls Cell Survival and Affects Organ Size. *Dev. Cell* **43**, 603–617.

Zhang, Y., Shen, H., Withers, H. G., Yang, N., Denson, K. E., Mussell, A. L., Truskinovsky, A., Fan, Q., Gelman, I. H., Frangou, C., et al. (2017b). VGLL4 Selectively Represses YAP-Dependent Gene Induction and Tumorigenic Phenotypes in Breast Cancer. *Sci. Rep.* **7**, 6190.

Zhang, R., Engler, A. and Taylor, V. (2018). Notch: an interactive player in neurogenesis and disease. *Cell Tissue Res.* **371**, 73–89.

Zhao, M., New, L., Kravchenko, V. V, Kato, Y., Gram, H., di Padova, F., Olson, E. N., Ulevitch, R. J. and Han, J. (1999). Regulation of the MEF2 family of transcription factors by p38. *Mol. Cell. Biol.* **19**, 21–30.

Zhao, L., Wang, L., Chi, C., Lan, W. and Su, Y. (2017). The emerging roles of phosphatases in Hedgehog pathway. *Cell Commun. Signal.* **15**, 35.

Zhou, H., Di Palma, S., Preisinger, C., Peng, M., Polat, A. N., Heck, A. J. R. and Mohammed, S. (2013). Toward a Comprehensive Characterization of a Human Cancer Cell Phosphoproteome. *J. Proteome Res.* **12**, 260–271.

Zolotarev, N., Fedotova, A., Kyrchanova, O., Bonchuk, A., Penin, A. A., Lando, A. S.,

Eliseeva, I. A., Kulakovskiy, I. V., Maksimenko, O. and Georgiev, P. (2016). Architectural proteins Pita, Zw5,and ZIPIC contain homodimerization domain and support specific long-range interactions in Drosophila. *Nucleic Acids Res.* **44**, 7228–7241.